AUTONOMOUS UNIVERSITY OF MADRID
FACULTY OF SCIENCES
PHD IN BIOMOLECULAR SCIENCES

TOLL-LIKE RECEPTOR 2 AND 4: DIFFERENTIAL SIGNALING, DIMERIZATION AND THE OUTCOME IN INFLAMMATION

Doctoral thesis

Sara Isabel Vaz Francisco

Madrid, April 2019

AUTONOMOUS UNIVERSITY OF MADRID
FACULTY OF SCIENCES
DEPARTMENT OF MOLECULAR BIOLOGY

TOLL-LIKE RECEPTOR 2 AND 4: DIFFERENTIAL SIGNALING, DIMERIZATION AND THE OUTCOME IN INFLAMMATION

Thesis for the degree of doctor philosophie in University Autonomous of Madrid by:
Sara Isabel Vaz Francisco, B.Sc and M.Sc in Biochemistry

Thesis Supervisors:
Dr. Manuel Fresno Escudero
Dra. Alicia Arranz de Miguel

The thesis was carried out in the Center of Molecular Biology– Severo Ochoa, Madrid and financed/supported by a predoctoral fellowship under the TOLLerant-ETN action, Marie Sklodowska-Curie grant agreement N° 642157 from the European Union Horizon 2020 program.

TABLE OF CONTENTS

ABBREVIATIONS

(IPS)-1 IFN-β promoter stimulator

AP1 Activator protein 1

BMDM Bone marrow-derived macrophages

c/EBPβ CCAAT-enhancer-binding proteins

CD14 Cluster of differentiation 14

CLR C-type lectin receptor

CpG DNA Unmethylated 2´- deoxyribo cytidine–phosphate–guanosine

CREB Cyclic AMP-responsive element-binding protein

DAMP Danger-associated molecular patterns

DCs Dendritic cells

dsRNA Double-strand RNA

ER Endoplasmic reticulum

Gal*p* D-Galactose

GlcNAc N-Acetyl-D-glucosamine

Glc*p* D-Glucose

Glc*p*N D-Glucosamine

HIV-1 Human immunodeficiency viruses

HMGB1 Protein high-mobility group box 1

HSP Heat shock proteins

HSV Herpes simplex virus

IFN Interferon

IFNAR Type I IFN-receptor

IgA Immunoglobulin A

IKK complex Inhibitor of nuclear factor-κB- kinase complex

Inl A and B Internalin A and B

iNOS Inducible nitric oxide synthase

IRAK IL-1R-associated kinase

IRF IFN-regulatory factor

IRF Interferon Regulatory Factor

KDO 3-deoxy-d-manno-oct-ulosonic acid

LBP Lipopolysaccharide binding protein

LLO Listeriolysin

LPS Lipopolysaccharide

L-Rha L-Rhamnose

LRR Leucin-rich repeats

Man*p* D-Mannose

MAPK Mitogen-activated protein kinases

MCP-1 Monocyte chemoattractant protein 1

MSK Mitogen and stress activated protein kinase

MyD88 Myeloid differentiation primary response 88

NEMO NF-κB essential modulator

NF-κB nuclear factor kappa-light-chain-enhancer of activated B cells

NK Natural killer cells

NLR Nucleotide-like receptors

NOD Nucleotide oligomerization domain

PAMP Pathogen-associated molecular patterns

PGN Peptidoglycan

PI3K Phosphoinositide 3-kinase

PKC Protein kinase C

polyI:C Polyinosinic-polycytidylic acid

PPRγ Peroxisome proliferator-activated receptor gamma

PRR Pattern recognition receptors

RIG Retinoic acid inducible gene

RIG-I-like receptors retinoic acid-inducible gene-I-like receptor

RIP1 Receptor-interacting serine/threonine-protein kinase 1

ROS Reactive oxygen species

ssRNA Single strand RNA

STAT Signal transducer and activator of transcription

STING Stimulator of interferon genes

TAB1 TGF-Beta Activated Kinase 1

TAK1 Transforming growth factor beta-activated kinase 1

TBK1 Serine/threonine-protein kinase

TGPI-mucins Glycosylphosphatidylinositol-anchored mucin-like glycoproteins

Th1 T helper type 1 cells

Th17 IL-17-producing helper T cells

TIR Toll/interleukin-1 receptor

TIRAP MyD88 adaptor-like Mal

TLR Toll-like receptor

TNF Tumor necrosis factors

TPL2 Tumor progression locus 2

TRAF6 Tumor necrosis factor receptor (TNFR)-associated factor 6

TRAM TRIF-related adaptor molecule

TRIF TIR domain containing adaptor inducing interferon-β

Ubc13 Ubiquitin-conjugating enzyme E2 13

Uev1A Ubiquitin-conjugating enzyme E2 variant 1A

Vip Vasoactive intestinal peptide

ABSTRACT

ABSTRACT

Toll-like receptors (TLRs) play a crucial role in the recognition of pathogen-derived components as a first line of defense against infections. TLR4 and TLR2 receptors play a key role due to their cell surface location and their ability to identify a diversified spectrum of pathogen components. The early signaling activation via TLR4 and TLR2 receptors was studied and the results presented in the first chapter of this work show that TLR2 ligands activated NF-κB and MAPKs earlier and exhibited a higher IL-10 /IL-12 ratio at later time points compared to TLR4 ligands. The results further show the involvement of the phosphatase MKP-1 in the control of the MAPK p38 activation and that MKP-1 contributes to pro-inflammatory cytokine's upregulation. Furthermore, p38 is critical for IL-10 expression in response to TLR2 ligands, which triggers the macrophage change to a M2 and regulatory phenotype in contrast to the M1 phenotype induced by TLR4 activation. Therefore, the early TLR2-mediated p38 induction contributes for the high IL-10 production as a virulence strategy to suppress host Th1 response against certain types of pathogens.

TLR2 activation induces type I interferon expression mediated by MyD88 and TRIF signaling pathways. The role of TRIF-IFN-β-signaling in TLR2-mediated inflammatory responses was investigated and the results presented in the second chapter indicate that TLR2 ligands induce IFN-β expression, dependent of receptor endocytosis which consequently activate the interferon transcription factors IRF3 and IRF7. TRIF signaling was found to be required for IFN-β induction and consequent expression of the cytokine IL-12 in response to TLR2 ligands. Moreover, TLR2 is determinant for *Listeria monocytogenes* recognition, however, modifications of this bacteria cell wall avoid its recognition. The *in vivo* administration of TLR2 ligands in a murine model of neonatal listeriosis showed lower levels of bacterial load in neonate's microglia, and *Listeria*-infected dendritic cells stimulated with TLR2 ligands presented higher levels of protective TNF-α and IL-12 cytokines, mediated by IFN-β. Therefore, TLR2 ligands exert a modulatory effect on cytokines with beneficial effects on the prevention of *Listeria* dissemination. This data points to TLR2 ligands as potential adjuvants in vaccine models for this bacterial infection.

TLR4 is considered the major receptor to recognize all LPSs. However, some atypical LPS's structures depart from the well-studied *E. coli* LPS and induce a TLR2-dependent inflammatory response in immune cells. The results in the third chapter demonstrate that the atypical LPS from *Ochrobactrum intermedium* is a TLR4/TLR2 agonist, inducing a weaker inflammatory response compared to *E. coli* LPS. Molecular docking analysis of *O. intermedium* LPS predicts a favorable formation of a TLR2/TLR4/MD-2 heterodimer, further confirmed by FRET. These imply that atypical LPSs may induce TLR4/TLR2 heterodimerization to decrease the bacteria activation of the innate immune system.

RESUMEN

Los receptores “Toll-like” (TLRs) tienen un papel clave en el reconocimiento de compuestos derivados de patógenos siendo una primera barrera contra las infecciones. TLR4 y TLR2 son importantes debido a su localización en la superficie celular y por su capacidad de reconocer una variad de moléculas derivadas de patógenos. Se estudió la señalización temprana por la activación de TLR4 y TLR2 fue y los resultados presentados en el capítulo 1 de este trabajo demuestran que ligandos de TLR2 activan NF-κB y MAPKs más tempranamente y exhiben un ratio IL-10/IL-12 más alto que los ligandos TLR4. Además, la fosfatasa MKP-1 controla la fosforilación de p38 y contribuye al incremento de citoquinas proinflamatorias. Nuestros resultados indican que p38 es importante para la expresión de IL-10 en respuesta a ligandos de TLR2, lo que induce un cambio del fenotipo de los macrófagos a tipo M2 y regulatorio, en lugar del tipo M1 que es inducido por la activación de TLR4. Por lo tanto, la activación temprana de p38 mediada por TLR2 contribuye para la alta producción de IL-10 como una estrategia de virulencia para suprimir la respuesta Th1 del hospedero contra determinados patógenos.

La activación de TLR2 induce la expresión de interferón tipo I mediado por la señalización dependiente de MyD88 y TRIF. El papel de la señalización TRIF-IFN-β en la respuesta inflamatoria inducida por TLR2 fue estudiado y los resultados descritos en el capítulo 2 indican que la activación de TLR2 lleva a una producción de IFN-β, dependiente de la internalización del receptor, lo que activa los factores de trascripción de interferón IRF3 y IRF7. La señalización por TRIF es necesaria para la inducir IFN-β y la citoquina IL-12 por la activación de TLR2. Además, TLR2 es importante para el reconocimiento de *Listeria monocytogenes*, sin embargo, modificaciones en la pared de esta bacteria evitan su reconocimiento inmunológico. La administración *in vivo* de ligandos TLR2 en un modelo murino de listeriosis neonatal disminuye la carga bacteriana en la microglía de los neonatos y su tratamiento en células dendríticas infectadas incrementa los niveles de TNF-α y IL-12, mediado por IFN-β. Por lo tanto, los ligandos TLR2 tienen un efecto modulador en los niveles de citoquinas y previenen la diseminación de la bacteria. Esto apoya el uso de ligandos TLR2 como potenciales adyuvantes en modelos de vacunas para esta bacteria.

TLR4 es conocido como el receptor de reconocimiento a los lipopolisacáridos (LPS). Sin embargo, algunos LPSs presentan una estructura distinta del bien estudiado LPS de *E. coli* y inducen respuestas inflamatorias dependientes de TLR2. Los resultados del capítulo 3 demuestran que el LPS de *Ochrobactrum intermedium* es un agonista TLR4/TLR2 y induce una respuesta inflamatoria más débil que el LPS de *E. coli*. Estudios de modelado molecular predicen que el *O. intermedium* LPS favorece la formación del heterodímero TLR2/TLR4/MD-2, que se confirmó por FRET. Esto indica que estos LPSs atípicos inducen la dimerización de TLR4 y TLR2 para evitar la detección de la bacteria por el sistema inmunológico.

INTRODUCTION

1 INTRODUCTION

The living organisms have evolved defense strategies by the immune system in order to combat the invading microbial pathogens. The immune system is classically divided into innate and adaptive systems. The innate immune system provides a first line of defense against a broad spectrum of pathogens.

Adaptive immunity confers a slower but more specific response, consisting in clonal expansion of antigen-specific cells that combat the infection and provide immunological memory.

1.1 Pattern recognition receptors

Macrophages, dendritic cells and neutrophils provide a first line of defense against many common microorganisms and are essential for the control of common bacterial and viral infections (Akira and Takeda, 2004b). These cells are able to discriminate between "self" and pathogens through the function of pattern recognition receptors (PRRs). PPRs can sense a pathogen infection by recognizing conserved pathogen-associated molecular patterns (PAMPs) (Charles A. Janeway, 2002). PRR-mediated recognition of pathogens by phagocytes triggers the degradation of invading pathogens by their engulfment, digestion and killing, followed by initiation of a cascade of inflammatory responses. It is now evident that PRRs also recognize noninfectious components that can cause tissue damage and endogenous molecules that are released during cellular injury, often termed as damage-associated molecular patterns (DAMPs) (Matzinger, 1994). Examples of DAMPs are the associated protein high-mobility group box 1(HMGB1), heat shock proteins (HSPs), purine metabolites derived from necrotic cells, as well as extracellular matrix fragments such as hyaluronan and biglycan generated by proteolytic enzymes from damaged cells. These endogenous stress signals once released play a similar role as PAMPs regarding their ability to activate inflammatory signaling pathways.

To date, four classes of PRRs families have been identified and characterized. These families consist of cytosolic PRRs such as the (NOD)-like receptors (NLRs) and RIG-I-like receptors (RLRs), as well as transmembrane proteins such as the Toll like receptors (TLRs) and C-type lectin receptors (CLRs). The RLR family consists of RNA helicases that detect viral double-stranded RNA. Activation of RLRs induce an antiviral response through the recruitment of the adapter protein IFN-β promoter stimulator (IPS)-1, the activation of the transcription factors interferon regulatory factor IRF3 and NF-κB, and subsequent induction of type I IFN. The NLR family consists of more than 20 members, and several respond to the various PAMPs, non-PAMP particles and cellular stresses. Upon recognition of ligands, this receptors trigger the production of pro-inflammatory cytokines, including the activation of the multiprotein-complex, the inflammasome, with consequent secretion of IL-1β and IL-18 (Kumar et al., 2011).

1.2 Toll-like receptors

Charles Janeway predicted in 1989 the existence of innate immunity PRRs able to recognize microbial products and link innate and adaptive immunity.

The discovery of TLRs began in the 1980s with the identification of the protein receptor IL-1R1. IL-1 is a pro inflammatory cytokine and it was reported to be an essential mediator of host defense (Dinarello, 1991) In 1991, the IL-1R1 cytosolic domain sequence was shown to be homologous to the cytosolic domain of a protein termed Toll, found in *Drosophila melanogaster*. Toll protein was initially identified as a gene product essential for the development of embryonic dorsoventral polarity in *Drosophila*. Subsequent studies showed that Toll was an important receptor for host defense against fungal infection in flies, which only have innate immunity (Lemaitre et al., 1996).

In 1997, the first human homolog of the Toll receptor was cloned (now termed TLR4) and showed the induction of gene's expression involved in inflammatory response (Medzhitov et al., 1997). In the next two years, a loss-of-function mutation of the mouse homologue of hToll was identified in a mouse strain that is unresponsive to lipopolysaccharide, revealing hToll as the signaling receptor for the bacterial LPS(Hoshino et al., 1999). Shizuo Akira and colleagues, who generated multiple TLR and adaptor molecule-knockout mice, have later contributed considerably to revealing the functions of the other TLRs and which specific ligands are recognized by each TLR (Akira and Takeda, 2004a; Shizuo Akira, 2006).

1.3 Macrophage phenotypes: host defense, wound healing and immune regulation

The recognition of microbes by TLRs is thought to follow a model, in which immune cells use different TLRs to detect several PAMPs, from different classes of microbes, simultaneously. This elicits different responses that are required to efficiently combat the pathogens present in the host (Underhill and Ozinsky, 2002). Triggering TLRs with distinct PAMPs induce the release of different patterns of cytokines and chemokines by macrophages, which drive these cells to assume different phenotypes and functions. Basically, macrophages can polarize in three distinct phenotypes (Sica and Mantovani, 2012). Microbial products such as LPS and pro-inflammatory cytokines (IFN-γ, TNF) confer a M1 type macrophage, that have enhanced microbicidal and capacity to secrete high levels of IL-12, IL-6, IL-23, TNF-α, iNOS and ROS species. M2-type macrophages are induced by signals such as glucocorticoids, DAMPs, IL-4, IL-13, and IL-10 and even by helminths-derived PAMPs. This class of macrophages is involved in parasite containment and promotion of tissue repair, through induction of arginase 1, IL-10 and PPRγ. The third class, termed regulatory macrophages have an anti-inflammatory activity. Two stimuli are needed to induce IL-10 production, for example, prostaglandins, glucocorticoids or adenosine with TLR ligands (Mosser and Edwards, 2008). Moreover, regulatory

macrophages can also downregulate IL-12 production. Therefore, IL-10/IL-12 can be used to define these class of macrophages.

1.4 TLR family

TLRs are expressed in many cell types, including macrophages, DCs, B cells, some types of T cells and even in non-immune cells such as fibroblasts, epithelial and endothelial cells. The expression of these receptors is dynamic, changing rapidly in response to pathogens, DAMPs and environmental stresses. The TLRs are type I transmembrane proteins, and due to the considerable homology in the cytoplasmic region, they are members of a larger superfamily that includes the interleukin-1 receptors. TLRs are composed of three major regions: the cytoplasmic, transmembrane and extracellular domain (Fig. I1). These structures belong to the leucine-rich repeat (LRR) family and form characteristic, horseshoe-like structures. As the cytoplasmic domain of TLRs shows high homology to that of the IL-1 receptor family, this domain is termed as Toll/IL-1 receptor (TIR) domain. The extracellular domain of TLRs contains 16 to 28 tandem copies of a consensus sequence leucine-rich repeat (LRR modules). This motifs mediate the recognition of PAMPs (Bell et al., 2003).

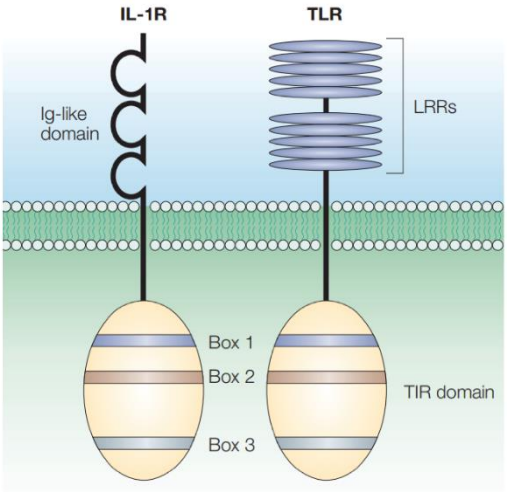

Fig. I1 TLR structure. The intracellular TIR domain is composed of ~200 amino acids in length, and the regions of homology comprise three conserved boxes, which are required for initiating downstream signaling pathways. The extracellular domain harbors tandem copies of LRR. These modules include highly conserved segment, LxxLxLxxNxL, in which "L" is Leu, Ile, Val, or Phe and "N" is Asn, Thr, Ser, or Cys and "x" is any amino acid. LRRs have a secondary structure composed of a beta strand and an alpha helix connected by a looped segment (Akira and Takeda, 2004b).

So far, 10 TLR family members have been identified in humans and 12 in mice, with TLR1–TLR9 being conserved in both species. TLR10 is expressed in humans but not in mice because of a stop codon in the murine TLR10 gene. TLR11, TLR12 and TLR13 have been lost from the human genome. Toll-like receptors play a central role in detecting all types of pathogens, including viruses, bacteria, and parasites. Moreover, TLRs are localized in various cellular compartments. More specifically, TLR1,2,4,5, and 6 are mainly found in the cell plasma membrane, where they can recognize “first contact” PAMPs from bacteria, fungi and parasites. TLR3, 7, 8 and 9 are sequestered in the ER in resting cells and rapidly traffic to endolysosomes in response to nucleic acids components from viruses and bacteria (Fig. I2) (Shizuo Akira, 2006). The proper distribution of TLRs in different cellular

compartments facilitates ligand accessibility for downstream signal transduction, and the endosomal localization of nuclei-acid-sensing TLRs allows the discrimination between self from non-self-nucleic acids.

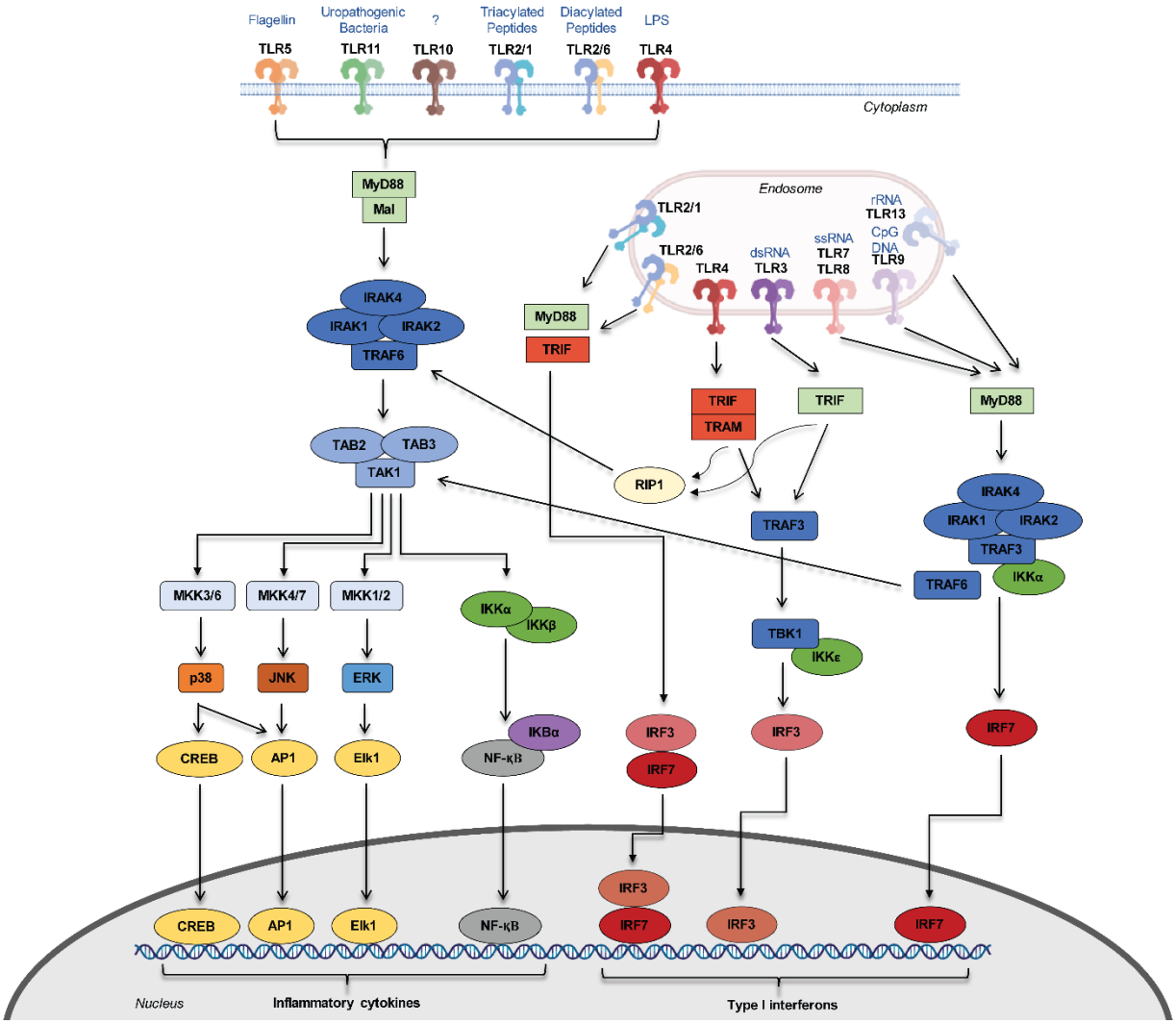

Fig.I2 TLR signaling and trafficking.

Overview of the distinct members of TLR family, their ligands and the TIR adaptors recruited upon ligand stimulation.

1.4.1 TLR2 subfamily

TLR1, TLR2, TLR6 and TLR 10 are commonly categorized into the TLR2 subfamily due to the amino acid sequence similarities and chromosomal localization. Phylogenetic analysis reveals that TLR10 is most related to TLR1 and TLR6, both of which mediate immune responses to a variety of microbial and fungal components in cooperation with TLR2. This receptor binds a wider array of ligands than any other member of the TLR family. These include lipopeptides, lipoteichoic acid from Gram-positive bacteria, lipoarabinomannan from mycobacteria, zymosan from fungi, tGPI-mucin from *Trypanosoma cruzi* and the hemagglutinin protein from measles virus (Shizuo Akira, 2006). TLR2 initiates immune

responses by recognizing diacylated and triacylated lipopeptides and the discrimination of the lipid portion of lipoproteins is controlled by whether TLR2 heterodimerizes with TLR1 or TLR6. Specifically, the TLR2/TLR1 heterodimer recognizes triacylated lipopeptides, whereas the TLR2/TLR6 heterodimer recognizes diacylated lipopeptides. In addition, TLR2-deficient (TLR2-/-) mice, which were found to be highly susceptible to challenge with Staphylococcus aureus or Streptococcus pneumoniae demonstrating the importance of TLR2 in the host defense against Gram-positive bacteria (Echchannaoui et al., 2002). Besides infectious diseases, TLR2 is also implicated in pathologic conditions such as rheumatoid arthritis, ischemia/ reperfusion injury, and allergy (O'Neill et al., 2009).

TLR10 is the only family member without a defined agonist or function, however recent studies have shown that TLR10 share some agonists with TLR1 like Pam3CSK4. Similar to TLR1 and TLR6, TLR10 also requires heterodimerization with TLR2 for the recognition of these agonists as well as microbial and fungi components. Nevertheless, TLR10 is not able to activate the downstream signaling mediators that are commonly associated with the TLR1 or TLR6 members (Guan et al., 2010). It is reported that hTLR10 transgenic mice exposed to TLR2 ligands produce fewer cytokines in vivo. TLR10 functions as an inhibitory receptor, exerting a modulatory effect in the TLR2-mediated cytokine production (Oosting et al., 2014). Indeed, TLR10 is the only member of the TLR family described so far as an inhibitory receptor.

TLR2 has been shown to functionally collaborate with other types of receptors such as dectin-1, a lectin family receptor that recognizes the fungal cell wall component β-glucan and zymosan, inducing its internalization. Moreover, TLR2 can interact with other co-receptors on the cell surface that assist PAMP recognition. These include CD36, which enhances immune responses to some TLR2/TLR6 ligands. The co-receptor CD14 is involved in the recognition of diacylated lipopeptide and lipoarabinomannan. (Gantner et al., 2003; Hoebe et al., 2005).

1.4.2 TLR4

TLR4 was the first TLR identified and was characterized as an LPS receptor through studies of two mouse strains, C3H/HeJ strain and C57BL/10ScCr that were nonresponsive to LPS. LPS, is a major constituent of the outer membrane of Gram-negative bacteria and is mostly present with six acyl chains, like *E. coli* LPS, which is one of the most potent agonists of the human innate immune system. LPS consists of three distinct domains: the lipid A composed by fatty acid chains linked to a disaccharide backbone; a core saccharide and the O-antigen that render LPS solubility. The core can be composed of up to 15 sugars and be identified as inner and outer core. Inner core is less variable, usually formed by 3-deoxy-d-manno-oct-ulosonic acid (KDO) sugars. In contrast, the outer core is more variable since it can comprise common residues such mannoses, heptoses, galactoses or distinct sugars, depending of

the bacterium strain. The O-antigen is the hydrophilic region of the LPS and strain-specific. It is usually composed of up to 50 repeating oligosaccharide units, with different kinds of monosaccharides, projected from the core towards the exterior of the bacterial surface (Silipo and Molinaro, 2010).

Accessory molecules such as LBP, CD14 are involved in LPS signaling, enhancing the TLR4 sensitivity to recognize LPS in minute concentrations (Haziot et al., 1996). LBP, which belongs to the lipid-binding/lipid transfer protein family, forms a high-affinity complex with LPS that is subsequently delivered to CD14. CD14 is present in the plasma membrane on myeloid cells or in a soluble form in the serum. It contains a hydrophobic pocket that comprises LPS FA chains. This protein delivers LPS to MD-2, a co-receptor associated with TLR4. In basal conditions, TLR4-MD-2 complex exist as monomers in the cell membrane. When LPS binds to MD-2, it induces the interaction of two monomers forming a TLR4/MD-2/TLR4*/MD-2* homodimer. This interaction promotes the dimerization of the intracellular domains, which leads to the activation of downstream signaling pathways and final immune response. It has been described that TLR4 is in constant translocation between Golgi complex and the cell surface to replenish its levels at the cell surface TLR4 for LPS recognition (Latz et al., 2002). In order to be transported to the surface, TLR4 needs to be glycosylated (Nagai et al., 2002). Alternatively, TLR4 can be translocated to endosomal compartments capable of recognizing phagocytosed bacteria. Upon receptor activation at the surface, the receptor is endocytosed, and activates TRIF signaling (Fig. I2). Endosomes mature into late endosomes and fuse with lysosomes where the receptor is degraded.

1.4.3 TLR9 subfamily

TLR7, TLR8 and TLR9 constitute the TLR9 subfamily, due to their high gene homology to each other. These receptors recognize nucleic acids derived from viruses and bacteria, as well as endogenous nucleic acids in pathological conditions. The activation of these receptors occurs by trafficking from the ER to the endolysosomes, where proteolytical cleavage generates functionally competent receptors. Thus, viral nucleic acids are efficiently recognized in these compartments, avoiding the activation by self-nucleic acids. TLR7 recognizes ssRNA derived from viruses such as vesicular stomatitis virus, influenza A and HIV-1 genomic RNA as well as from the host (Diebold et al., 2004). TLR7 also detects RNAs from bacteria such as Group B *Streptococcus* in endolysosomes in conventional DCs (cDCs) (Mancuso et al., 2009). TLR8 is phylogenetically more similar to TLR7 and recognizes viral ssRNA, however, although it is expressed in mice, it appears to be nonfunctional (Heil et al., 2004). TLR9 senses CpG DNA motifs from bacterial DNA and viral dsDNA such as herpes simplex virus (HSV) and oligonumerine cytomegalovirus (MCMV) (Hemmi et al., 2000).

1.4.4 TLR3

TLR3 recognizes genomic RNA purified from dsRNA viruses such as reovirus and dsRNA produced during the course of replication of single-stranded RNA (ssRNA) viruses such as RSV, encephalomyocarditis virus (EMCV) and West Nile virus (Alexopoulou et al., 2001; Wang et al., 2004). TLR3 triggers immune responses by producing type I IFN and inflammatory cytokines to prevent viral spread. TLR3 also recognizes viral dsRNA synthetic analog polyI:C. Noteworthy, the recognition mechanism of nucleic acids by TLR3 was clarified by solving and analyzing the crystal structure of hTLR3 ectodomain (Bell et al., 2005; Choe et al., 2005; Liu et al., 2008). The horseshoe-like shape of the receptor comprises a large surface area to facilitate dsRNA recognition. The ligand binds to the N-terminal and C-terminal portions of TLR3 ectodomain stabilizing the formation of a TLR3 homodimer. TLR3 deficiency in humans is associated with susceptibility to herpes simplex virus (HSV)-1 and TLR3-deficient mice are susceptible to infection with murine cytomegalovirus (MCMV) (Tabeta et al., 2004; Zhang et al., 2007). TLR3 is present in conventional DCs, macrophages as well as in epithelial cells.

1.4.5 TLR5

TLR5 recognizes flagellin, the major constituent of bacteria flagella and is a potent activator of innate immune responses. TLR5 is highly expressed on the basolateral surface of intestinal epithelial cells, sensing the invasion of flagellated bacteria in the gut. In addition, TLR5 is highly expressed in lamina propria DCs (LPDCs), in the small intestine. Specifically, in the presence of flagellin, LPDCs induce the differentiation of naïve B cells into IgA-producing plasma cells and promote the differentiation of naïve T cells into Th17 and Th1 cells (Uematsu et al., 2008). Moreover, lamina propria DCs can produce retinoic acid that contribute for these humoral and cellular responses. Thus, LPDCs plays a critical role in regulating both innate and adaptive immune response in the intestine through TLR5. Moreover, TLR5 is present in lung epithelial cells, protecting the respiratory tract from flagellated bacteria. Indeed, a polymorphism in the ligand binding site of TLR5 compromises the TLR5-driven signaling and is associated with susceptibility to pneumonia, caused by *L. pneumophila*, a flagellated bacterium (Hawn et al., 2003). Thus, these findings indicate the important role of TLR5 in microbial recognition at the mucosal surface.

1.4.6 TLR11, 12, 13 subfamily

TLR11 is present in mice but not in humans and is localized in endolysosomes and is highly expressed in the kidney and bladder epithelial cells. TLR11 senses uropathogenic bacteria, observed by TLR11-

deficient mice that were susceptible to the infection with these bacteria (Zhang et al., 2004). TLR11 also recognizes profilin-like molecule derived from the intracellular protozoan *Toxoplasma gondii*, which functions as an actin-binding protein, implicated in the parasite mobility and/or invasion (Yarovinsky et al., 2005). These findings show a role for this receptor in host recognition of protozoan pathogens.

TLR12 is an intracellular TLR and it was found to also recognize *Toxoplasma's* profilin, similar to TLR11. However, the levels of expression of each TLR differ in tissues. TLR12 expression is restricted to myeloid cells, macrophages, and lymphoid cells. TLR11 is more expressed at epithelial surfaces, though it can also be expressed in macrophages and DCs. TLR12 and TLR11 were found to heterodimerize in response to *Toxoplasma gondii* in mice to induce an optimal response towards the parasite (Andrade et al., 2013).

TLR13 is also an intracellular receptor, localized in the endolysosomes. It was identified a bacterial 23S ribosomal RNA (rRNA) sequence as a ligand for TLR13 (Hidmark et al., 2012; Oldenburg et al., 2012). TLR13 may be important for the detection of specific viruses since is able to recognize the vesicular stomatitis virus to activate innate immune antiviral responses (Shi et al., 2011).

1.5 Classical TLR signaling pathways

The interaction of TLRs with their ligands trigger the activation of signaling pathways, by promoting the dimerization of TLRs or by altering the conformation of existing dimers. This ligand-receptor engagement leads to the induction of inflammatory cytokines and type I IFNs for host defense. TLR signaling begins with the recruitment of different TIR-domain containing adaptor molecules such as MyD88, TRIF, Mal (TIRAP) and TRAM that will interact with the receptor TIR domains. Mal and TRAM adaptors bridge MyD88 and TRIF to the TIR to facilitate downstream signaling (Oshiumi et al., 2003; Yamamoto et al., 2002) (Fig. I2). MyD88 is recruited by all TLRs except TLR3 and initiate the MyD88-dependent signaling with activation of the transcription factor NF-κB and mitogen-activated protein kinases (MAPKs) to induce inflammatory cytokines in macrophages and dendritic cells. In addition to MyD88, TLR4 and TLR2 subfamily recruits TIRAP adaptor for MyD88-dependent signaling initiation but not TLR5 nor TLR 7-9 subfamily. Particularly, TLR7 and TLR9 only recruit MyD88 adaptor to induce type I IFNs via IRF7 and IRF1 transcription factors. On the other hand, TRIF is used by TLR4 and TLR3, initiating the TRIF-dependent cascade which activates NF-κB and IRF3 for the induction of inflammatory cytokines and type I IFNs (Shizuo Akira, 2006). Unlike TLR3, TLR4 recruits TRIF through TRAM mediated by endocytosis, and it has been considered the only TLR capable of activating both MyD88 and TRIF-dependent signaling pathways (Kagan et al., 2008). However, recent publications report that TLR2 can also recruit TRAM/TRIF and induce IFN-β in BMDM (Nilsen et al., 2015).

1.5.1 MyD88-dependent signaling pathway

MyD88 adaptor is important to link TLRs with the downstream signaling molecules. After association with receptor complex, MyD88 recruits and activates the kinase IRAK4. IRAK1 and IRAK2 are sequentially recruited and activated by phosphorylation forming a complex that subsequently interacts with TRAF6. This enzyme forms a complex with E2 ubiquitin-conjugating enzymes Ubc13 and Uev1A to catalyze the formation of lysine63-linked polyubiquitin chains. These chains activate the complex TAK1 that then activates the IKK complex. NF-κB inhibitory protein, IkBα is consequently phosphorylated and undergoes degradation by the ubiquitin-proteasome system, allowing nuclear translocation of NF-κB and binding to the promoters of target genes. TAK1, can simultaneously phosphorylate the MAPKKs MEK1/MEK2, MEK3/MEK6 and MEK4/MEK7 to phosphorylate MAPKs ERK1/2, p38 and JNK respectively. Besides the MAP3K TAK1, the activation of ERK1 and ERK2 is mediated by the upstream kinase TPL2 (Arthur and Ley, 2013).MAPKs are important for the induction of transcription factors such as cyclic AMP-responsive element-binding protein (CREB) and activator protein 1 (AP1) to promote the transcription of inflammatory cytokines genes (Akira, 2010).

1.5.2 TRIF-dependent signaling pathway

TRIF-dependent signaling activation leads to induction of NF-κB and IRFs. TRIF recruits TRAF6 and RIP1 to activate TAK1 via mechanisms similar to those in the MyD88-dependent pathway. However, TRIF interacts with RIP1 and undergoes K63-linked polyubiquitination. RIP1 also interacts with TRADD, and this multiprotein complex is required for NF-κB activation. Moreover, TRIF can also recruit TRAF3, which activates the noncanonical IKKs TBK1 and IKKi that induce IRF3 and IRF7 activation. Phosphorylated IRFs translocate to the nucleus and initiate the transcription of type I interferons (Fig. I2) (Akira, 2010). IRF3 and IRF7 share the greatest structural homology and have gained much attention as the key regulators of type I IFN gene expression induced by viruses. IRF3 is constitutively expressed and resides in the cytosol in the latent form in resting cells. Upon TLR activation, IRF3 is phosphorylated at Ser396, 398, 402, 404, and 405 in site 2 of the C-terminal regulatory region, which alleviates auto-inhibition and causes IRF3 nuclear translocation. Once in the nucleus, IRF3 is phosphorylated at site 1 (Ser385 or Ser386), which is required for IRF3 dimerization. IRF3 can form dimers with itself or with IRF7. These complexes bind to the promoters of type I IFN genes to facilitate their expression. Unlike IRF3, IRF7 is expressed in low amounts in unstimulated cells and is strongly induced upon stimulation. IRF7 can form a homo or heterodimers with IRF3 and each can differentially activate type I IFN. IRF3 activates more IFN-β, whereas IRF7 can activate efficiently both IFN-α and IFN-β genes (Honda et al., 2006). Once activated, IRF7 induces the type I IFN amplification loop determinant for later responses (Zhao et al., 2015).

1.6 Regulation of MAPKs: role of dual-specificity protein phosphatases

The phosphorylation state of MAPKs is controlled, among others, by dual-specificity protein phosphatases (DUSPs, also known as MKPs), which dephosphorylate both the threonine and tyrosine residues in the activation loop of MAPKs, thereby inactivating them. MKPs contain a highly conserved C-terminal catalytic domain and a less conserved N-terminal region that engages the substrate. Three major phosphatase subfamilies are classified according with their sequence similarity, substrate specificity and subcellular localization. The subfamily formed by MKP-1 (DUSP-1), PAC-1 (DUSP2), MKP-2 (DUSP4) and HVH3 (DUSP5) is primarily localized in the nuclear compartment and encoded by immediate-early genes. The second subfamily comprises MKP-3 (DUSP6), MKP-X (DUSP7) and MKP-4 (DUSP9). They are present in the cytoplasm and preferentially recognize ERK1 and ERK2 *in vitro*. HVH5 (DUSP8), MKP-5 (DUSP10) and MKP-7 (DUSP16) constitute the third subgroup as they preferentially recognize JNK and p38. Different DUSPs are expressed in different cell types even between different immune cell types. In macrophages and stimulated leucocytes high levels of MKP-1, PAC-1 and MKP-7 are found. Studies with MKP-1 KO peritoneal macrophages show that this phosphatase regulates p38 and JNK with little effect on ERK. PAC-1 have preference to dephosphorylate ERK (Liu et al., 2007). Some DUSPs including MKP-1, MKP-2, VHR (DUSP3) and MKP-X are post-translationally regulated through phosphorylation which alters their stability. It has been shown that when MKP-1 is phosphorylated by ERK the half-life of DUSP1 is increased by twofold to threefold (Brondello et al., 1999).

1.7 Role of TLR2 and NOD receptors in the recognition of *Listeria monocytogenes*

1.7.1 Listeriosis

Listeria monocytogenes is a pathogenic gram-positive bacterium responsible for foodborne illness in humans and animals, commonly designated listeriosis. The infection is originated via ingestion of contaminated food causing febrile gastroenteritis in healthy persons (Vazquez-Boland et al., 2001). The annual number of *Listeria* infection cases remains low due to the high level of resistance to the infection from immunocompetent individuals. However, listeriosis is one of the deadliest foodborne diseases and occurs mainly in high-risk groups such as elderly or immunocompromised individuals and pregnant women. The common symptoms are manifested as septicemia, when infection is spread to distinct organs and meningitis/encephalitis, when the infection invades the brain.

1.7.2 *Listeria* dissemination, virulence factors and intracellular life cycle

The first site of infection occurs in the intestine and *L. monocytogenes* stimulate DCs and resident macrophages, leading to an increase of Th1 type cytokines. Thus, immune responses are already elicited in the early stage of infection. Moreover, *L. monocytogenes* can cross the intestinal epithelium barrier through the invasion of enterocytes, specifically globet cells and M cells. The invasion of these cells requires the interaction of listeria protein surface InlA or InlB enterocyte-E-cadherin receptors (Chiba et al., 2011; Lecuit et al., 2001). After translocation *L. monocytogenes* spreads to the liver, spleen and lymph nodes. Most of the bacteria that reach the liver is cleared from the circulatory system through Kupffer cells, neutrophils, NK and DCs action. However, *L. monocytogenes* can enter in hepatocytes through internalin B that binds to hepatocyte receptors and eventually replicate. In the spleen, bacteria inactivation by resident immune cells is less efficient than in the liver, which leads to extensive bacterial replication. In the case of immunosuppressed individuals, if the infection is not controlled at this stage, listeria disseminates to secondary organs including the central nervous system (CNS) and the placenta in pregnant women. The mechanism used by the bacteria to reach the CNS is not clear, however, some evidences propose that phagocytic cells behave as "Trojan horses", transporting bacteria to the brain (Drevets, 1999). Upon crossing the blood - brain barrier, the bacteria invade and propagate in microglia cells. In the case of pregnant women, a similar mechanism is used by bacteria that is transported through maternal macrophages to trophoblast cells by cell-to-cell spread (Bakardjiev et al., 2005), This bacteria replication is enhanced by the immunosuppressive state associated to pregnancy to protect the fetus from rejection by the mother (Weinberg, 1987). Pregnancy listeriosis occurs mainly at the third trimester and can lead to different clinical symptoms, such as fetal loss, stillbirth or premature birth. Newborns can develop septicemia at the first days and later on meningitis, commonly termed neonatal listeriosis (Janakiraman, 2008)

L. monocytogenes presents several virulence factors determinant for cellular invasion, survival and multiplication. Invasion of non-phagocytic cells is induced by interaction of listeria surface internalin A with the receptor E-cadherin, and internalin B to GAG receptors and c-Met receptors, respectively. Vip, a protein anchored in the *Listeria* peptidoglycan (PGN) and the endoplasmic reticulum-resident chaperone Gp96 interaction promote the bacterium invasion in cells (Cabanes et al., 2005). *Auto* protein is described to control the products released from the bacteria surface. GtcA glycosylates teichoic acids present in the bacteria cell wall contributing to *Listeria* invasion in epithelial cells (Faith et al., 2009). MprF (multiple peptide resistance factor) is implicated in the synthesis of L-PG membrane phospholipid and increases invasiveness of bacteria in epithelial cells and macrophages (Thedieck et al., 2006). Following cell invasion, *L. monocytogenes* escapes from the intracellular phagosomes through membrane lysis mediated by bacterial listeriolysin (LLO) and the phospholipases PlcA and PlcB. Once in the cytosol, *L. monocytogenes* expresses actin-assembly-inducing protein Act A that induces actin polymerization and allows bacteria movement through the cytoplasm. The internalin InlC

then regulates the passage of bacteria to neighboring cells (Pamer, 2004). In addition, *L. monocytogenes* can escape from autophagy through ActA and internalin InlK action (Cossart, 2011).
Upon dissipation of the bacteria through the bloodstream, the resident macrophages, especially Kupffer cells phagocytize the bacteria. In response to the infection, macrophages secrete TNF-α and IL-12. These cytokines induce NK cells to produce IFN-γ, which in turns activate macrophages and neutrophils to produce reactive species important for macrophage-mediated killing of bacteria.

1.7.3 *Listeria* recognition by PRRs and signal transduction

Listeria expresses several TLR ligands such as PGN, flagellin and bacterial DNA, but TLR2 appears to be the most important TLR for surface recognition of *L. monocytogenes* (Torres et al., 2004). The early response is likely dependent of the classical MyD88-pathway (Fig. I3). Once the bacterium invades macrophages and escapes from the phagosomes, NOD1 and NOD2 can recognize peptidoglycan fragments (Leber et al., 2008), leading to the induction of pro-inflammatory cytokines. In addition, *Listeria* activates the formation of the inflammasome leading to the maturation of IL-1β and IL-18 (Warren et al., 2008). On the other hand, the innate response against infection by *L. monocytogenes* includes the synthesis of type I IFNs.
Bacterial secondary messengers c-di-AMP, c-di-GMP and bacterial DNA activate the cytosolic receptor DDX41, DAI, cGas that recruit STING adaptor and transcription factors IRF3 and IRF7 to induce IFN- β (Archer et al., 2014; Burdette et al., 2011; Woodward et al., 2010). Moreover, the production of IFN-β in response to *L. monocytogenes* was found to be dependent of TLR2 in peritoneal macrophages (Aubry et al., 2012), whereas in bone marrow-derived macrophages is independent of TLRs (O'Connell et al., 2005; Stockinger et al., 2004), which indicates that specific macrophage populations have developed different recognition strategies for *Listeria*.

1.7.4 Evasion of host IFN responses by *Listeria*

Previous published data points for a detrimental role of type I IFNs to the host, during *L. monocytogenes* infection (Auerbuch et al., 2004; O'Connell et al., 2004). Type I IFNs were suggested to induce the downregulation of IFN-γ receptor and the induction of T cell apoptosis, which have a negative impact in the immune response. However, recent studies have demonstrated that type I IFNs can provide protection to the host during *Listeria* infection. Infection of mice with *L. monocytogenes* via gastrointestinal route benefited from the IFN induction in contrast of mice infected intraperitoneally (Kernbauer et al., 2013). Moreover, *L. monocytogenes* induces type I IFNs at later stages compared to the rapid responses induced by viral pathogens (Pontiroli et al., 2012). Therefore, the infection route

and the timing of host type I IFNs production in response to *Listeria* are determinant factors for an efficient control of the bacterium.

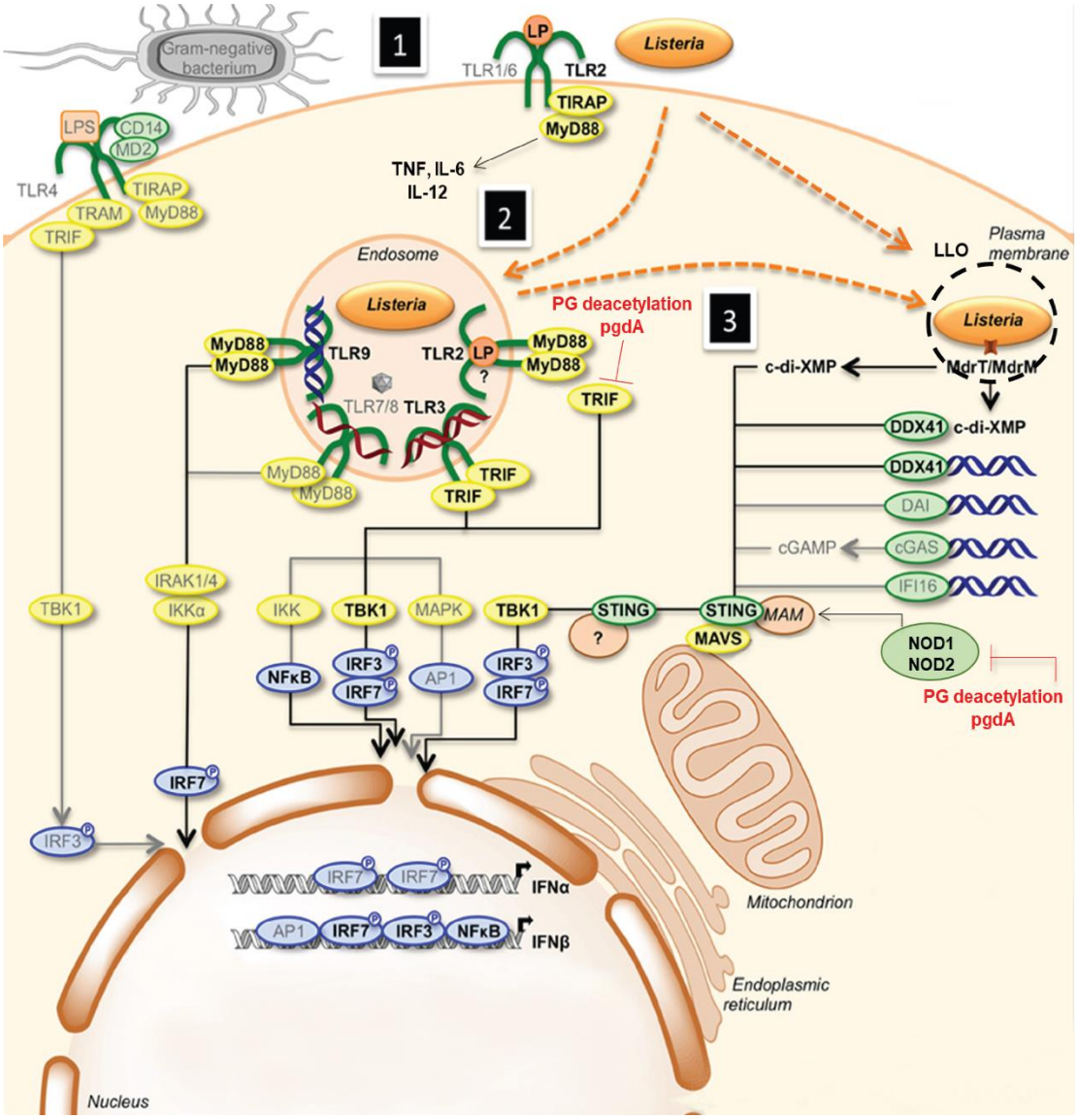

Fig. I3 Activation of extracellular TLR and cytosolic receptors in response to Listeria monocytogenes. Bacteria lipoproteins are recognized at the surface by TLR2, which induces production of inflammatory cytokines via MyD88 signaling. TLR2 is internalized and together with intracellular TLRs recognize PAMPs (lipoproteins, peptidoglycan and nucleic acids), which lead to TRIF-IRF3 and IRF7 signaling for type I IFN production. Cells infected by the bacteria release di-nucleotide and nucleic acids that activate cytosolic receptors such as DDX41, DAI, cGas and IFI16, as well as peptidoglycan recognized by NOD receptors. These receptors activate STING adaptor to promote IFN-β induction. Peptidoglycan deacetylation lows its recognition by these receptors and the bacteria evades from the immune system. Image adapted from (Dussurget et al., 2014).

L. monocytogenes has the capacity to invade and replicate in macrophages, therefore circumventing the early innate immune responses. PGN modification is another mechanism used by the bacteria to evade the host immune system. PGN is a polymer that comprises alternated residues of N-acetylglucosamine and N-acetylmuramic acid crosslinked by peptide chains. Lipoteichoic acid, tri- and

di-acylated lipoproteins are constituents of the gram-positive bacteria cell wall (Chandler and Ernst, 2017).

PGN modifications prevent the release of bacterial components, which includes PGN, and other cell wall components. However, the action of host lysozymes releases these cell wall components, which activate TLR2 as well as intracellular receptors such as NOD1 and NOD2. Indeed, previous studies demonstrated that PGN deacetylation by the deacetylase pgdA prevents its degradation by host lysozymes and the consequent release of PAMPs (lipoproteins, LTA). *Listeria* pgdA mutants were found to be hypersensitive to lysozymes and rapidly killed by macrophages, Moreover this strain induced a stronger INF-β induction and pro-inflammatory cytokines compared to the WT strain, mediated by TLR2 and NOD1 activation (Boneca et al., 2007). Further studies revealed that *Listeria* pgdA mutants require endosomal TLR2-TRIF signaling activation to induce IFN- β production (Aubry et al., 2012). Other pathogenic bacteria comprise pgdA orthologs, which suggests that PGN deacetylation is a general mechanism evolved by gram-positive bacteria to escape from PRR-mediated immune recognition (Psylinakis et al., 2005; Vollmer and Tomasz, 2000; Wang et al., 2009).

1.8 TLR4 and TLR2 structure

1.8.1 Structure of TLR2/1 and TLR2/6 complexes

Bacterial lipoproteins are mostly composed of triacylated cysteines in their N-terminal, whereas mycoplasma lipopeptides such as MALP-2 and FSL-1 contain diacylated cysteines. Studies have provided structural insights into the mechanisms by which the heterodimers TLR2/1 and TLR2/6 discriminate the structures of lipoproteins. The crystal structure of the extracellular domain of TLR2 in association with TLR1 and a synthetic triacylated lipopeptide, Pam3CSK4, revealed that they form M-shaped structures (Fig. I4A) (Jin et al., 2007). In the crystal structure, the lipid chains of the ligand bridge the TLRs; two of the three lipid chains are inserted into an internal hydrophobic pocket in TLR2, and the remaining amide-bound lipid chain is inserted into the narrower channel of TLR1. The crystal structure of mTLR2/TLR6 -Pam2CSK4 complex was solved (Fig. I4B) (Kang et al., 2009). Diacylated lipopeptides lack the amide-bound lipid chain, which is essential for TLR2/TLR1 response. Thus, it has higher affinity for TLR6 since its pocket contains two bulky phenylalanines at the entrance and a high hydrophobic area. Therefore, the amide-bound lipid chain of triacylated lipopeptides is not able to interact with TLR6. Modeling of TLR10/TLR2 lipopeptide complex reveals structural similarity to the solved crystal structure TLR2/1/lipopeptide complex. Similar to TLR1, the model predicts a hydrophobic channel on the convex surface of TLR10 that accommodates the amide-linked lipid chain of the Pam3CSK4 lipopeptide (Guan et al., 2010).

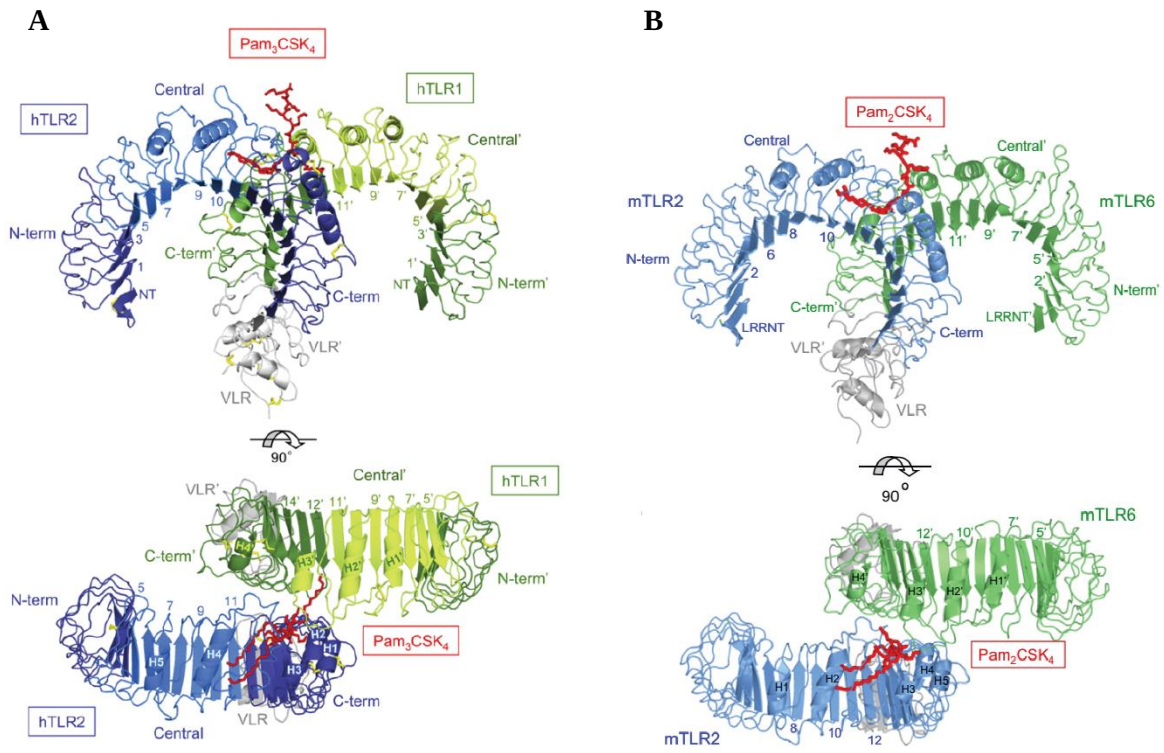

Fig. I4 Overall structure in side and top view of **A)** human TLR1/TLR2/Pam3CSK4 complex and **B)** mouse TLR6/TLR2/ Pam2CSK4 complex. Ligands are displayed in red. Each TLR structure represents the three domains: N-terminal, central domains and C-terminal (Jin et al., 2007; Kang et al., 2009).

1.8.2 TLR4/MD-2/LPS complex crystal structure

The crystal structure of TLR4/MD-2 receptor with *E. coli* LPS indicates the formation of an M-shaped structure made up of two molecules of TLR4 and two molecules of MD-2 (Park et al., 2009). *E. coli* LPS lipid A contains a β (1→ 6) linked phosphorylated glucosamine disaccharide backbone and C12 and C14 acyl chains there are directly linked to the disaccharide, and the secondary acyl chains are esterified with the hydroxyl groups of primary acyl chains (Fig. I5A). *E. coli* lipid A is accommodated in the MD-2 pocket such that five of six acyl chains are buried inside the pocket and the sixth chain is exposed to the surface of MD-2 (Fig. I5B). MD-2 pocket size is unchanged and the additional space for lipid binding is generated by glucosamine backbone displacement upwards. The two phosphates of this backbone are important for dimerization, through interaction with positively charged lysine and arginine residues in TLR4, TLR4*, and at the entrance of MD-2 pocket (e.g. Lys91, Ser118, Ser120 and Lys122 for MD-2 and Arg264, Lys341, Tyr296 for TLR4). The exposed FA chain contributes to complete the dimerization interface, interacting with TLR4* (Gln 436). The sugars present in the inner core of *E. coli* LPS consist of three units of 3-deoxy-d-manno-2-octulosonic acid (KDO I, II, III) and three units of heptosyl-2-keto-3-deoxy-octulosonate (Hep I, II, III) which stablish hydrogen bonds with MD-2 and TLR4 (e.g., Tyr296, Asp294, Lys341 Lys122) but not with TLR4*. Thus, it is speculated

that the core has a minor role in the immunological activity of LPS. The number of acyl chains in the lipid A can affect TLR4 dimerization. In contrast to the hexaacylated *E. coli* lipid A, the tetraacylated precursor molecule, lipid IVA or the synthetic molecule Eritoran display antagonistic activity for TLR4 signaling. The crystal structures of lipid IVA or Eritoran in complex with TLR4/MD-2 were solved (Ohto et al., 2007; Ohto et al., 2012). The four-acyl lipid A is completely buried in the MD-2 pocket to fill the empty space and cannot promote the hydrophobic dimerization at the surface. This downwards shift of the lipid A greatly affects the interaction of the two phosphate groups with the positively charge groups in the MD-2 and TLR4 surface. Bacteria such as *Yersinia pestis* expresses a hexa-acyl lipid A at 28ºC, but this structure is mainly tetra-acylated at 37ºC (host temperature)(Kawahara et al., 2002). In addition, *F. tularensis* regulates lipid A acyl chain length according to temperature where at 37ªC, express a lipid A with longer acyl chains, thus attenuating TLR4 recognition (Okan and Kasper, 2013).

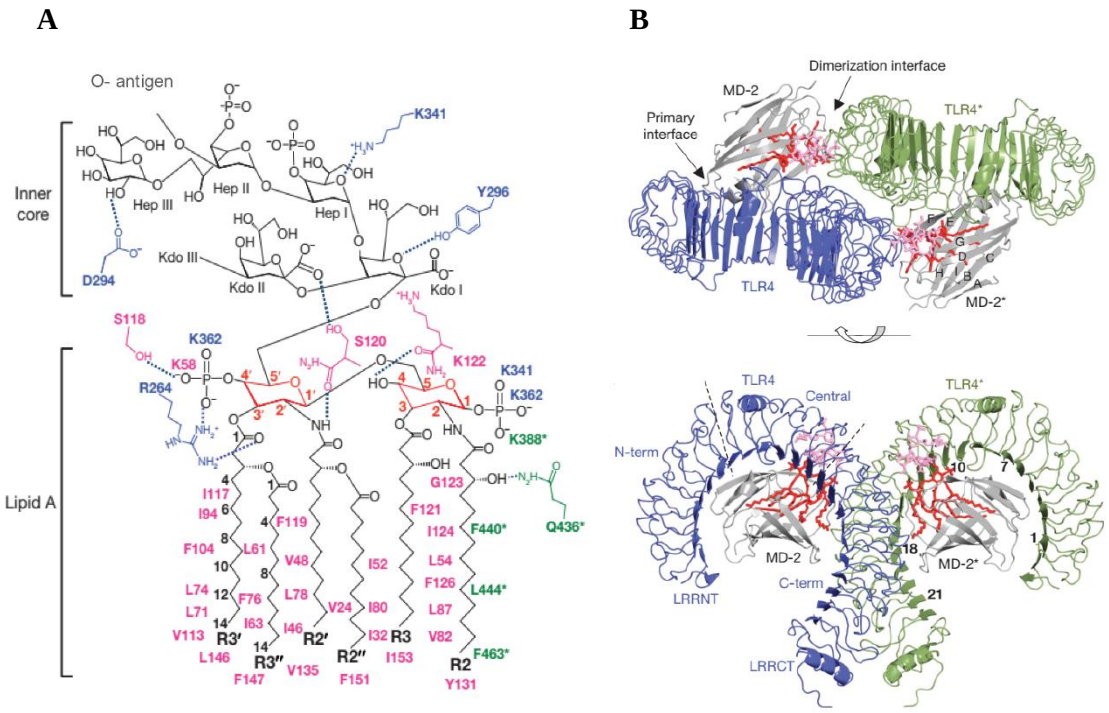

Fig. I5 A) Full *E. coli* LPS structure composed of lipid A acylated chains linked to a 1,4′-diphosphorylated β (1→6) glucosamine (GlcN) disaccharide (in red). To the lipid A is attached a core oligosaccharide and a distal O-antigen. The inner core is composed of KDOs and heptoses with phosphate residues. Hydrogen bonds with MD-2 residues are shown in pink and with TLR4 residues in blue. **B)** Full structure in side and top view of the human dimer TLR4/MD-2/*E.coli* LPS. The lipid A component of *E. coli* LPS is coloured red, and the inner core carbohydrates of the LPS are coloured pink (Park et al., 2009).

Besides the number of acyl chains, the number of phosphate groups is another bacterial strategy to low recognition by the immune system. *Francisella tularensis* lack one phosphate group in one of the

backbone sugars and is considered to contribute for its weak TLR4 agonistic activity (Molinaro et al., 2015). *Porphyromonas gingivalis* can harbor different lipid A species, from non-phosphorylated to mono or di-phosphorylated and penta- and tetra-acylated structures, depending on the temperature. At 37 º C, tetra-acylated non-phosphorylated lipid A is predominant. Thus, the number of acyl chains and phosphates groups in the lipid A greatly influence TLR4/MD-2 dimerization and the consequent host immune response.

1.9 Atypical LPS recognition by TLR2 receptor

Several studies have highlighted that the biological activity of some LPSs is not restricted to TLR4. Indeed *Leptospira interrogans, Legionella pneumophila and Rhizobium* species sin-1 LPSs induce TLR2-mediated inflammatory responses in immune cells (Burns et al., 2010; Girard et al., 2003; Hirschfeld et al., 2001; Werts et al., 2001). These LPSs, typically termed non-classical LPSs show a different structure and composition compared with the classical enterobacterial-type LPSs. These LPSs contain a diaminoglucose disaccharide backbone and at least one very long fatty acid chain (VLCFAs) in the lipid A domain. α-Proteobacteria like *Brucella* and *Ochrobactrum* express this type of LPS (Fig. I6A). *Brucella* is an animal pathogen and evolved a stealthy strategy to avoid innate immunity recognition. In contrast, *Ochrobactrum* is a soil-living organism but is another opportunistic bacterium and phylogenetically is the closest member to *Brucella*. Both bacteria express LPSs with a similar lipid A but distinct core saccharide and O-antigen. The lipid A comprises six acyl chains in amide linkages and include a VLCFA with 28 carbons (Lapaque et al., 2006). The N-linked fatty acyl chains role in the low endotoxicity of these LPSs is not clear. It is speculated that provides more stability to the outer membrane at elevated temperatures and extreme pH due to the greater bond strength (Trent et al., 2006). *Ochrobactrum* LPS contains a core with two KDO molecules, a side branch composed of Man*p* and Glc*p*N residues. The KDO II connects the lipid A to the O-antigen followed by a Gal*p* and Glc*p* sugars (Fig. 6A). On the other hand, *Brucella* LPS harbors a core saccharide with a larger side branch comprising four Glc*p*N residues and the other branch contains a Glc*p* linked to KDO II (Barquero-Calvo et al., 2009; Fontana et al., 2016). *Ochrobactrum intermedium* LPS showed immunostimulant properties for prevention and treatment of sepsis, as well as adjuvant for vaccines in immunosuppressed animals (Ovejero Guisasola, 2012). This LPS contains a hexaacyl-lipid A made of a diaminoglucose disaccharide backbone and two very long FA chains (VLCFAs) with 19 and 28 carbons (Fig. I6B).

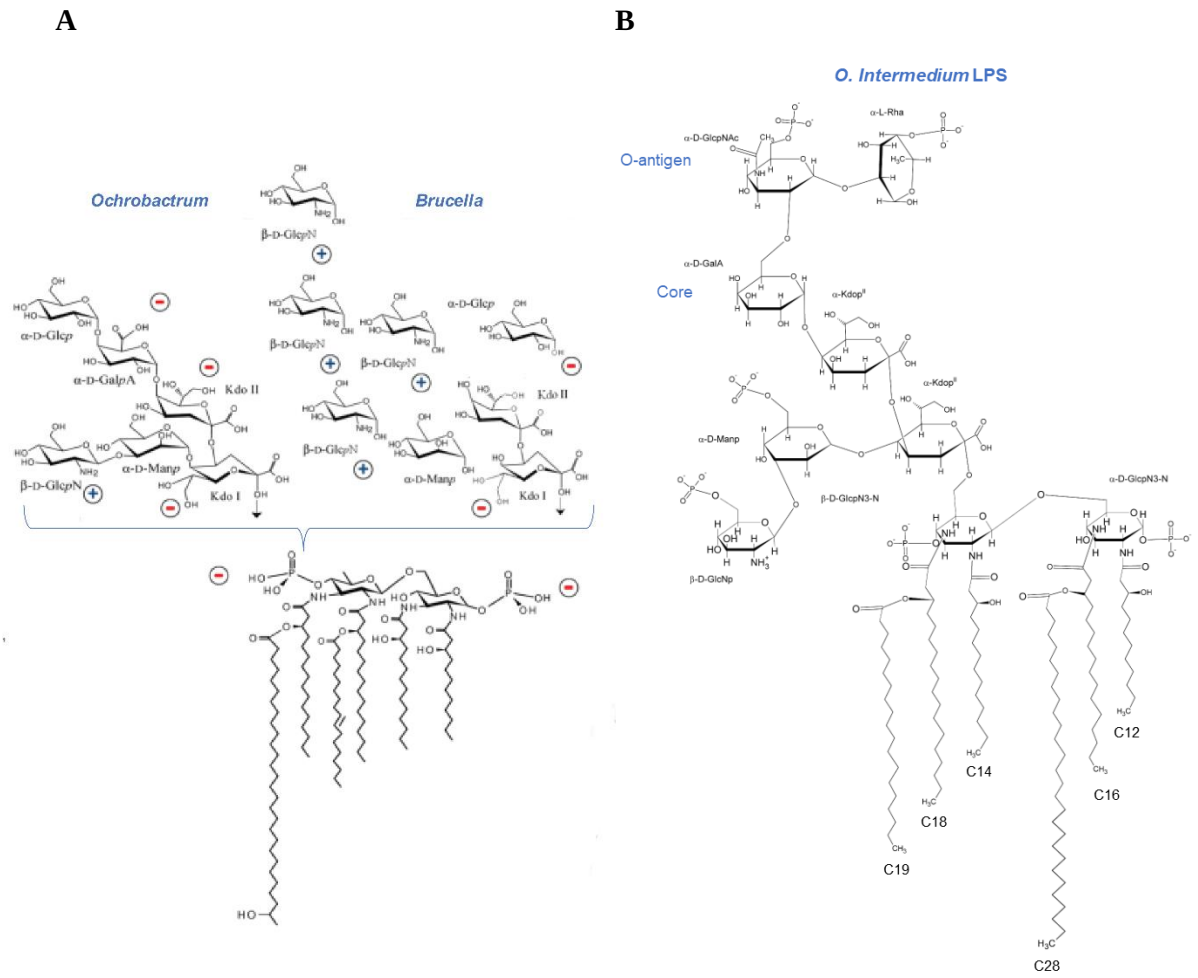

Fig. I6 Structure model of **A)** *Ochrobactrum* and *Brucella* lipid A and core saccharide portion (adapted from (Barquero-Calvo et al., 2009). **B)** *Ochrobactrum intermedium* LPS. The lipid A is composed of a linked 2,3-diamino-2,3-dideoxyglucose backbone with two phosphate groups and four fatty acid chains attached, carrying two radical groups (C19 and C28 chains). The core oligosaccharide is composed of two KDO molecules, glucosamines, mannose and galactose

Similar to *O. anthropi*, the *O. intermedium* core comprises a Man*p* and Glc*p*N but both contain a phosphate group. However, the O-antigen core branch contains sugars such as acetylated Glc*p*N and rhamnose. This core composition departs from the typical heptose sugar repetitions observed in *E. coli* core (Brooke and Valvano, 1996; Velasco et al., 2000). The presence of these VLCFAs and a diverse sugar core reduce the reactivity of these LPSs. This was observed previously, where cell stimulation with high concentrations of *Brucella* LPS, induced a weak final response (Barquero-Calvo et al., 2009; Duenas et al., 2004).

It was previously demonstrated cytoplasmic TLR2-TLR4 binding through enzyme complementation assays (Lee et al., 2004). Moreover, other study have highlighted that TLR2 is required along with TLR4 for the response to gram-negative bacterial LPS, and involves a physical interaction between TLR2 and TLR4 in cells from renal tubules (Good et al., 2012). This supports the concept of TLR4 and TLR2 heterodimers formation, depending of the ligand.

AIM OF STUDY

2 AIM OF STUDY

The overall aim of this study was to increase our understanding of TLR2 signaling, receptor dimerization and inflammatory response pattern compared to TLR4 signaling. Understanding TLR2 biology and function is important, as these receptors can be targets for immune modulating compounds against certain bacterial infections.

In this study, the objectives were as follows:

1. Study the differential signaling in response to TLR2 and TLR4 ligands and the consequence in the final inflammatory response;
2. Determine the role of TRIF signaling in TLR2-mediated inflammatory response and the effect of TLR2 ligands in the prevention of the gram-positive bacteria *Listeria monocytogenes;*
3. Address the ability of the atypical *Ochrobactrum intermedium* LPS to induce the heterodimerization of TLR4 and TLR2 receptors.

MATERIALS AND METHODS

3 MATERIALS AND METHODS

3.1 Materials

3.1.1 Reagents

Name	Reference	Commercial House
E. coli LPS	L8274	Sigma
Pam3CSK4	tlrl-pms	InvivoGen
FSL-1	tlrl-fsl	InvivoGen
Ochrobactrum intermedium LPS	patent WO2010/139352	
PD98059	BML-EI360-0005	Enzo Life Sciences
PKC_{ζ} inhibitor	BML-P219-0500	Enzo Life Sciences
U0126	19-147	Merck Milipore
SB203580	152121-47-6	Cayman
SB239063	S0569	Merck
FR180204	SML0320	Merck
5Z-7-oxozeaenol	66018-38-0	Calbiochem
Manumycin A	52665-74-4	Calbiochem
Dynasore	D7693	Merck
Chlorpromazine	C8138	Merck
Chloroquine	C6628	Merck
Recombinant mouse IFN-β	8234-MB-010	R&D systems
Anti-mouse IFN-β	32400-1	PBL assay Science
Recombinant murine GM-CSF	315-03	Peprotech
Metafectene Pro	T040	Biontex

3.1.2 Antibodies

Name	Reference	Commercial house	Application
IκBα	9242	Cell Signaling	WB
p38	9212	Cell Signaling	WB
pp38 (Thr180/Tyr182)	9211	Cell Signaling	WB
ERK1/2	9102	Cell Signaling	WB
pERK1/2 (Thr202/Tyr204)	9101	Cell Signaling	WB
MKP1 V-15	sc-1199	Santa Cruz Biotechnology	WB
IRF3	4302	Cell Signaling	WB
pIRF3 (Ser396)	4947	Cell Signaling	WB
IRF7	ab109225	Abcam	WB
pIRF7 (Ser437/438)	24129	Cell signaling	WB
β-actin	sc-47778	Santa Cruz Biotechnology	WB
TLR2 CD282 T2.5	121802	Biolegend	FACS/IF
TLR4	Ab13556	Abcam	FACS
F4/80	12-4801-80	eBioscience	FACS
CD16/CD32 Fc block	553142	BD Biosciences	FACS
Anti-rabbit Alexa Fluor 647	A-31573	ThermoFisher	FACS
Anti-mouse Alexa Fluor 647	A-31571	ThermoFisher	FACS
Anti-mouse Alexa Fluor 555	A-31570	ThermoFisher	IF
DAPI	268298	Merck	IF
Prolong Glass Anti-fade	P-36982	ThermoFisher	IF
Anti CD11b MicroBeads	130-049-601	Miltenyi Biotec	MACS

3.1.3 Primers for quantitative real-time PCR

Gene	Primer Sequence (5`→3`)
TNF-α	F: CCACCACGCTCTTCTGTCTAC R: AGGGTCTGGGCCATAGAACT
IL-1β	F: TGTGAAATGCCACCTTTTGA R: GGTCAAAGGTTTGGAAGCAG
IL-6	F: TGATGCACTTGCAGAAAACA R: ACCAGAGGAAATTTTCAATAGGC
IL-10	F: ATCGATTTCTCCCCTGTGAA R: TGTCAAATTCATTCATGGCCT
IL-12p40	F: TGGTTGCCATCGTTTTCCTG R: ACAGGTGAGGTTCACTGTTTCT
iNOS	F: TGAAGAAAACCCCTTGTGCT R: TTCTGTGCTGTCCCAGTGAG
ARG1	F: AGAGATTATCGGAGCGCCTT R: TTTTTCCAGCAGACCAGCTT
MKP-1	F: CTACCAGTACAAGAGCATCCC R: AACTCAAAGGCCTCGTCCAG
IFN-β	F: AACCTCACCTACAGGGCGGACTTCA R: CCCACGTCAATCTTTCCTCTTGCTTT
ifit1	F: GTCAACTGTGAGTGCTTCCATCC R: TCAGGGCAGAAAAGTCAAGGC
GAPDH	F: AGGTCGGTGTGAACGGATTTG R: TGTAGACCATGTAGTTGAGGTCA
RPL13A	F: ATCCCTCCACCCTATGACAA R: GCCCCAGGTAAGCAAACTT

3.1.4 Cell lines

The murine macrophage cell line RAW264.7 was cultured in RPMI 1640 medium (Gibco) (2mM L-glutamine, antibiotics), supplemented with 5% FBS. Cells were cultured in 12-well plates for protein or in 6-well plates for RNA and serum deprived for 18 hours prior stimulation. HEK293T were cultured in DMEM (Gibco) (2mM glutamine, 2mM AANE, antibiotics) with 5% FBS.

3.1.5 Mice

C57BL/6 female mice, TLR2, TLR4 and TLR2/4 KO mice were obtained from S. Akira. All mice were bred and maintained in the animal facilities of the Centro de Biologia Molecular Severo Ochoa in Universidad Autonoma de Madrid. All animal procedures were performed according to the European and Spanish regulations.

3.2 Methods

3.2.1 Ligands and inhibitors preparation

Pure TLR4 ligand LPS, synthetic TLR2/1 ligand Pam3CSK4 and TLR2/6 ligand FSL-1 were resuspended in sterile PBS 1x and added to the culture medium to the indicated concentrations.
Inhibitors were dissolved in DMSO and added to the culture medium at the indicated concentrations (DMSO final concentration at 0,1%).

3.2.2 *In vivo* model of neonatal listeriosis

Pregnant C57BL/6 female mice were infected with bacterial suspensions of Listeria in PBS (10000 CFUs/mL) by intravenously injection at 11 days of gestation (infected mother´s group). FSL-1 was administrated (10ug/Kg) at the same time as the infection in pregnant mice (infected and treated mothers' group). A control group consisted in mice injected only with PBS (non-infected group). 4 days after birth, neonates from infected and infected and treated mothers were sacrificed to obtain the brain for CFU measurement and for isolation of primary microglia cells for cytokine quantification. The neonate´s liver and spleen were also harvested for CFU measurement. Mothers from control, infected and infected and treated group were sacrificed to isolate the liver and spleen for bacteria load quantification and blood sera was extracted for cytokine measurement. Organs were homogenized by mechanical disruption in a 70µM strainer. Serial dilutions of the homogenates were plated on BHI agar plates and colonies were counted after overnight incubation at 37ºC.

3.2.3 Microglia isolation by MACS

Microglia cells were obtained from neonate brains with 4-days. The brains were homogenized and the obtained cells are incubated with an antibody against CD11b coupled to magnetic beads for 15 min at

4ºC. Microglia cells are finally isolated by magnetic separation and cultured for further supernatant collection.

3.2.4 Isolation of primary macrophages

3.2.4.1 Isolation of mouse peritoneal macrophages

Peritoneal macrophages (PM) were isolated from 6-8-week-old pathogen-free mice. Briefly, mice were injected intraperitoneally 1 mL of 4% thioglycollate. Four days later, cells were harvested by peritoneal lavage with cold PBS. Cells were recovered by centrifugation and cultured in RPMI 1640 (2mM L-glutamine, antibiotics) with 5% FBS. Cells were seeded into 12 or 6-well-pates at a density of 1 x 10^6 cells/well. Cells were allowed to adhere for 2 h and then the medium was changed to remove non-adherent cells. After 24 h, medium was replaced with new complete medium before the respective treatment.

3.2.4.2 Isolation of mouse bone marrow-derived macrophages and dendritic cells

Bone-marrow cells were isolated from femurs of female 6-8-week-old mice and collected in ice cold PBS. Bones were flushed with RPMI 1640 (2mM L-glutamine, antibiotics) supplemented with 5% FBS. These cells were cultured in 6-well plates with medium + 20% L929 supernatants (a source of M-CSF) to differentiate in macrophages or with GM-CSF to differentiate in dendritic cells until day 7, where a homogeneous population of adherent macrophages was obtained. Cells were then deprived of L929 supernatants or GM-CSF for 2 h before carrying out the stimulation assays. MKP-1 and TRIF KO macrophages were obtained from a collaboration with Rosario Perona(xx) and Gloria Gonzalez-Aseguinolaza respectively (Center for Applied Research, Pamplona, Spain).

3.2.5 Mouse dendritic cell's infection assay

DC's were cultured in RPMI 1640 with 5% FBS. After 7 days of differentiation DC' s were infected with Listeria at a MOI 1:10 (cells/bacteria), centrifuged 5min at 700g for bacteria infection synchronization, followed by incubation at 37ºC for 15 min. Following phagocytosis, cells were washed and incubated in 5% FBS/RPMI medium with gentamicin (30ug/mL) for 45 min, to kill non-internalized extracellular bacteria. After infection, cells were treated with the different ligands and supernatants were collected after 6 and 24 hours of treatment for cytokine detection by ELISA. Cells

were lysed in 0.2% Triton X-100 at 24 hours, and the number of viable bacteria released from the cells was assessed after serial dilutions of the lysates on BHI agar plates.

3.2.6 Real-time quantitative PCR

Total cellular RNA was isolated using NZyol Reagent (NZYTech). cDNA was prepared by reverse transcription (GoTaq 2-Step RT-qPCR System, Promega) and amplified by PCR using SYBR® Green PCR Master Mix and ABI Prism 7900HT sequence detection system (Applied Biosystems) All samples were run in triplicate. All quantifications were normalized to the housekeeping genes, GADPH and RPL13A to account for the variability in the initial concentration of RNA and in the conversion efficiency of the reverse transcription reaction (ΔCT) and to values from control samples. The relative quantity (RQ) was calculated as $RQ = 2^{-\Delta\Delta CT}$

3.2.7 Enzyme-Linked Imunosorbent Assay (ELISA)

Cytokine concentration was determined for IL-10, TNF-α, IL-6 and IL2-p40 and IFN-β using ELISA kit purchased from R&D systems or CBA kit. Briefly, experimental supernatants were collected and centrifuged at 3,000 g for 5 min. Supernatants were analyzed in duplicate per manufacturers protocol.

3.2.8 Protein extraction and Western blot

Cells were washed with ice-cold PBS and solubilized in ice-cold lysis buffer (50mM Tris pH 7,5, 150 mM NaCl, 1% Triton X-100, 1mM EDTA, 10% Glycerol + Phosphatase and Protease inhibitors from Roche). Protein concentration was determined by the bicinchoninic acid (BCA) method (Pierce). Western blot analyses were performed as follows: equal protein amount (20 µg) from each cell lysate were loaded and separated on SDS 10% polyacrylamide gel and transferred to a nitrocellulose membrane (Bio-Rad). Membranes were blocked with 3% BSA for 1 h and incubated with the primary antibodies overnight. The membranes were then incubated with HPR-conjugated secondary antibodies for 1 h. The membranes where developed using ECL substrate (BioRad).

3.2.9 Fluorescence-activated cell sorting (FACS)

$3x10^5$ cells were washed with PBS and blocked with 1% BSA with CD16/CD32 Fc block antibody for 20 min at 4ºC. Cells were consequently incubated with anti-TLR2 CD282 T2.5 antibody or TLR4 antibody for 20 min (1:100). Cells were incubated with an anti-mouse or anti-rabbit secondary antibody Alexa Fluor 647 for 20 min at 4ºC. Cells were incubate with formalin 10% for 10 min and finally

ressuspended in PBS with 1% BSA. Cells were analysed in FACS Canto II, collecting 30 000 events per sample and the results were analysed in FlowJo 7.0 software.

3.2.10 Immunofluorescence

Raw 264.7 cells were plated in coverslips, into 24-well plate at seeded at density of 1 x 10^5 cells/well overnight, in RPMI 1640 (2mM L-glutamine, antibiotics) with 5% FBS. The next day, cells were stimulated with LPS, Pam3CK4 or FSL-1 for 3 mqin. Cells were washed 3 times with PBS 1x and fixed with PFA 4% for 10 min. Cells were incubated with 50 mM NH_4Cl, pH 8 for 10 min to eliminate the autofluorescence. The cells were then blocked 1% BSA for 1 hour and incubated with the primary antibodies anti-TLR2 CD282 T2.5 (1:200). Cells were further incubated with Anti-mouse Alexa Fluor 555 (1:1000) for 1 hour. Cells were consequently stained with DAPI (1: 7500). Coverslips were mounted in slides with Prolong Glass Anti-fade. The samples were observed in Zeiss LSM 710 Confocal Microscope.

3.2.11 Molecular docking

3.2.11.1 Ligands construction and preparation

The full structure of E. coli LPS was extracted from the (TLR4/MD-2/E. coli)2 complex retrieved from the Protein Data Bank (PDB) under the accession code 3FXI. The 3D structure of *Ochrobactrum intermedium* LPS was constructed using PyMOL molecular graphics (DeLano, 2002). *O. intermedium* LPS structure was then divided into fragments: IV core (fragment containing the saccharide core of the LPS), IV28 (fragment with the two fatty acid chains containing 12 and 16 carbons and the third 28 carbon acyl chain attached to C16), IV19 (fragment containing the two lipid chains with 14 and 18 carbons and the third 19 carbon lipid chain attached to C18), IV lipid A (all the lipid A part containing the two phosphorylated glucosamines and the six fatty acid chains). Cuts were introduced as hydrolysis of ether bonds, thus a hydrogen atom was added to the oxygen atom of the fragment. The full ligands and the fragments were minimized with Schrodinger Maestro software (Schrödinger, 2018) using the OPLS3 force field (Harder et al., 2016).

3.2.11.2 Construction of a TLR4/TLR2 dimer and TLR2/MD-2 monomer models

The crystal structure of hTLR2/6 dimer (2Z7X) and hTLR4 (3FXI) were retrieved from the PDB. PyMOL software was used to superimpose TLR2 to one of the TLR4 from the dimer. The final structure comprises TLR4/MD-2 dimer as found in 3FXI and TLR2 that was superimposed, the remaining atoms were deleted. The TLR2/MD-2 model was obtained by superimposition of hTLR2/6 dimer and hTLR4 dimer, deleting atoms from TLR4 and one of the MD-2. The structures went through a minimization with Amber14 (Case, 2014) under the ff14SB (Maier et al., 2015) to minimize the newly constructed TLR4/TLR2 interface.

3.2.11.3 Ligand-protein docking for full LPS and fragments

The Gasteiger charges were computed for ligands and receptors using the AutodockTools 1.5.6 software (Sanner, 1999) and non-polar hydrogens of the receptors were merged. The structure of the receptors was kept rigid whereas all ligands were set to be partially flexible considering the rotable and non-rotable bonds determined by the program. Autodock Vina (Oleg Trott, 2010) was used to perform the docking calculations. Each ligand was docked into different regions of hTLR2 monomer and hTLR2/TLR4/MD2 heterodimer complex. For all the docking boxes, the point spacing was set as 1 Å. For hTLR2, a docking was performed with the box covering the TLR2 pocket (Docking A) with a center placed between residues Phe284, Leu282 and Asn274, and a box size of 40, 36, 30 (X, Y, Z).
For hTLR2/TLR4/MD-2 heterodimer, a docking was performed in the region behind hTLR2 containing the N-terminal and central subdomains (Docking B), were the box was centered between residues Arg321, His318 and Asn290 with a size of 37, 50, 50 (X, Y, Z). Other box was set to cover the interface of TLR2 and TLR4 receptor (Docking C) with center coordinates of Lys324 (TLR4), Tyr376 (TLR2) and Asn379 (TLR2) (X, Y, Z) and size 37, 50, 50 (X, Y, Z). The docking was also performed inside the MD-2 pocket (Docking D) setting a box where the center of coordinates were Phe119 (TLR4), Ile52 (MD-2) and Ser57 (MD-2) (X, Y, Z) and size 36, 38, 50 (X, Y, Z). A docking covering the entire hTLR2/TLR4/MD-2 heterodimer was also performed (Docking E), setting a box with the center coordinates Glu321 (TLR4), Glu375 (TLR2) and Lys378 (TLR2) and the size was 45, 84, 62 (X, Y, Z). The determination of the best result from each docking was based on the predicted binding energy and the mode of interaction of the ligands. Docking poses were analyzed and structural images were generated in PyMol.

3.2.12 Cell transient transfection and FRET imaging

Analysis of association of the TLR4 and TLR2 monomers by LPS *O. intermedium* stimulation was performed by FRET (Förster resonance energy transfer), using CFP-tagged TLR2 and YFP-tagged TLR4 monomers. HEK293T cells were seeded in 6-well plates ($3x10^5$ cells/well) and incubated overnight in DMEM with FBS 5% without antibiotics. In the next day, cells were transiently transfected using Metafectene Pro (Biontex). Cells were co-transfected with 0.5 µg of plasmid mixture of pcDNA3-TLR4-YFP, pcDNA3-TLR2-CFP or transfected with each plasmid (molar ratio 1:1). Cells were also transfected with the plasmid pCMV-ECFP-EYFP that expresses the tandem CFP:YFP construct, which served as a positive control for FRET. Briefly, DNA and metafectene were diluted in Optimem for 5 min and then the DNA was mixed to the Metafectene during 15 min, to a ratio of DNA:Metafectene 1:3. This mix was added to the cell medium and incubated for 6 hours. Then, cells were seeded in eight-well glass bottom chambers ($4x10^4$ cells/well) and incubated overnight in phenol red-free DMEM with FBS 5% and HEPES 25mM. Next day, cells were stimulated with LPS *O. intermedium* at a final concentration of 1 µg/mL.

FRET between TLR2 and TLR4 proteins was calculated by measuring sensitized emission fluorescence of CFP-YFP pair using NIS Elements 4.40 software on the Nikon Eclipse Ti-E confocal microscope. Images of live cells were captured at 60x magnification, under oil immersion. In sensitized emission FRET, the acceptor (YFP) emission is measured as a result of donor (CFP) excitation. Images from three channels are acquired: CFP channel (a CFP excitation and emission filter), a YFP channel (a YFP excitation and emission filter) and a FRET channel (containing a CFP excitation filter and a YFP emission filter). CFP and YFP channel are used to correct the FRET image, because the donor emission can bleed-through into the FRET channel and because CFP excitation wavelength can excite the acceptor YFP, giving false positive FRET signals. Thus, cells expressing only TLR2-CFP or only TLR4-YFP are used as controls. First, images of cells expressing TLR4-YFP were taken, exciting YFP with a 513-laser line and the 458 laser, each time collecting images in the FRET channel (Em 527 nm). Then, images of cells expressing TLR2-CFP were obtained, exciting CFP at 458 nm and acquiring images in both the CFP (Em 480nm) and FRET channel. These images are used to calculate the correction factors A (percentage of YFP in the FRET channel) and B (percentage of CFP in the FRET channel). ROIs were drawn in images of cells expressing only TLR4-YFP as well as in regions without cells to correct for background. The average of intensity values from all acquired YFP images give the correction factor A. The same procedure was performed for images of cells expressing only TLR2-CFP to calculate the correction factor B. Applying the following equation:

$$\mathbf{FRET_{Corr} = FRET_{Raw} - (A * YFP) - (B * CFP)}$$

A corrected FRET image ($FRET_{Corr}$) is obtained from the $FRET_{Raw}$ image of cells co-expressing TLR4-YFP and TLR2-CFP as well as for the CFP:YFP construct. The FRET efficiency is shown as a color-coded scale of values between 0 and 100%. Quantification of the number of FRET positive structures in the cells, as well, as the mean fluorescence intensity of each structure was determined in ImageJ, applying a threshold in grayscale images, to eliminate the background and only select positive FRET signal structures.

3.2.13 Statistics

Analysis was performed with GraphPad Prism 5 software. Statistical analysis between two groups was performed using two-tailed unpaired Student's *t*-test. Two or more groups were compared with one-way ANOVA with Bonferroni post-test.

RESULTS

4 RESULTS

4.1 CHAPTER 1: TLR4 and TLR2 differential kinetics on early signaling activation: the outcome in inflammation

4.1.1 TLR4 and TLR2 ligands induce a distinct cytokine pattern

TLR's activation by various microbial-derived components induce distinct inflammatory responses in macrophages that may fine-tune the acquired immune response. To determine whether TLR2 and TLR4 differ in their ability to activate macrophage responses, Raw264.7 cells were stimulated with specific ligands for TLR4 (LPS), TLR2/1 (Pam3CSK4) and TLR2/6 (FSL-1). The LPS stimulus induced higher trnascription levels of IL-6, IL-12p40, TNF-α and iNOS but lower induction of IL-10 cytokine and ARG1 than TLR2 ligands (Fig. 1).

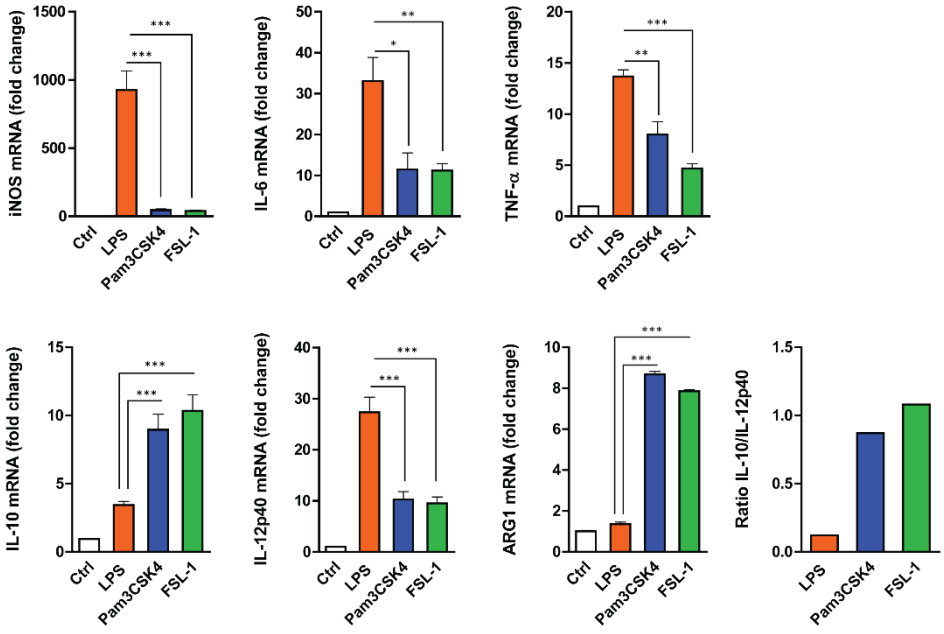

Fig. 1 TLR4 and TLR2 ligands induce a distinct cytokine expression pattern in Raw264.7 cell line.
Raw264.7 cells were stimulated with LPS (100 ng/mL), Pam3CSK4 (1 µg/mL) and FSL-1 (100 ng/mL) for 24 h. Cytokines mRNA expression was assayed by quantitative RT-PCR, normalized to GAPDH, and presented relative to unstimulated cells (Ctrl). Data are representative of three independent experiments (mean ± SEM.) (*p < 0.05, **p < 0.01, and ***p < 0.001).

On the other hand, TLR2 ligands induced higher levels of IL-10 and ARG1, but lower activation of pro-inflammatory cytokines than LPS. To ensure that the differential cytokine induction observed in Raw264.7 cells was not a cell-line occurrence, the same experiment was performed using wild-type

peritoneal macrophages (PM). When these cells were treated with LPS, Pam3CSK4 or FSL-1, a similar pattern on cytokine's induction was observed by TLR4 and TLR2 activation (Fig. 2).

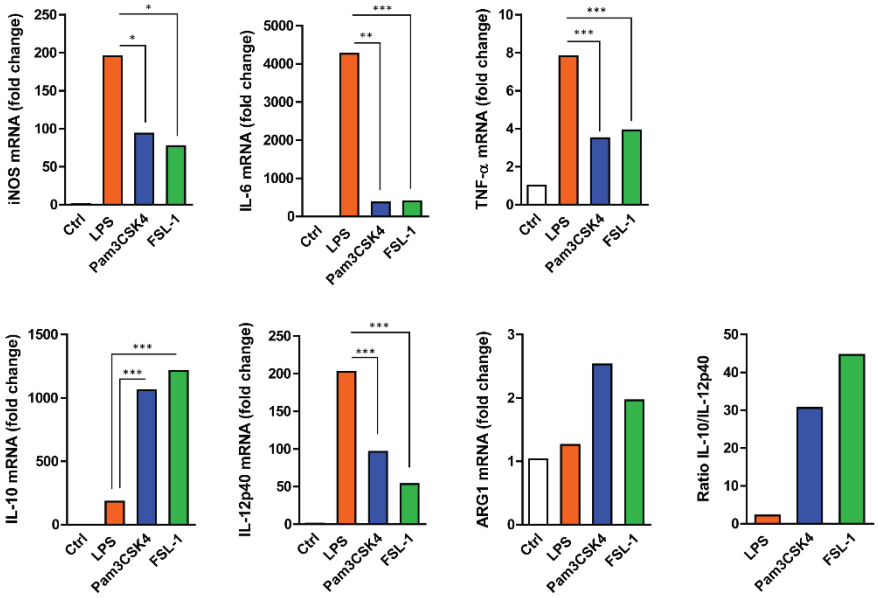

Fig. 2 TLR4 and TLR2 ligands induce a distinct cytokine expression pattern in peritoneal macrophages.
Peritoneal macrophages were stimulated with LPS (100 ng/mL), Pam3CSK4 (1 µg/mL) and FSL-1 (100 ng/mL) for 24 h. Cytokines mRNA expression was assayed by quantitative RT-PCR, normalized to GAPDH, and presented relative to unstimulated cells (Ctrl). The results are shown as mean ± SEM of three independent experiments (* $p<0.05$, ** $p<0.01$, and *** $p<0.001$).

This indicates that TLR2 ligands induce a more anti-inflammatory response compared to TLR4 ligands observed by the higher IL-10/IL-12p40 ratios. Furthermore, there was also some differences between distinct TLR2 ligands, since FSL-1 induced a higher IL-10/IL-12p40 ratio compared with Pam3CSK4, which suggests that distinct TLR2 ligands can elicit slightly different inflammatory responses. Moreover, these results demonstrate that both immune cell types (cell line vs primary cell) have a similar cytokine induction profile via TLR4 and TLR2 receptors.

4.1.2 TLR4 and TLR2 ligands exhibit different kinetics on NF-κB and MAPK pathways activation

Since TLR4 and TLR2 receptor's activation induce a distinct cytokine pattern, the next step was to examine whether TLR4 and TLR2 ligands could differentially activate the cell signaling pathways. Raw 264.7 cells were serum starved and then stimulated for 3, 10, 30 and 60 minutes with LPS, Pam3CSK4 or FSL-1. We detected NF-κB activation by IκBα degradation in response to LPS around 30 and 60 min. Similar kinetics was observed for activation of MAPKs ERK and p38, where detectable

phosphorylation appears at 30 and 60 min (Fig. 3). Interestingly, TLR2 ligands activate these signaling pathways faster; by 3 min after stimulation, IκBα degradation and the phospho-MAPKinase pathway activation markers were clearly visible and, in a dose-dependent manner (Fig. 4).

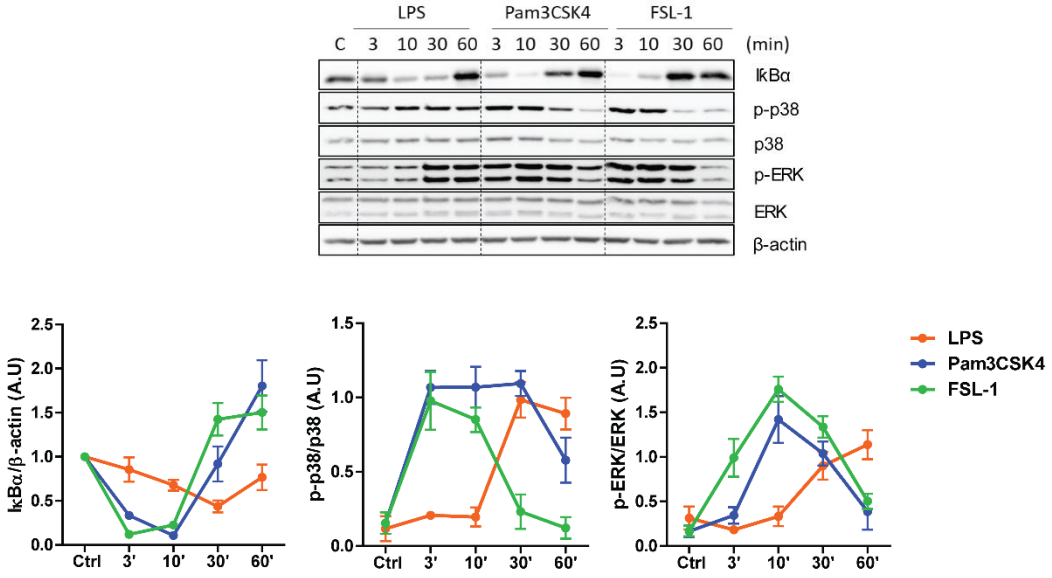

Fig. 3 TLR4 and TLR2 ligands exhibit different kinetics on NF-κB and MAPK pathways activation.
Raw 264.7 cells were treated with LPS (100 ng/mL), Pam3CSK4 (1 µg/mL) and FSL-1 (100 ng/mL) at 3, 10, 30 and 60 min and stained with the antibodies indicated on the right side of the panels. The graphics below show the quantification of band intensities of the Western blots. The results are shown as mean ± SEM of three independent experiments.

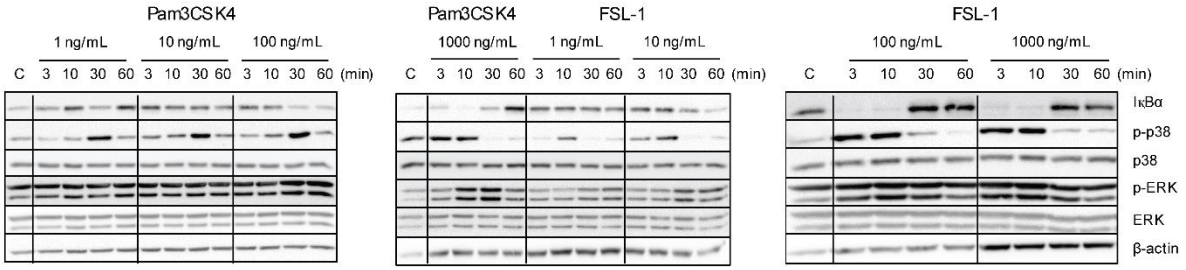

Fig. 4. Raw264.7 cells were stimulated with incremental doses of Pam3CSK4 and FSL-1indicated in the image at 3, 10, 30 and 60 min and stained with the indicated antibodies. The image is representative of one experiment.

Despite the striking difference in the activation kinetics between TLR4 and TLR2 ligands, no apparent changes in the signal strength of activation were observed. In peritoneal macrophages, a similar kinetic signature was observed (Fig. 5). Peritoneal macrophages from TLR2 KO and TLR4 KO mice were also used to confirm the ligands stimulation-specificity. Upon stimulation of TLR2 KO macrophages, TLR2 ligands were unable to activate MAPK or NF-κB pathways, indicating the specificity of these ligands for TLR2 receptor. As expected, LPS was able to activate these cells but not TLR4 KO macrophages.

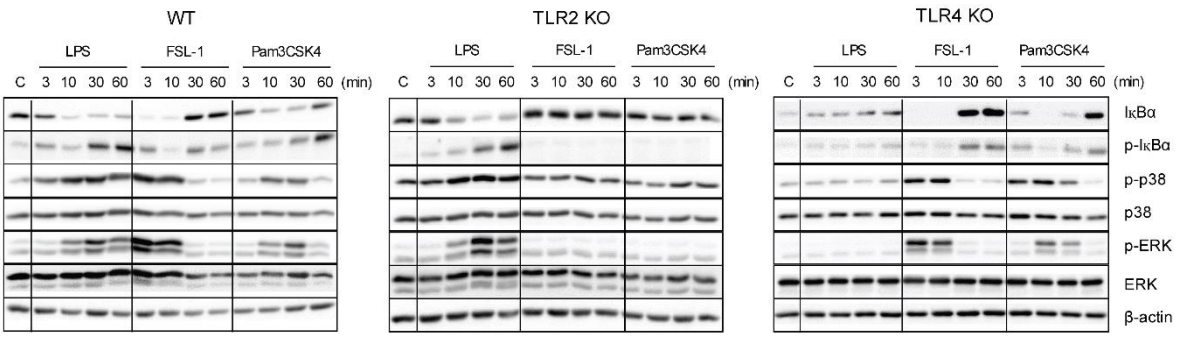

Fig. 5 TLR4 and TLR2 ligands responses are specific of TLR4 and TLR2 receptor respectively.

WT peritoneal macrophages, TLR2 KO and TLR4 KO peritoneal macrophages were left untreated (c) or treated with LPS (100 ng/mL), Pam3CSK4 (1 µg/mL) and FSL-1 (100 ng/mL) at 3, 10, 30 and 60 min. The data are representative of two independent experiments.

4.1.2.1 MEK- independent mechanism contributes for ERK1/2 activation by TLR2 ligands in the Raw264.7 cell line

To study the differential kinetic signaling between TLR4 and TLR2 ligands, special focus was given to investigate whether different upstream ERK and p38 activators could be induced via TLR4 or TLR2 activation. To this end, Raw264.7 cells were pretreated with TAK1 inhibitor (5Z-7-oxzeaenol) and MEK 1/2 inhibitors (PD98059 and U0126) once these mediators are described to be implicated in ERK activation. In the presence of TAK1 inhibitor, ERK and p38 phosphorylation were reduced upon stimulation with TLR4 and TLR2 ligands (Fig. 6A) suggesting that TAK1 is an upstream activator for these MAPKs. The same pattern was observed for the stimulation of peritoneal macrophages (Fig. 6B). The role of the MEK1/2 kinase in ERK activation by TLR2 activation was addressed. Cells were pretreated with MEK1/2 inhibitor PD98059 that has been described has an inhibitor of MEK1 activation and to a lesser extent MEK2, with IC50 values of 4 µM and 50 µM respectively (Alessi et al., 1995). A 50 µM concentration of PD98059 was sufficient to fully block ERK phosphorylation upon stimulation of LPS (Fig. 7). However, this inhibitor only inhibited a small fraction of ERK phosphorylation in response to Pam3CSK4 and FSL-1. To ascertain that this phenomenon was not dueto a limited inhibition of MEK2 activity, a higher dose of PD98059 was tested (100 µM), but ERK phosphorylation in response to Pam3CSK4 and FSL-1 was maintained (Fig. 8).

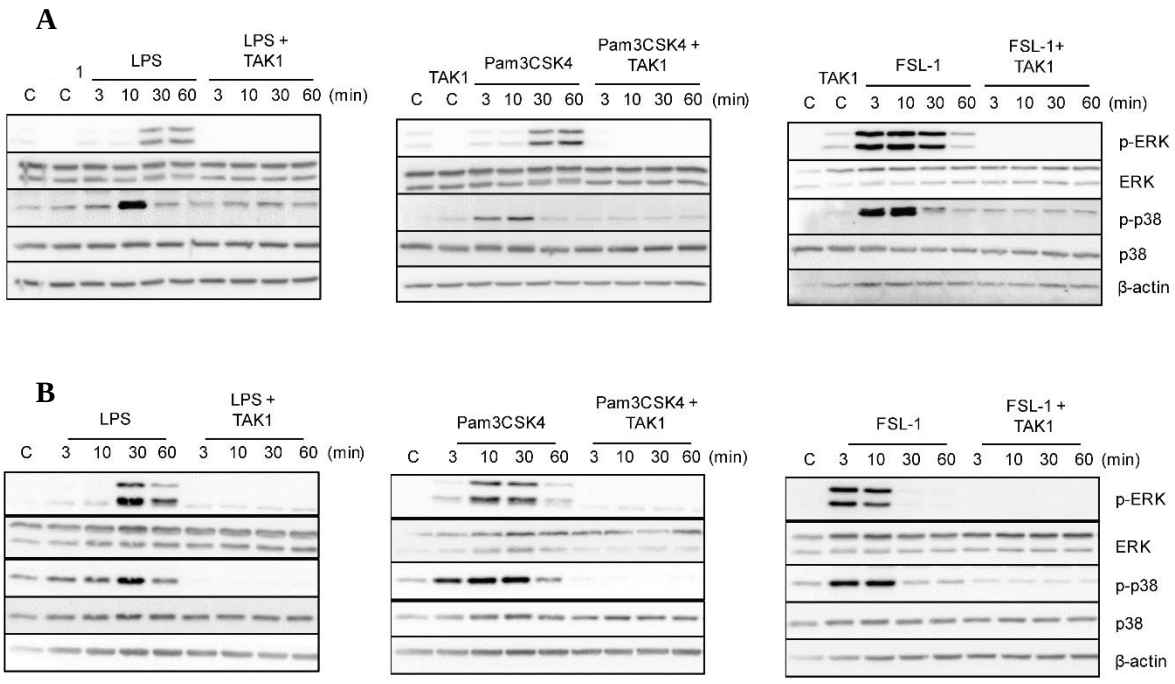

Fig. 6 TAK1 is an upstream activator of ERK and p38 in the Raw264.7 cell line and peritoneal macrophages.
A) Raw264.7 cells and **B)** peritoneal macrophages were pretreated with 1 µM 5Z-7-oxzeaenol ("TAK1") for 30 min. Cells were left unstimulated (c) or stimulated with LPS (100 ng/mL), Pam3CSK4 (1 µg/mL) and FSL-1 (100 ng/mL) at 3, 10, 30 and 60 min. A representative western blot is shown of three independent experiments.

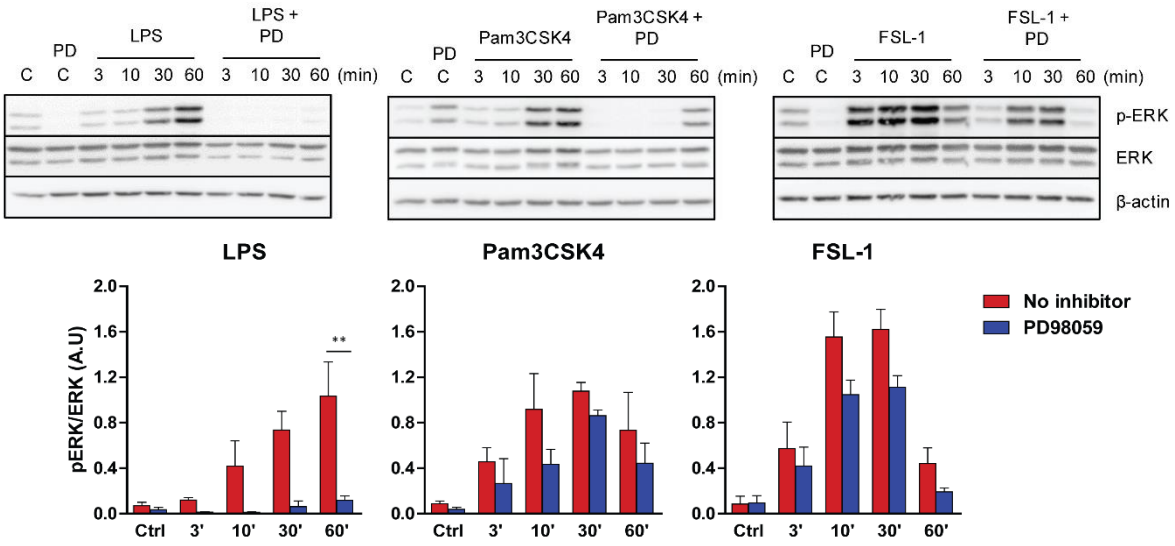

Fig. 7 PD98059 weakly inhibits ERK activation in response to TLR2 ligands in the Raw 264.7 cells line.
Raw 264.7 cells were pretreated with 50 µM PD98059 ("PD") for 30 min. Cells were left unstimulated (c) or stimulated with LPS (100 ng/mL), Pam3CSK4 (1 µg/mL) and FSL-1 (100 ng/mL) at 3, 10, 30 and 60 min. A representative western blot experiment is shown of three experiments. Graphics show quantification of band intensities of the upper western blot. The values of p-ERK 1/2 bands were normalized to the total ERK 1/2 protein. Data are representative of three independent experiments (mean ± SEM.) (*$p < 0.05$, **$p < 0.01$, and ***$p < 0.001$).

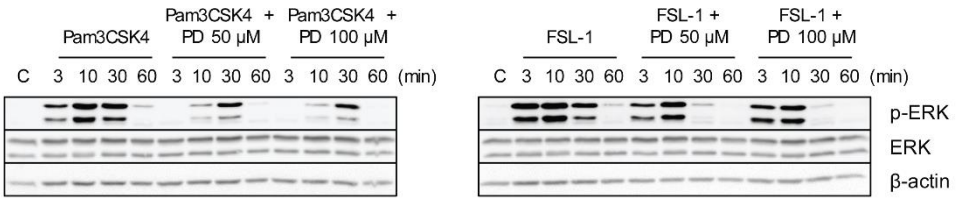

Fig. 8 Raw 264.7 cells were pretreated with two doses of PD98059 ("PD") as displayed in the images for 30 min. Cells were left unstimulated (c) or stimulated with Pam3CSK4 (1 µg/mL) and FSL-1 (100 ng/mL) at 3, 10, 30 and 60 min. A representative experiment is shown from one experiment.

U0126 was tested in Raw264.7 cells since this inhibitor has 100-fold higher affinity for MEK1/2 than PD98059, with similar IC50 values for MEK1 and MEK2 (0,06 µM and 0,07 µM respectively) (Favata et al., 1998). In the presence of U0126 inhibitor, ERK activation by LPS was fully impaired. However, in response to Pam3CSK4, ERK phosphorylation peak appeared at 60 min, and was inhibited to 67% in the presence of U0126 (Fig. 9). Regarding FSL-1 stimulation, ERK activation was higher at 10 and 30 min and when treated with U0216, ERK phosphorylation was still observed (approx. 25%).

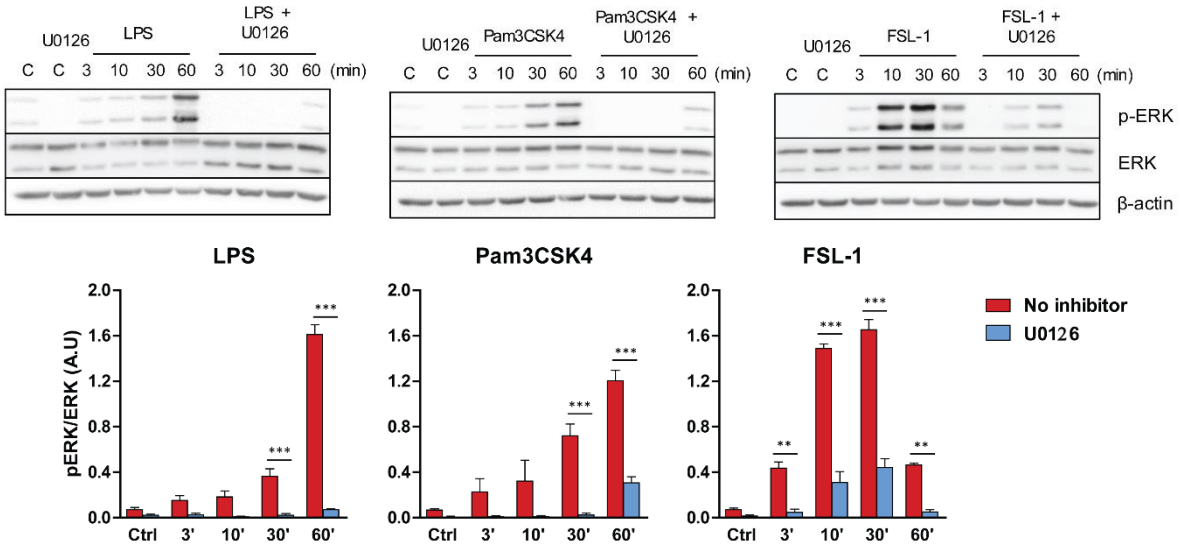

Fig. 9 A **MEK-independent mechanism contributes for TLR2-mediated ERK activation in the Raw264.7 cell line.** Raw 264.7 cells were pretreated with 1 µM U0126 for 30 min. Cells were left unstimulated (c) or stimulated with LPS (100 ng/mL), Pam3CSK4 (1 µg/mL) and FSL-1 (100 ng/mL) at 3, 10, 30 and 60 min. A representative western blot experiment is shown of three experiments. Graphics show quantification of band intensities of the upper western blot. The values of p-ERK 1/2 bands were normalized to the total ERK 1/2 protein. Data are representative of three independent experiments (mean ± SEM.) (*$p < 0.05$, **$p < 0.01$, and ***$p < 0.001$).

These results show that PD98059 and at a lesser extent U0126, weakly inhibits ERK activation in response to TLR2 ligands. This phenomenon prompted us to examine the effect of these inhibitors on ERK activation in primary cell macrophages. Peritoneal macrophages were pretreated with each MEK

inhibitor and stimulated with the three different ligands. ERK phosphorylation in response to the three ligands was impaired in the presence of PD98059 inhibitor as well as in the presence of U0126 (Fig. 10A and 10B).

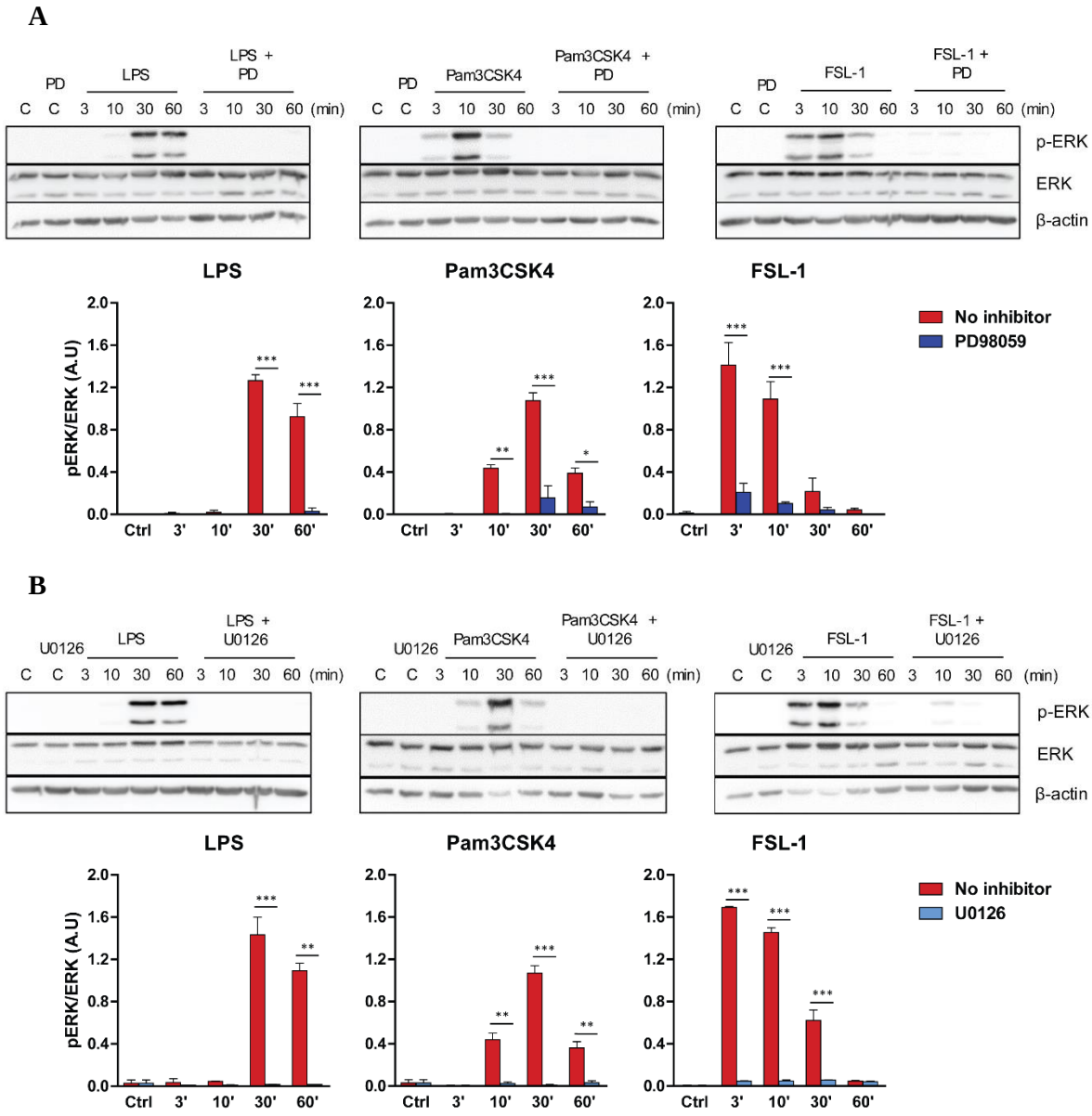

Fig. 10 PD98059 and U0126 inhibitors downregulate ERK activation in peritoneal macrophages, regardless of the stimuli.

Peritoneal macrophages were pretreated with **A)** with 50 µM PD98059; **B)** with 1 µM U0126 for 30 min. Cells were left unstimulated (c) or stimulated with LPS (100 ng/mL), Pam3CSK4 (1 µg/mL) and FSL-1 (100 ng/mL) at 3, 10, 30 and 60 min. A representative Western blot is shown of two experiments. Graphics show quantification of band intensities of the upper western blot. All densitometry values of the p-ERK 1/2 band were normalized to the total ERK 1/2 protein. Data are representative of two independent experiments (mean ± SEM.) (*p < 0.05, **p < 0.01, and ***p < 0.001).

The same effect was observed for LPS and FSL-1 stimulated bone marrow-derived macrophages (BMDM) pretreated with PD98059 (Fig. 11). Therefore, a TAK1-MEK- independent mechanism contributes for ERK1/2 activation by TLR2 ligands only in the Raw264.7 cell line.

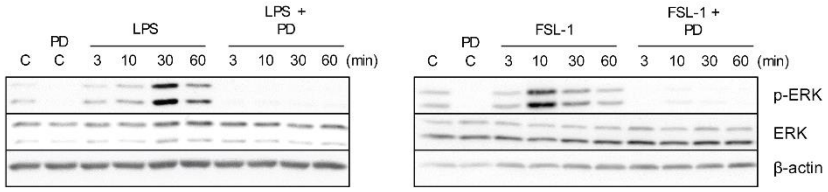

Fig. 11 PD98059 inhibitor downregulates ERK activation in BMDM, regardless of the stimuli.
Bone marrow-derived macrophages were pretreated with 50 μM PD98059 ("PD") for 30 min. Cells were left unstimulated (c) or stimulated with LPS (100 ng/mL) and FSL-1 (100 ng/mL) at 3, 10, 30 and 60 min. A representative experiment is shown from one experiment.

4.1.2.2 ERK activation by TLR2 ligands is Ras-dependent and PKCζ–partially dependent in Raw264.7 cells

It is described that Ras-MEK as well as PKCζ-MEK pathways are activated by LPS and induce ERK phosphorylation (Monick et al., 2000; Pathak et al., 2004). Moreover, PI3K-mTOR, TPL2 are also described to contribute for ERK activation in response to LPS. Therefore, PI3K, TPL2, Ras and PKCζ inhibitors were tested in order to access their influence in the MEK-independent pathway activated by TLR2 ligands in Raw264.7 cells. Inhibition of PI3K (wortmannin) and TPL2 did not affect ERK activation upon TLR2 ligands stimulation (data not shown). On the other hand, cells stimulated with LPS show ERK activation at 30 and 60 min, which is impaired in the presence of Ras inhibitor (Fig. 12A). The same effect is observed for Pam3CSK4 and FSL-1 stimulation as ERK phosphorylation is present mainly at 3, 10 and 30 min and disappears in the presence of the inhibitor. However, the effect of PKCζ inhibition in ERK phosphorylation differs. PKCζ inhibition impairs strongly ERK activation in response to LPS and a partial decrease is observed by stimulation with Pam3CSK4 and FSL-1. ERK activation by FSL1, which occurs at 3 and 10 min, is inhibited by approx. 33% (Fig. 12B). These results imply that Ras is a common upstream mediator for ERK activation by TLR4 and TLR2 ligands and TLR2 ligands, mainly FSL-1 partially activate ERK through PKCζ kinase. Therefore, these results show that in response to TLR2 ligands a TAK1-Ras dependent but MEK-independent pathway, together with PKCζ activity, contribute to ERK activation in the Raw264.7 cell line.

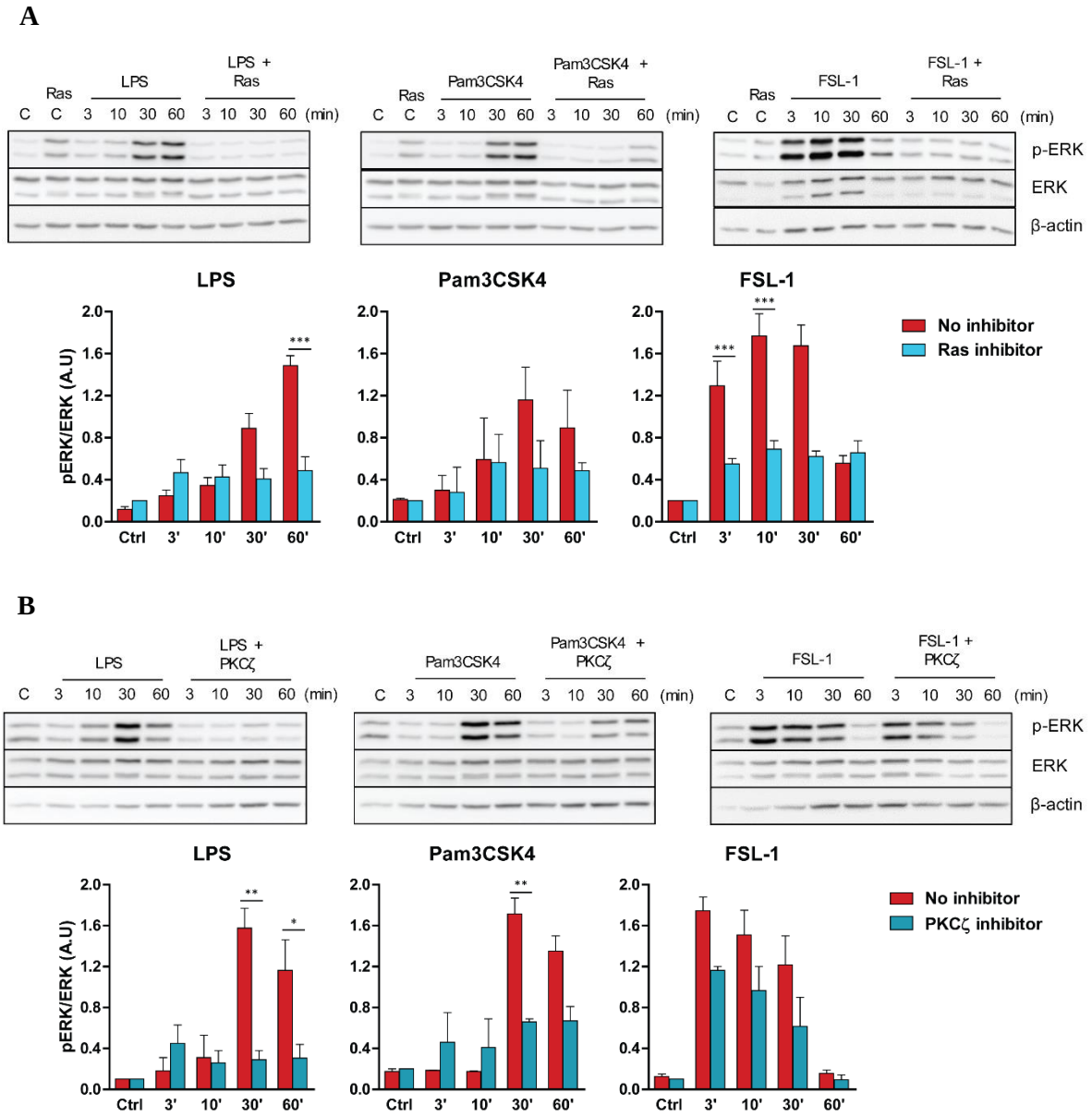

Fig. 12 ERK activation by TLR2 ligands is Ras-dependent and PKCζ –partially dependent in Raw264.7 cells.
Cells were pretreated with **A)** 10 µM Manumycin ("Ras inhibitor"); **B)** with 10 µM PKCζ inhibitor (PKCζ) for 30 min. Cells were left unstimulated (c) or stimulated with LPS (100 ng/mL), Pam3CSK4 (1 µg/mL) and FSL-1 (100 ng/mL) at 3, 10, 30 and 60 min. A representative experiment is shown of two experiments. Graphics show quantification of band intensities of the upper western blots. All densitometry values of the p-ERK 1/2 band were normalized to the total ERK 1/2 protein. Data are representative of two independent experiments (mean ± SEM.) (*$p < 0.05$, **$p < 0.01$, and ***$p < 0.001$).

4.1.2.3 p38 activation is dependent of an autophosphorylation mechanism in the Raw264.7 cell line but not in primary macrophages

The MAP kinase p38 activation is well described to be mediated by the classical TAK1-MEK3/6 pathway in response to TLR ligands. However, a study using a human B cell line describes that LPS induces p38α by an autophosphorylation mechanism dependent of TAB1 kinase, which does not occur in the presence of TLR2 ligand lipoproteins (Ge et al., 2002). Considering this, we decided to investigate the effect of p38 inhibition upon stimulation with TLR4 and TLR2 ligands. For this experiment, Raw264.7 cells were stimulated with LPS, Pam3CK4 and FSL-1 in the absence or presence of a p38 inhibitor (SB203580) and p38 phosphorylation was determined by WB. Cells stimulated with LPS exhibited p38 activation mainly at 30 and 60 min and the presence of p38 inhibitor fully impaired the phosphorylation of this kinase. However, cell treatment with these inhibitors only partially affected p38 phosphorylation mediated by TLR2 ligands (Fig. 13A).

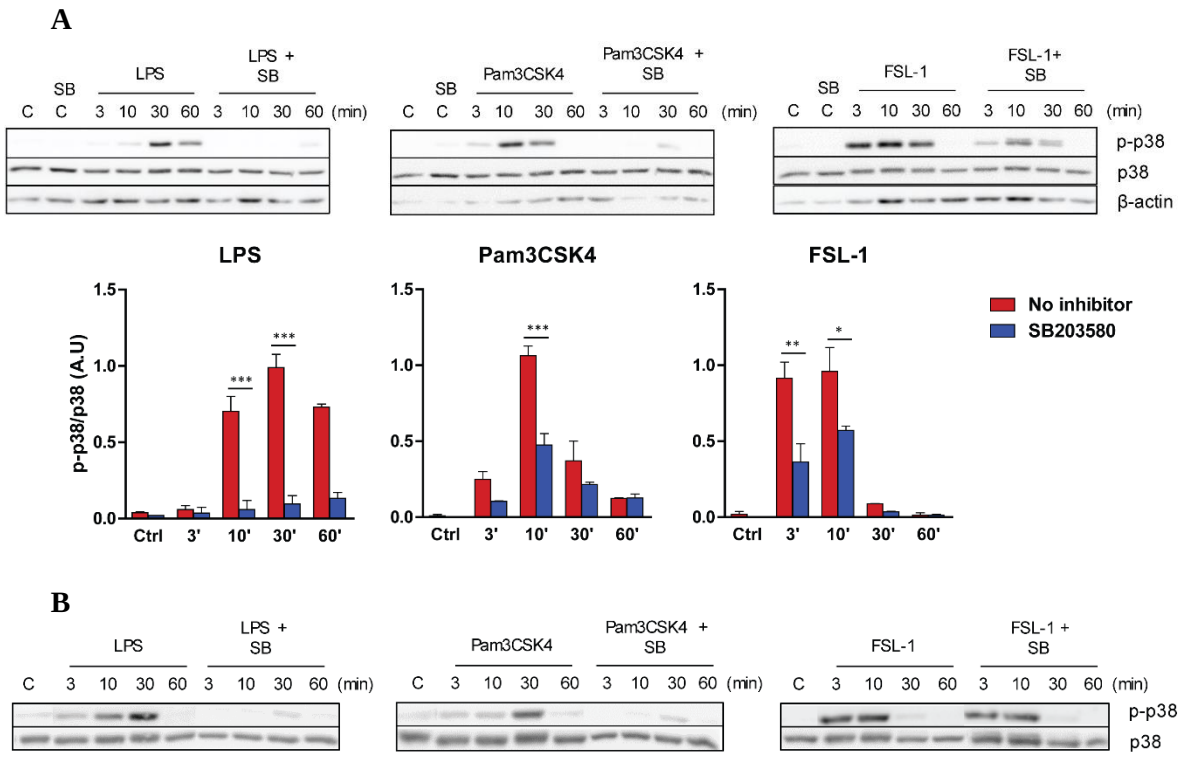

Fig. 13 p38 activation is dependent of an autophosphorylation mechanism in the Raw264.7 cell line

Raw264.7 cells were pretreated with **A)** 10 µM SB203580 and **B)** 1 µM of SB239063. Cells were left unstimulated (c) or stimulated with LPS (100 ng/mL), Pam3CSK4 (1 µg/mL) and FSL-1 (100 ng/mL) at 3, 10, 30 and 60 min. Graphics show quantification of band intensities of the upper western blot. All densitometry values of the p-p38 band were normalized to the total p38 protein. Data are representative of two independent experiments (mean ± SEM.) (*p < 0.05, **p < 0.01, and ***p < 0.001).

To confirm this result, another p38 inhibitor, SB239063 was also tested and the same result was obtained (Fig. 13B). In peritoneal macrophages, p38 phosphorylation state was not altered in the presence of the inhibitor, regardless of the stimulus (Fig. 14).

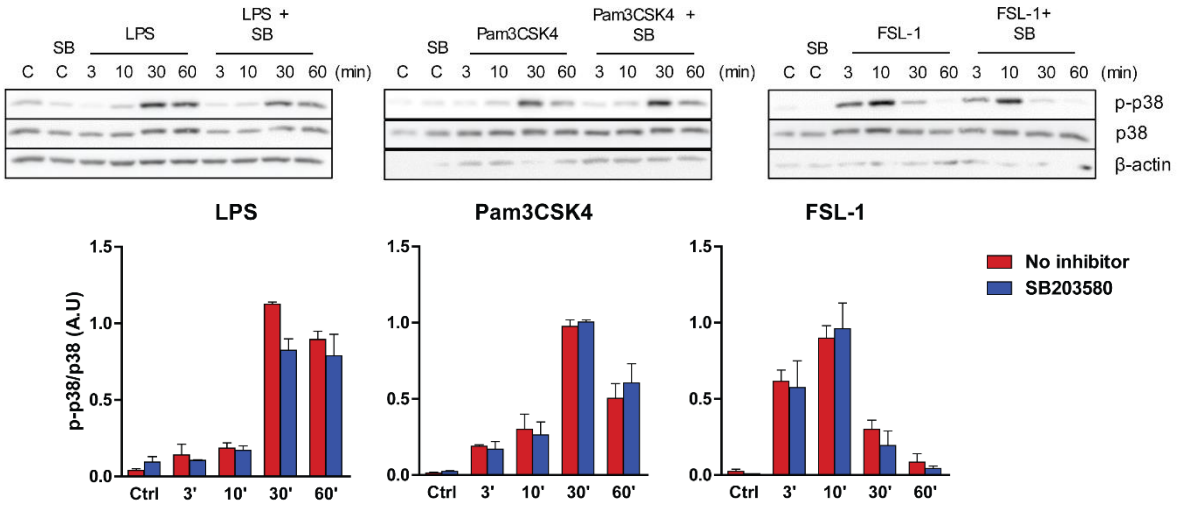

Fig. 14 p38 phosphorylation is not affected by the inhibitor SB203580 in peritoneal macrophages.
Peritoneal macrophages were pretreated with 10 µM SB203580. Cells were left unstimulated (c) or stimulated with LPS (100 ng/mL), Pam3CSK4 (1 µg/mL) and FSL-1 (100 ng/mL) at 3, 10, 30 and 60 min. At each time point, cells were lysed, and the cell lysate was subjected to immunoblotting. Graphics show quantification of band intensities of the upper western blot. All densitometry values of the p-p38 band were normalized to the total p38 protein. Data are representative of two independent experiments (mean ± SEM.) (*$p < 0.05$, **$p < 0.01$, and ***$p < 0.001$).

This data demonstrates that LPS and at some extent Pam3CSK4 and FSL-1 induce p38 by an autophosphorylation mechanism, only observed in the Raw264.7 cell line.

These results demonstrate that: (i) Raw264.7 cell line, but not primary macrophages, activate different upstream mediators of p38 and ERK signaling, which is dependent of the initial stimulus; (ii) TLR4 and TLR2 differential kinetic signaling cannot be explained by differences on the upstream signaling cascades, at least in primary macrophages.

4.1.3 MKP-1 role in MAPKs de-activation and inflammatory response by TLR4 and TLR2 ligands

4.1.3.1 MKP-1 exhibits different activation and regulation kinetics by TLR4 and TLR2 activation

Previous results confirmed that MAPKs activation occurs earlier in response to TLR2 ligands compared to LPS. Furthermore, p38 and ERK phosphorylation induced by TLR2 declines faster, at 30 and 60 min compared with the TLR4 ligand LPS, which occurs after 60 min (Fig. 2A and B). To understand the cause of these differences on p38 and ERK dephosphorylation, we sought to understand the possible role of phosphatases, more specifically MKP-1. This phosphatase was described to be induced and stabilized through phosphorylation by ERK in LPS-stimulated cells. Moreover, MKP-1 has higher affinity to dephosphorylate p38 and JNK rather than ERK. (Brondello et al., 1999). Stimulation of Raw264.7 cells and peritoneal macrophages with the TLR ligands exhibit MKP-1induction (Fig. 15A). In response to LPS, MKP-1 was induced at 60 min after stimulation, whereas in response to TLR2 ligands, mainly FSL-1, MKP-1 was detected earlier, at 30 min. A similar kinetic pattern was observed for MKP-1 transcription, however in peritoneal macrophages MKP-1 mRNA levels started to decay at 60 min (Fig. 15B). This data indicates that TLR2 ligands induce MKP-1 transcription and expression earlier compared to the TLR4 ligand LPS.

Since MKP-1 protein was reported to be stabilized by phosphorylation, increasing its half-life, protein and mRNA levels were quantified at later time points (Fig. 15C, left panel). LPS stimulation induced MKP-1 transcription at 2 hours followed by a decrease at 4 hours and reaching the basal levels at 6 hours after stimulation (this is in accordance with a previous published work) (Crowell 2014). Strong protein levels were observed for MKP-1 at 2 hours in LPS-stimulated cells and at 4 and 6 hours after stimulation, some MKP-1 protein maintains stabilized (Fig. 15C, right panel). This shows that although MKP-1 transcription declines after 6 hours of stimulation, some protein is still present at this time point. On the other hand, when activated by TLR2 ligands, MKP-1 transcription is rapidly declined after 2 hours of stimulation. Nonetheless, at a protein level, we still observe a strong MKP-1 band for Pam3CSK4 at 2 hours of stimulation, but fainter in response to FSL-1. This indicates that in Pam3CSK4 and mainly FSL-1-stimulated cells, the duration of MKP-1 activation was lower compared to LPS-stimulated macrophages. In summary, these results show that MKP-1 transcription and expression levels were induced earlier and declined faster by TLR2 activation compared to TLR4.

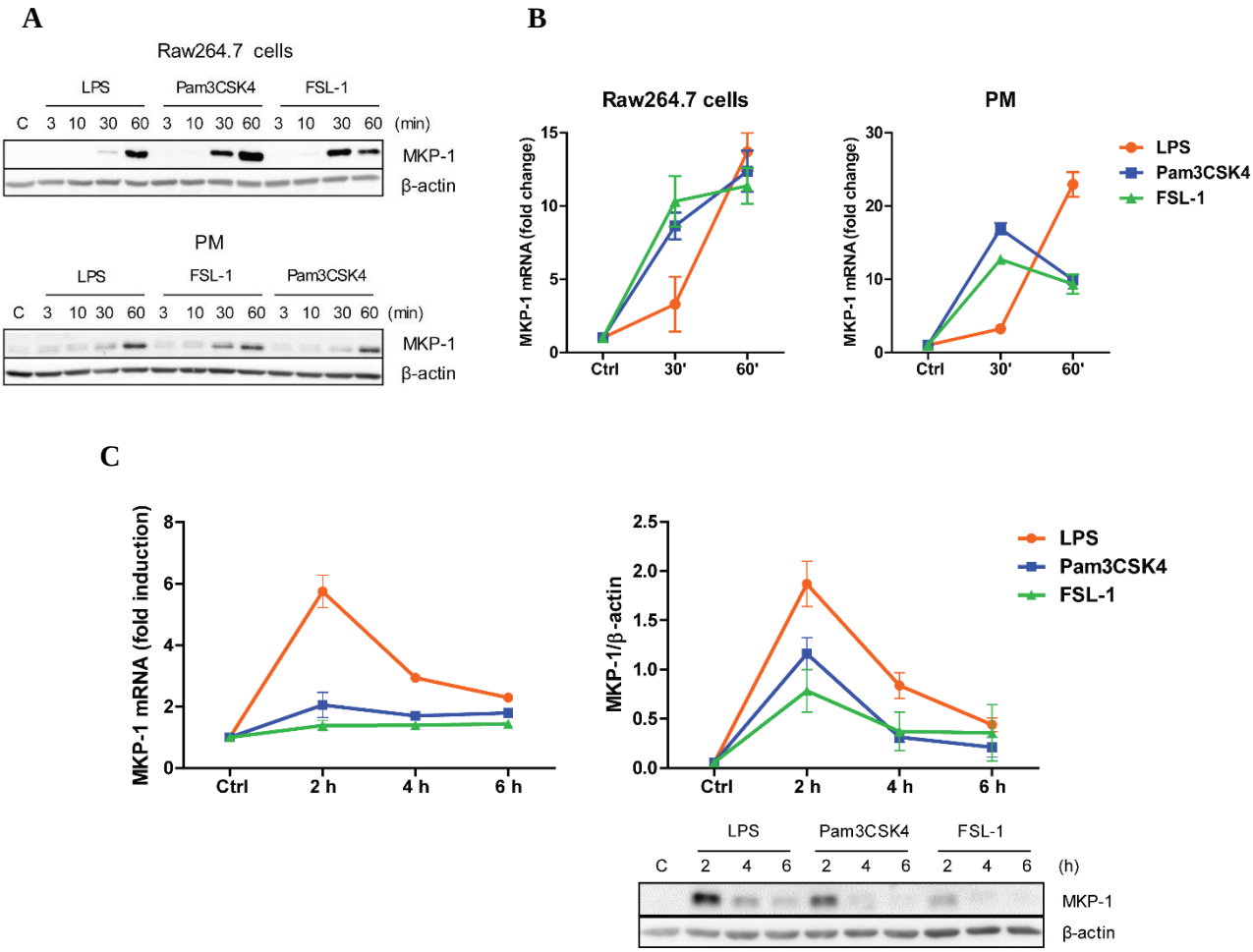

Fig. 15 MKP-1 exhibits different activation and regulation kinetics by TLR4 and TLR2 activation.
A) Raw264.7 cells and peritoneal macrophages were left unstimulated (c) or stimulated with LPS (100 ng/mL), Pam3CSK4 (1 µg/mL) and FSL-1 (100 ng/mL) at 3, 10, 30 and 60 min. **B)** MKP-1 mRNA levels after cell stimulation with the three ligands at 30 and 60 min. **C)** Peritoneal macrophages stimulated at later time points as indicated by LPS, Pam3CSK4 and FSL-1. MKP-1 mRNA levels and protein were measured by qPCR and WB. Data are representative of two independent experiments (mean ± SEM.) (*p < 0.05, **p < 0.01, and ***p < 0.001).

Since previous published data (Chen et al., 2002) describes that MKP-1 activation is induced by ERK, inhibition of ERK and p38 was performed to evaluate whether MKP-1 expression is affected differentially via TLR4 and TLR2 activation. Raw264.7 cells stimulated with LPS show a complete abrogation on MKP-1 expression in the presence of ERK inhibitor, as well as a significant abrogation in the presence of p38 inhibitor (Fig. 16A). Thus, ERK and in part, p38 contribute for MKP-1 induction in response to LPS. MKP-1 expression was impaired in the presence of ERK inhibitor, but not affected when treated with SB203580, in response to Pam3CSK4 and FSL-1. Therefore, TLR2 ligands, mainly FSL-1 induced MKP-1 expression mediated mainly by ERK, whereas TLR4 activated MKP-1 was mediated primarily by ERK, with p38 playing a minor role. On the other hand, peritoneal macrophages treated with the TLR2 ligands showed a complete downregulation of MKP-1 expression in the presence of both inhibitors (Fig. 16B).

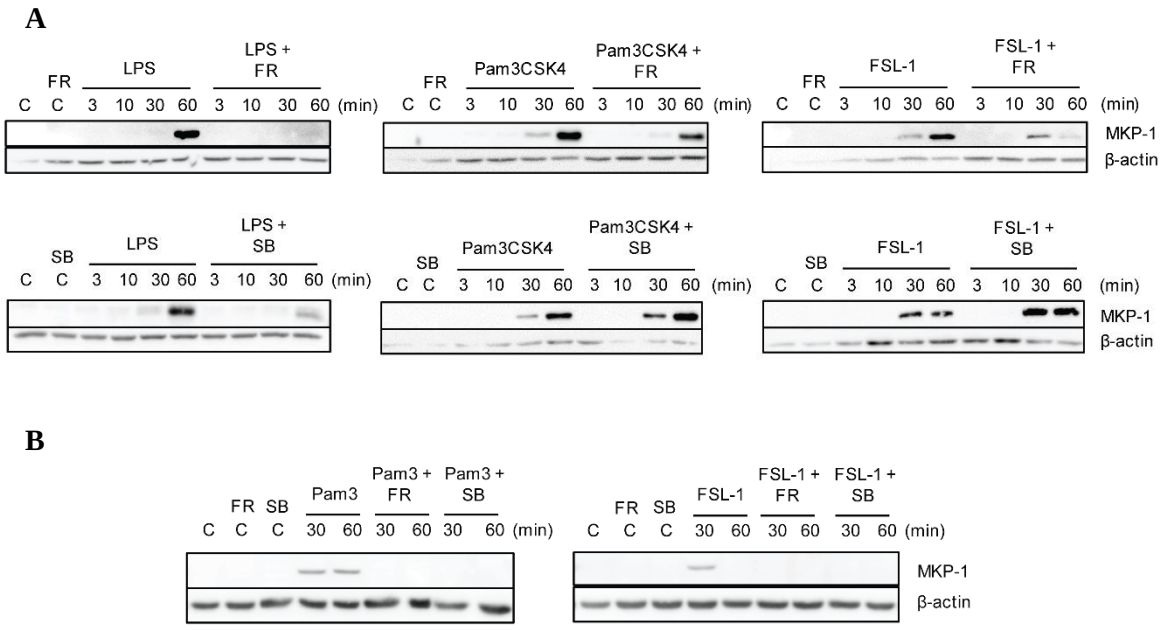

Fig. 16 MKP-1 induction is mediated by p38 and ERK in primary macrophages.

A) Raw264.7 cells were pretreated with 10 µM FR180204 ("FR") or 10 µM SB203580 ("SB"). Cells were left unstimulated (c) or stimulated with LPS (100 ng/mL), Pam3CSK4 (1 µg/mL) and FSL-1 (100 ng/mL) at 3, 10, 30 and 60 min. **B)** Peritoneal macrophages were pretreated with the same inhibitors and then stimulated with Pam3CSK4 and FSL-1 for 30 and 60 min. Images are representative of two independent experiments.

4.1.3.2 MKP-1 phosphatase controls p38 but not ERK phosphorylation in response to TLR2 stimulation

Previous data demonstrated that MKP-1 controls p38 activation in response to TLR4 activation (Chi et al., 2006; Zhao et al., 2006). Therefore, the MKP-1 role in MAPKs activation in response to FSL-1 was addressed. WT and MKP1-deficient macrophages were treated with FSL-1 for 1 hour. Macrophages deficient in MKP-1 exhibited a prolongation p38 phosphorylation but not for ERK comparing with WT (Fig. 17). Therefore, besides TLR4, MKP-1 will preferably regulate p38 phosphorylation in response to TLR2/6 stimulation.

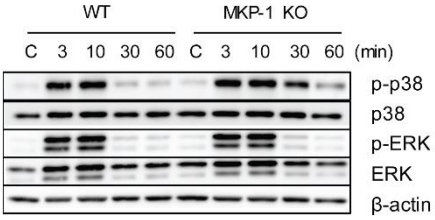

Fig. 17 WT and MKP-1 KO peritoneal macrophages were left unstimulated (c) or stimulated FSL-1 (100 ng/mL) at 3, 10, 30 and 60 min. β-actin was used as protein loading control. Image representative of one experiment.

4.1.3.3 MKP-1 differentially controls pro and anti-inflammatory cytokines in response to TLR2 ligands

Since MKP-1 expression is differentially regulated via TLR4 and TLR2 activation, and previous studies reported a role of MKP-1in cytokines regulation induced by LPS (Chi et al., 2006; Zhao et al., 2006), the effect of this phosphatase on TLR2-mediated cytokine induction was studied at later time points (Fig. 18).

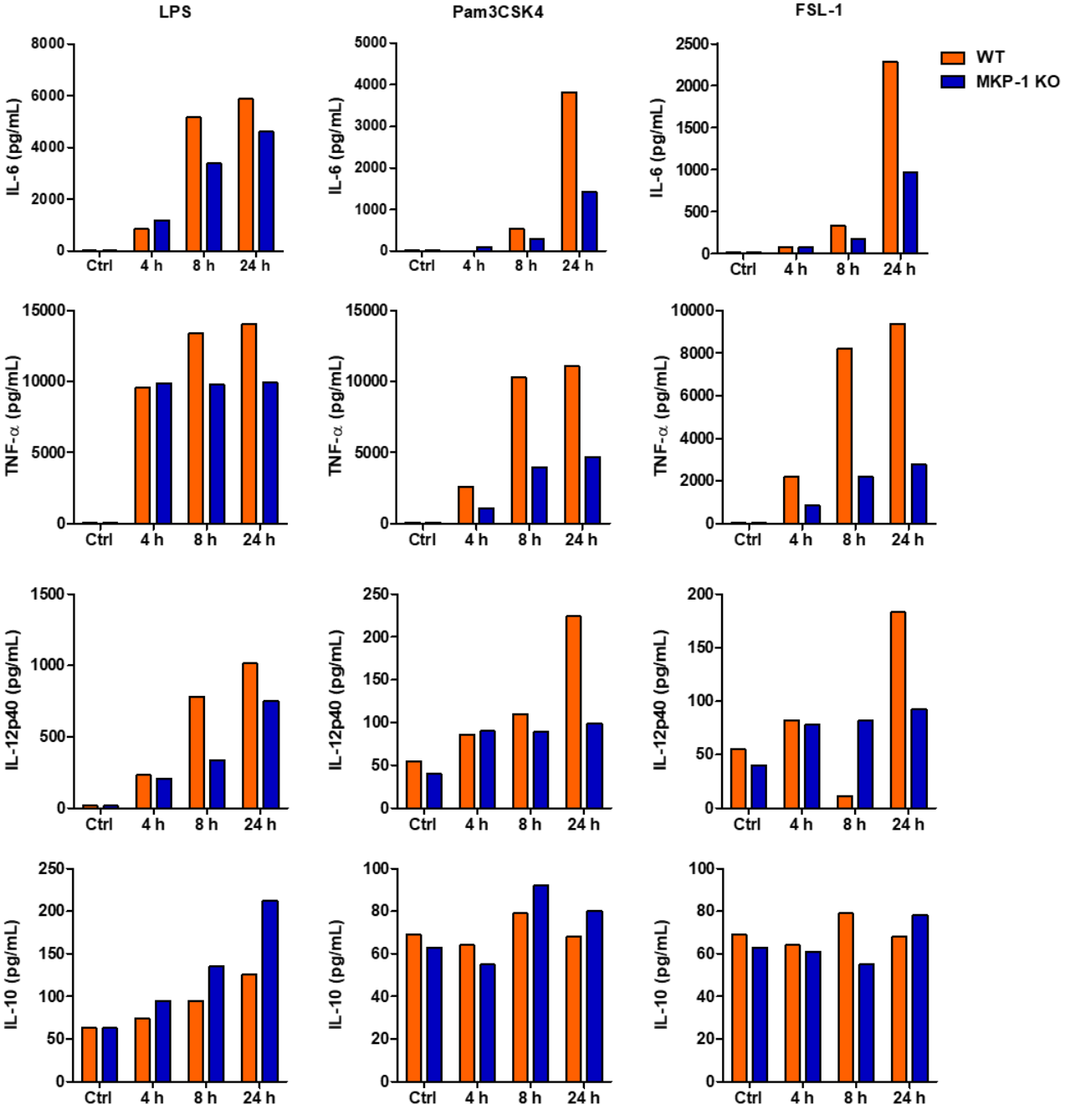

Fig. 18 MKP-1 differentially regulates pro and anti-inflammatory cytokine's expression.
WT and MKP-1 KO peritoneal macrophages were left unstimulated (Ctrl) or stimulated with LPS (100 ng/mL), Pam3CSK4 (1 µg/mL) and FSL-1 (100 ng/mL) at 4, 8, and 24 hours. At each time point, cell supernatant was collected, and cytokines were measured by ELISA. The results are representative of on experiment.

Stimulation of WT and MKP-1 deficient peritoneal macrophages with TLR4 and TLR2 ligands at 4, 8 and 24 hours was carried out, followed by cytokine´s quantification. In the absence of MKP-1, a decrease in TNF-α, IL-12p40 and IL-6 levels was observed over time, but the effect was stronger in response to TLR2 ligands stimulation at 8 and 24 hours, compared to LPS. On the other hand, IL-10 levels increased at 8 and 24 hours in MKP-1 deficient macrophages stimulated with LPS, whereas in response to TLR2 ligands the IL-10 levels were similar to WT cells (Fig. 18). This indicates that MKP-1 upregulates pro-inflammatory cytokines, which is more pronounced by TLR2 activation, but regulates IL-10 expression at later stages of the inflammation process.

4.1.4 p38 is critical for later IL-10 expression by TLR2 ligands

Published data describes that IL-10 expression is dependent of p38 activation in response to LPS (Kim et al., 2008). Thus, the next step was to investigate the effect of p38 and ERK inhibition in the cytokine's induction by the TLR2 ligands. A time-course kinetics was performed to determine the changes of cytokine levels in Raw2634.7 cells pretreated with SB203580 or FR180204 and stimulated with TLR4 or TLR2 ligands for 4, 8 and 24 hours (Fig. 19). Stimulation with TLR2 ligands gave a similar pattern for TNF-α induction, however IL-6 levels were lower at earlier time points compared to the levels induced by LPS. Nevertheless, at 24 hours, p38 has a regulatory role in IL-6 induction in response to Pam3CSK4 and FSL-1, similarly observed in response to LPS. However, IL-10 levels are highly increased at 24 hours in response to TLR2 ligands and fully dependent of p38. The effect of p38 and ERK inhibition on cytokine's expression was further evaluated in peritoneal macrophages pretreated with p38 and ERK inhibitors and stimulated with TLR ligands for 24 hours. The pro-inflammatory cytokines TNF-α, IL-6 and IL-12 were not apparently affected in the presence of the p38 inhibitor, however (Fig. 20A). On the other hand, IL-10 levels were strongly decreased by p38 inhibition. A similar pattern was observed for the cytokine transcription levels in stimulated-peritoneal macrophages (Fig. 20B). These results imply that ERK and p38 are important for pro-inflammatory cytokines induction at early time points of inflammation, whereas p38 contributes for later anti-inflammatory IL-10 production in response to TLR4 and TLR2 ligands.

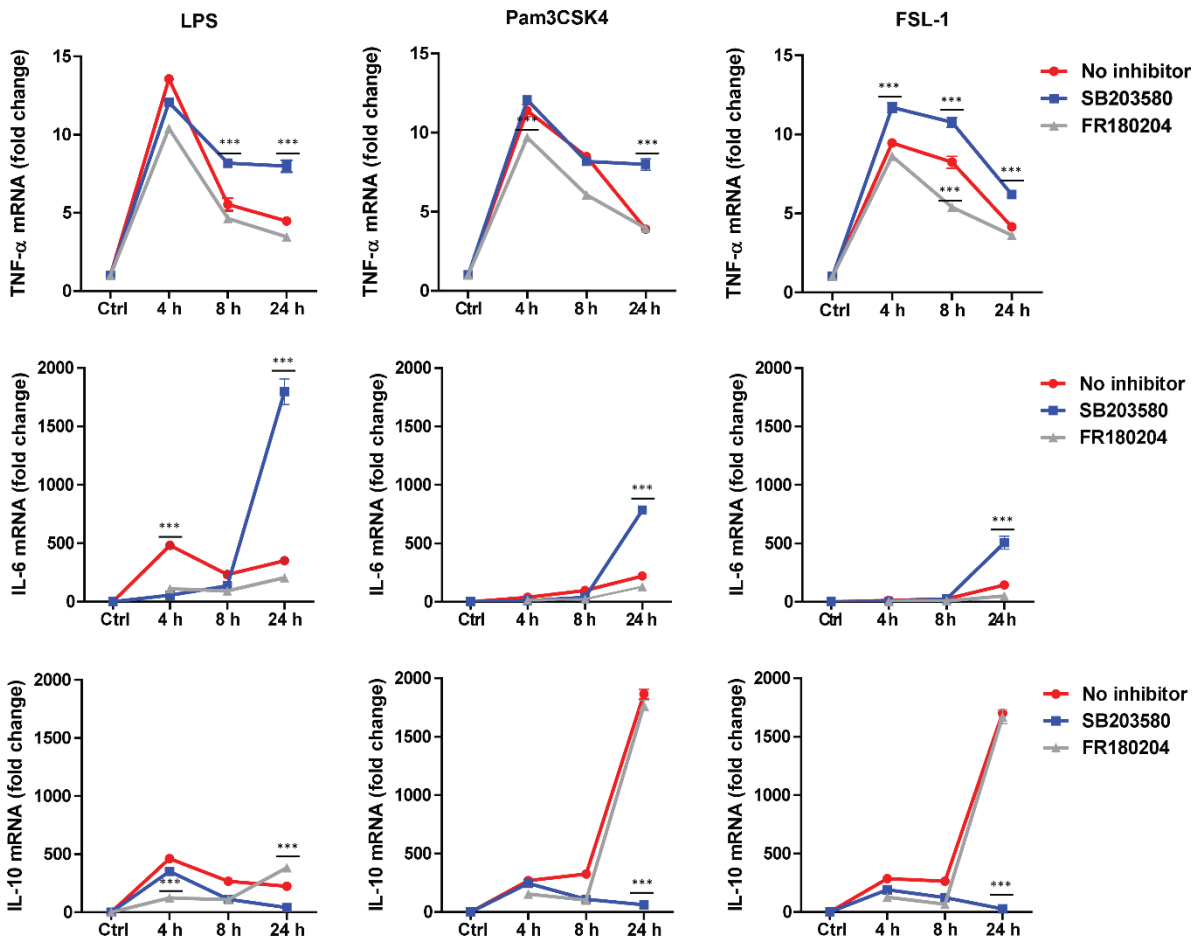

Fig. 19 p38 contributes for later IL-10 production in response to TLR ligands in Raw264.7 cells.

Raw264.7 cells were pre-treated with 10 µM SB203580 or 10 µM of FR180204 for 30 min and then stimulated with LPS (100 ng/mL), Pam3CSK4 (1 µg/mL) and FSL-1 (100 ng/mL) for 24 hours. Cytokines mRNA expression was assayed by quantitative RT-PCR, normalized to GAPDH, and presented relative to unstimulated cells. Protein levels were also measured by ELISA. Data are representative of two independent experiments (mean ± SEM.) (*$p < 0.05$, **$p < 0.01$, and ***$p < 0.001$).

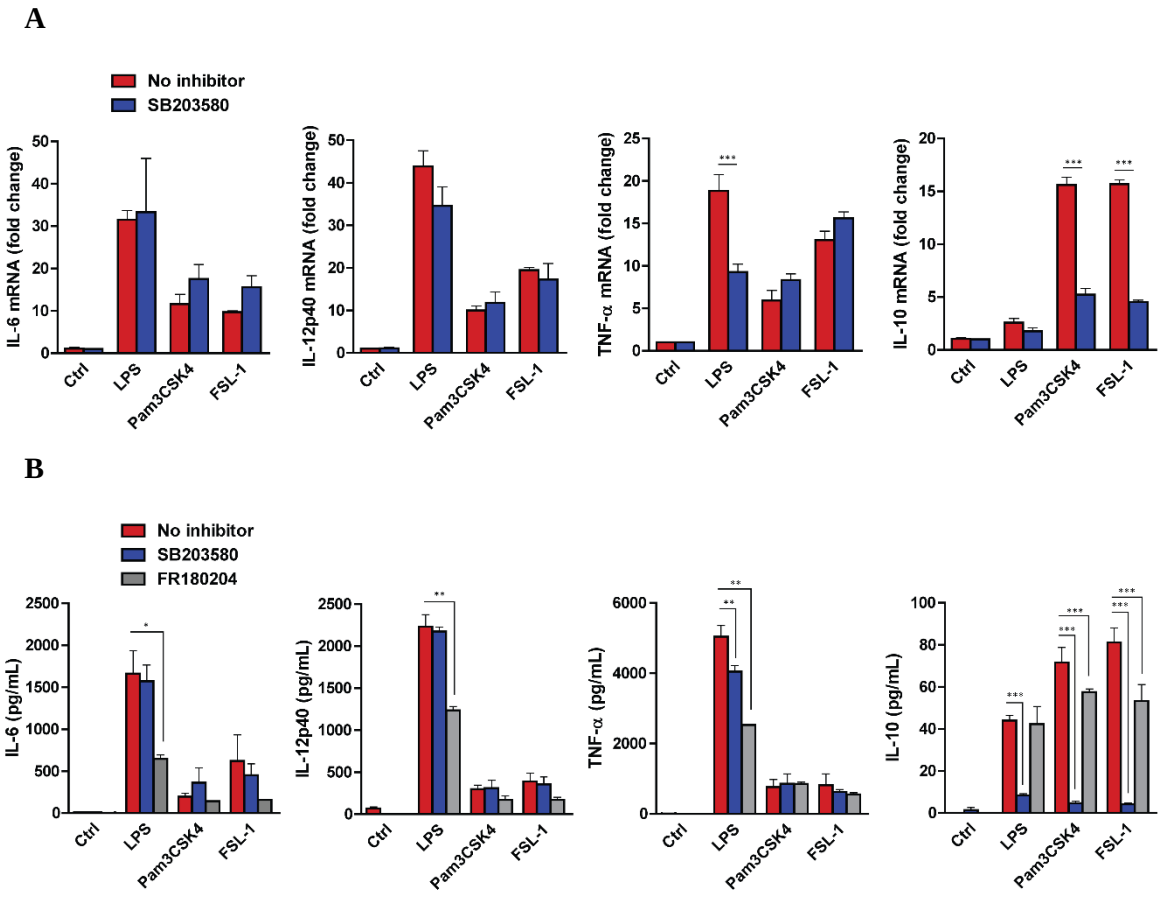

Fig. 20 p38 contributes for later IL-10 production in response to TLR ligands, in peritoneal macrophages.

Peritoneal macrophages were pre-treated with 10 µM SB203580 or 10 µM FR180204 for 30 min and then stimulated with LPS (100 ng/mL), Pam3CSK4 (1 µg/mL) and FSL-1 (100 ng/mL) for 24 hours. **A)** Cytokine mRNA levels and **B)** Cytokine protein levels were measured by qPCR and ELISA. Data are representative of three independent experiments (mean ± SEM.) (*$p < 0.05$, **$p < 0.01$, and ***$p < 0.001$).

4.2 CHAPTER 2: TRIF-IFN-β signaling dependence in TLR2 inflammatory responses

4.2.1 TLR2 ligands induce type I interferon in an endocytosis-dependent manner

Over the years, it had been suggested that only TLR4 and the endosomal receptors TLR3 and TLR7 signaling could activate the TRIF-IFN-β signaling pathway. However, recent published work from Dietrich et al and Stack et al show that TLR2 ligands are also capable of inducing the mediator IFN-β in bone marrow-derived macrophages (Dietrich et al., 2010; Stack et al., 2014). Given this, type I IFN activation by TLR2 ligands was explored in other macrophages subtypes, in this case peritoneal macrophages as well as in the mouse cell line Raw264.7.

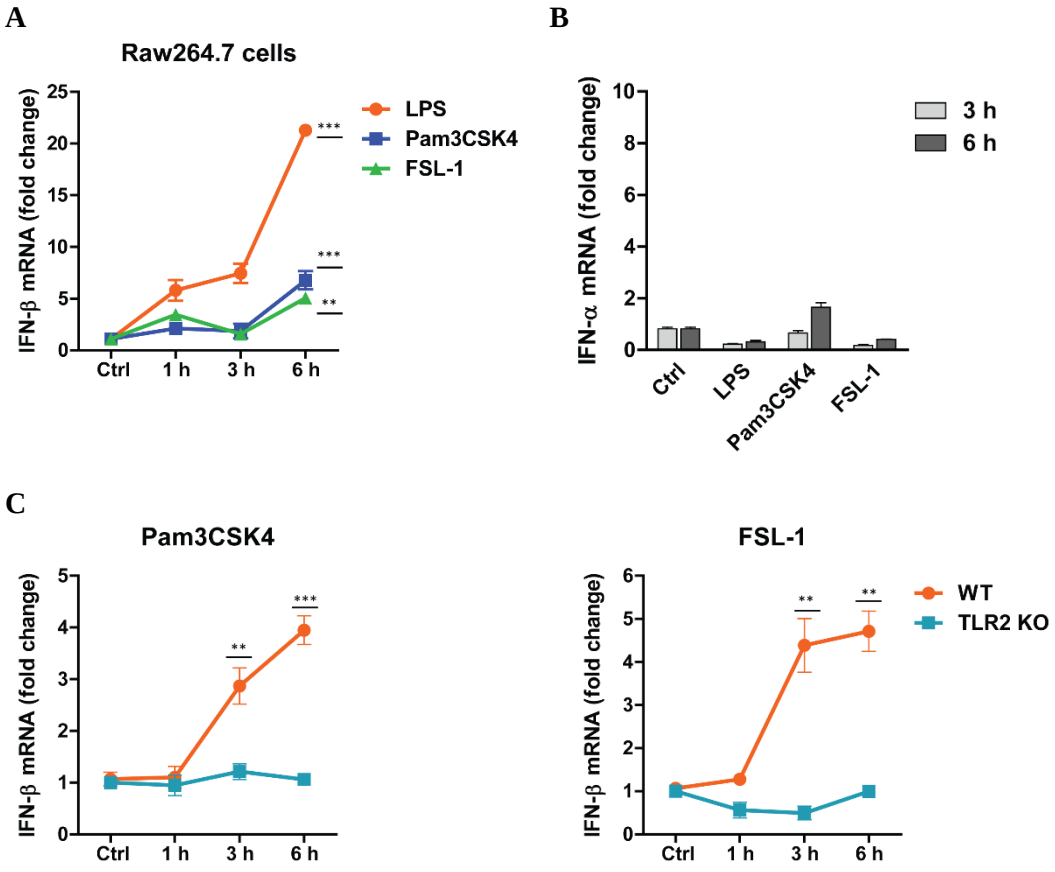

Fig. 21 TLR2 ligands induce IFN-β in the Raw264.7 cell line and in peritoneal macrophages.
A) Raw264.7 cells were stimulated with LPS (100 ng/mL), Pam3CSK4 (1 µg/mL) and FSL-1 (100 ng/mL) for the different times indicated. **B)** WT peritoneal macrophages were stimulated with the three ligands for 2 and 6 hours. **C)** WT and TLR2 KO peritoneal macrophages were stimulated with the three ligands for the different times indicated. IFN-α/β mRNA levels were assayed by quantitative RT-PCR. The results are shown as mean ± SEM of two independent experiments (* $p<0.05$, ** $p<0.01$, and *** $p<0.001$).

A time course analysis was performed to determine the kinetics of IFN-β gene induction by stimulation of Raw264.7 cells with LPS, Pam3CSK4 and FSL-1 for 1, 3 and 6 hours. LPS induced transcription of IFN-β, which increased along the time and at 6 hours IFN-β levels are 4 times more compared to IFN-β induced by TLR2 ligands (Fig. 21A). On the other hand, the isotype IFN-α is not induced by TLR4 and TLR2 ligands (Fig. 21B). Moreover, stimulated peritoneal macrophages induce IFN-β levels at 6 hours in response to Pam3CSK4 and FSL-1 and this IFN-β was specific to TLR2 receptor activation (Fig. 21C). This data suggests that peritoneal macrophages and mouse Raw 264.7 macrophage cell line have a similar response regarding type I IFN induction by TLR2 activation. It is described that LPS-mediated IFN-β induction requires the internalization of TLR4 receptor. The next step was to examine whether IFN-β induction by TLR2 ligands is linked to an endocytosis mechanism.

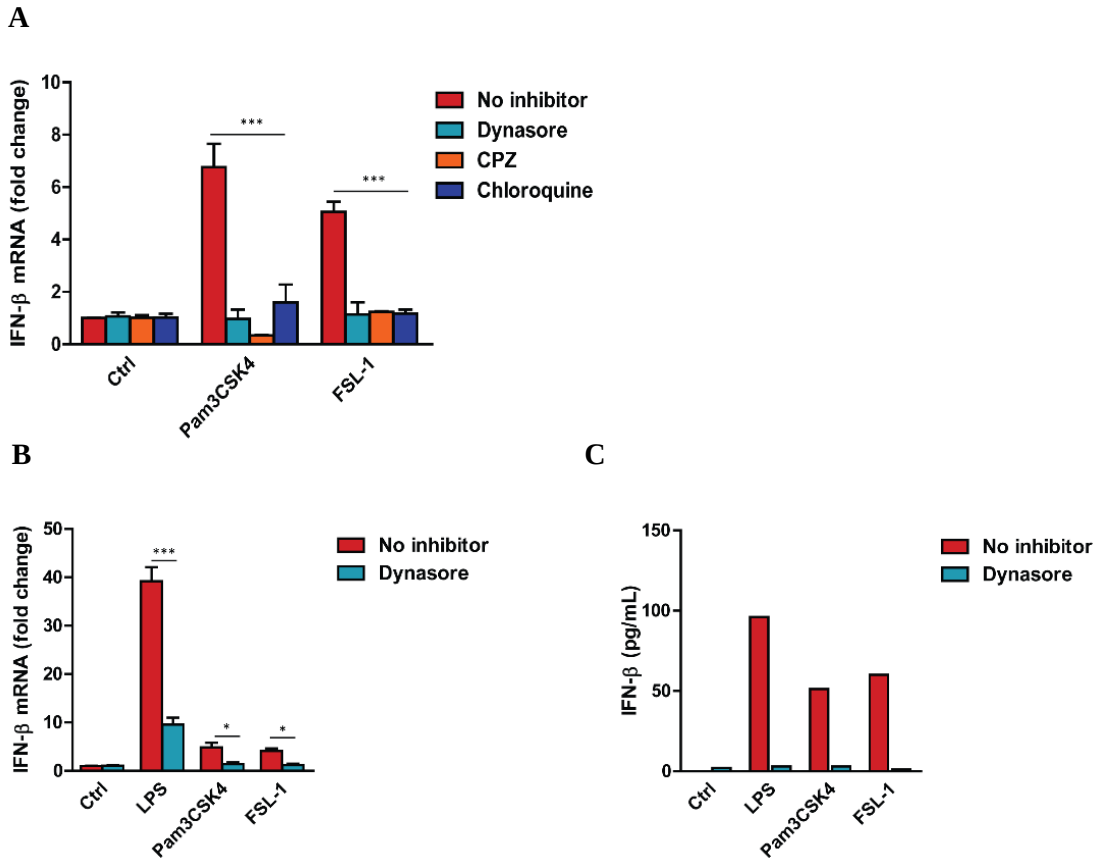

Fig. 22 IFN-β induction by Pam3CSK4 and FSL-1 requires TLR2 internalization

A) Raw264.7 cells were pretreated with 80 µM dynasore, 10 µg/mL chlorpromazine (CPZ) and 100 µM chloroquine. Cells were left unstimulated (Ctrl) or were stimulated with Pam3CSK4 (1 µg/mL) and FSL-1 (100 ng/mL) for 6 hours. The results are shown as mean ± SEM of two independent experiments. **B)** Peritoneal macrophages were pretreated with 80 µM dynasore and stimulated with Pam3CSK4 (1 µg/mL) and FSL-1 (100 ng/mL) for 6 hours. The data is shown as mean ± SEM of three independent experiments (* $p<0.05$, ** $p<0.01$, and *** $p<0.001$). **C)** IFN-β expression from peritoneal macrophages was also measured by ELISA. The results were obtained from one experiment.

Raw264.7 cells were pretreated with three different endocytic inhibitors, dynasore, chlorpromazine and chloroquine. The first two inhibitors disrupt clathrin-dependent endocytosis, although dynasore, a dynamin GTPase inhibitor, is also described to disrupt clathrin non-dependent endocytic pathways. Chloroquine prevented the endosome acidification and subsequent fusion with the lysosomes. The presence of the three inhibitors severely impaired TLR2-driven IFN-β, suggesting that IFN-β was triggered from acidified endosomal compartments (Fig. 22A). Treatment of peritoneal macrophages with dynasore also affected IFN-β production induced by TLR2 ligands (Fig. 22B and 22C). Since IFN-β production in response to TLR2 ligands is dependent of an endocytosis process, TLR2 internalization upon Pam3CSK4 and FSL-1 stimulation of Raw264.7 cells was evaluated (Fig. 23).

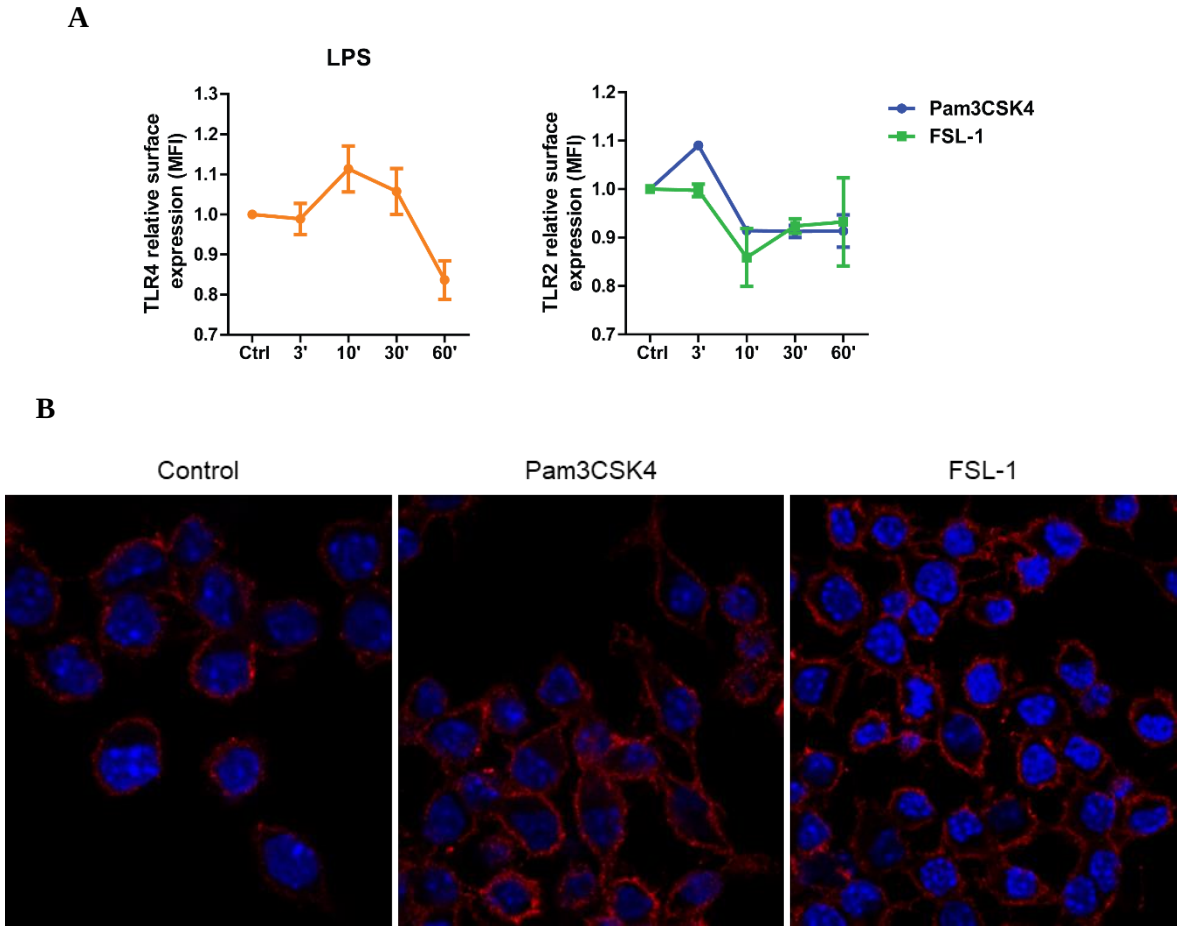

Fig. 23 Pam3CSK4 and FSL-1 induce TLR2 internalization.

A) Raw264.7 cells were left unstimulated (Ctrl) or stimulated with LPS (100 ng/mL), Pam3CSK4 (1 µg/mL) and FSL-1 (100 ng/mL) for 3, 10, 30 and 60 min. Cell surface expression levels of TLR4 or TLR2 are represented as (MFI) mean fluorescence intensity. **B)** Raw264.7 cells were left unstimulated (Control) or were stimulated with Pam3CSK4 (1 µg/mL) and FSL-1 (100 ng/mL) for 3 min, stained with Anti-TLR2 (red) and imaged by confocal microscopy. The images are representative of two independent experiments.

Cells were stimulated with LPS and TLR4 uptake was addressed as a reference. Upon stimulation with LPS, TLR4 cell surface levels increased at 3 min and reached a peak at around 10 min, followed by internalization after 30 min (Fig. 23A). TLR2 ligands, mainly Pam3CSK4 induced a slight but faster increase in TLR2 surface expression followed by a rapid uptake 3 min after stimulation. After 10 min a slow increase of TLR2 levels at the surface extended along the time. In addition, through immunofluorescence, Pam3CSK4 and FSL-1-stiumlated cells showed higher TLR2 localization at the cell surface, as well as some present in the cytoplasm, compared with non-stimulated cells (Fig. 23B). Therefore, as it occurs for TLR4, TLR2 is also internalized upon stimulation, however this process occurs earlier and at a lesser extent as for TLR4.

4.2.2.1 TLR2 ligands activate IRF3, IRF7 and IFN-β mediated in part by TRIF

The transcription of IFN-β depends on the activation of IRFs (interferon regulatory factors). IRF3 and IRF7 have been implicated in the activation of type I IFN genes in response to TLR4, TLR3 and TLR9, respectively. Previous studies support that IFN-β by TLR2 ligands is IRF7-dependent in BMDMs (Dietrich et al., 2010; Nilsen et al., 2015; Stack et al., 2014) and that FSL-1 induces IRF3 and IRF7 phosphorylation in the Raw264.7 cell line. However, so far it was not addressed the activation of IRF3 or IRF7 by TLR2 signaling in peritoneal macrophages. Our results show that LPS induces IRF3 activation in peritoneal macrophages, observing higher levels of phosphorylation at 30 and 60 min (Fig. 24A). Pam3CSK4 activates higher p-IRF3 levels mainly at 30 min and FSL-1induces IRF3 phosphorylation earlier, however the phosphorylation levels obtained are lower compared to LPS and Pam3CSK4 stimulation. Thus, FSL-1 is a weaker IRF3 inducer compare to the other ligands. In addition, a similar pattern was observed for IRF7 activation in response to LPS, observing higher levels of IRF7 phosphorylation at 60 min. On the other hand, Pam3CSK4 showed high activation of IRF7 at 30 min and FSL-1 showed higher levels of phosphorylated IRF7 at 3, 10 and 30 min compared with the other ligands. Therefore, FSL-1 exhibits a weaker activation of IRF3 phosphorylation but a faster induction of IRF7 phosphorylation. To ensure these observations were not due to possible LPS contamination in TLR2 ligand preparations, the same experiment was performed in TLR4 KO peritoneal macrophages (Fig 24B). IRF3 and IRF7 phosphorylation was impaired in LPS-stimulated cells deficient in TLR4, but detectable in response to TLR2 ligands, thus confirming a TLR2 specific response. Furthermore, Raw264.7 cells stimulated with Pam3CSK4 and FSL-1 ligands induced IRF3 phosphorylation in Ser 396 at 30 min, although to a lesser extent compared to LPS stimulation, which was observed at 60 min (Fig. 24C). Therefore, in addition to LPS, TLR2 ligands can induce the phosphorylation of IRF3 and IRF7 in primary macrophages and in the Raw264.7 cell line, however, IRF3 activation mediated by TLR2 ligands is weaker compared to LPS.

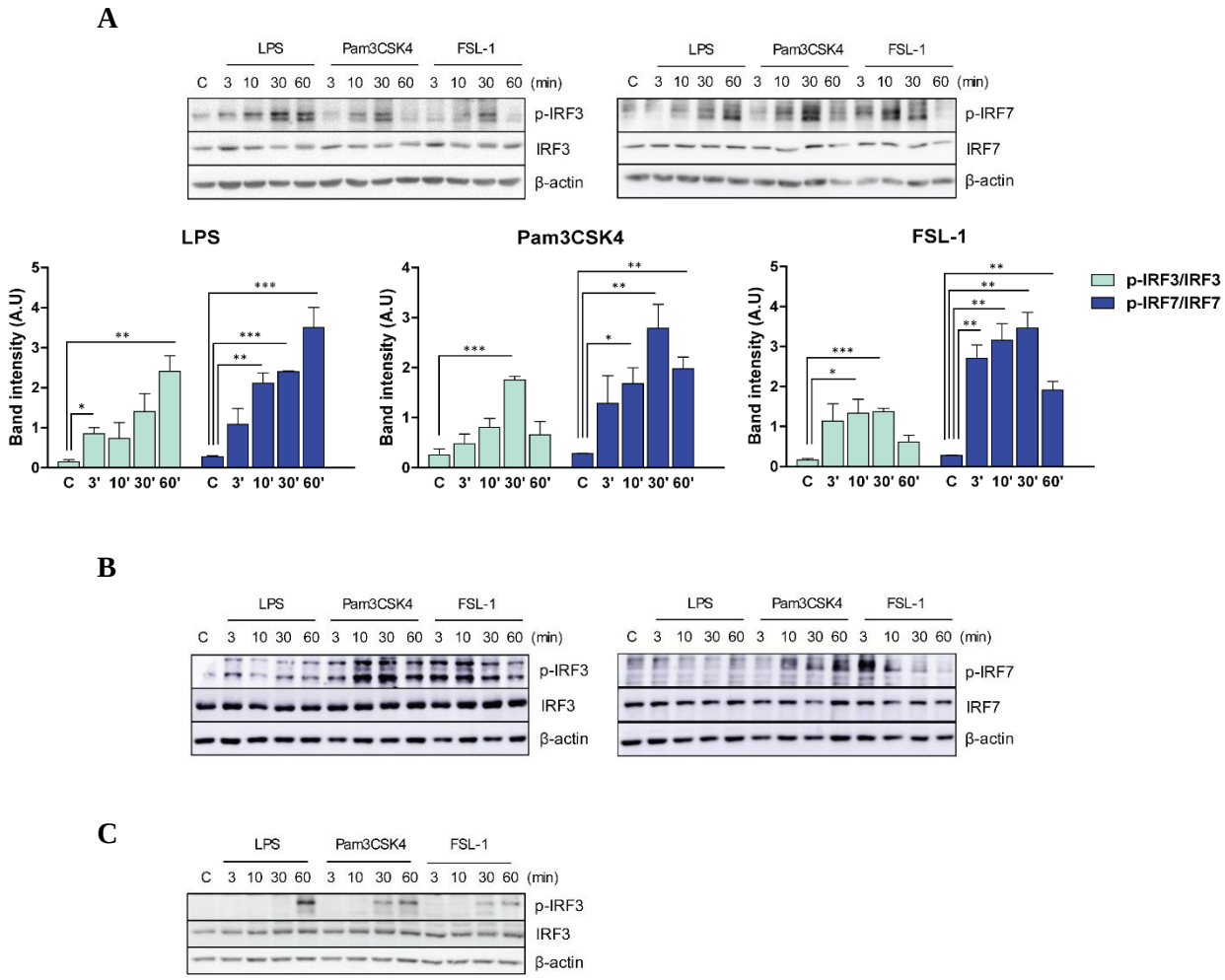

Fig. 24 TLR2 ligands activate IRF3 and IRF7 in peritoneal macrophages and in the Raw264.7 cell line.

A) WT peritoneal macrophages were left unstimulated (c) or stimulated with LPS (100 ng/mL), Pam3CSK4 (1 µg/mL) and FSL-1 (100 ng/mL) for 3, 10, 30 and 60 min. Graphics show quantification of band intensities of the upper western blots. The values of p-IRF3 and p-IRF7 bands were normalized to the total IRF3 and IRF7 protein respectively. Data are representative of three independent experiments (mean ± SEM.) (*p < 0.05, **p < 0.01, and ***p < 0.001). **B)** TLR4 KO peritoneal macrophages were left unstimulated (c) or stimulated with LPS (100 ng/mL), Pam3CSK4 (1 µg/mL) and FSL-1 (100 ng/mL) for 3, 10, 30 and 60 min. Images are representative of two independent experiments. **C)** Raw264.7 cells were unstimulated (c) or stimulated with LPS (100 ng/mL), Pam3CSK4 (1 µg/mL) and FSL-1 (100 ng/mL) for 3, 10, 30 and 60 min.

Furthermore, to determine the endocytosis dependency for IRF3 and IRF7 activation by TLR2 ligands, WT peritoneal macrophages were pretreated with dynasore (Fig 25). IRF3 and IRF7 phosphorylation was blocked by dynasore in response to LPS. In Pam3CSK4 and FSL-1-stimulated cells, IRF3 and IRF7 phosphorylation was impaired by dynasore, mainly at 10 and 30 min. Thus, similar to TLR4, the TLR2 signaling requires endocytosis to activate IRF3 and IRF7.

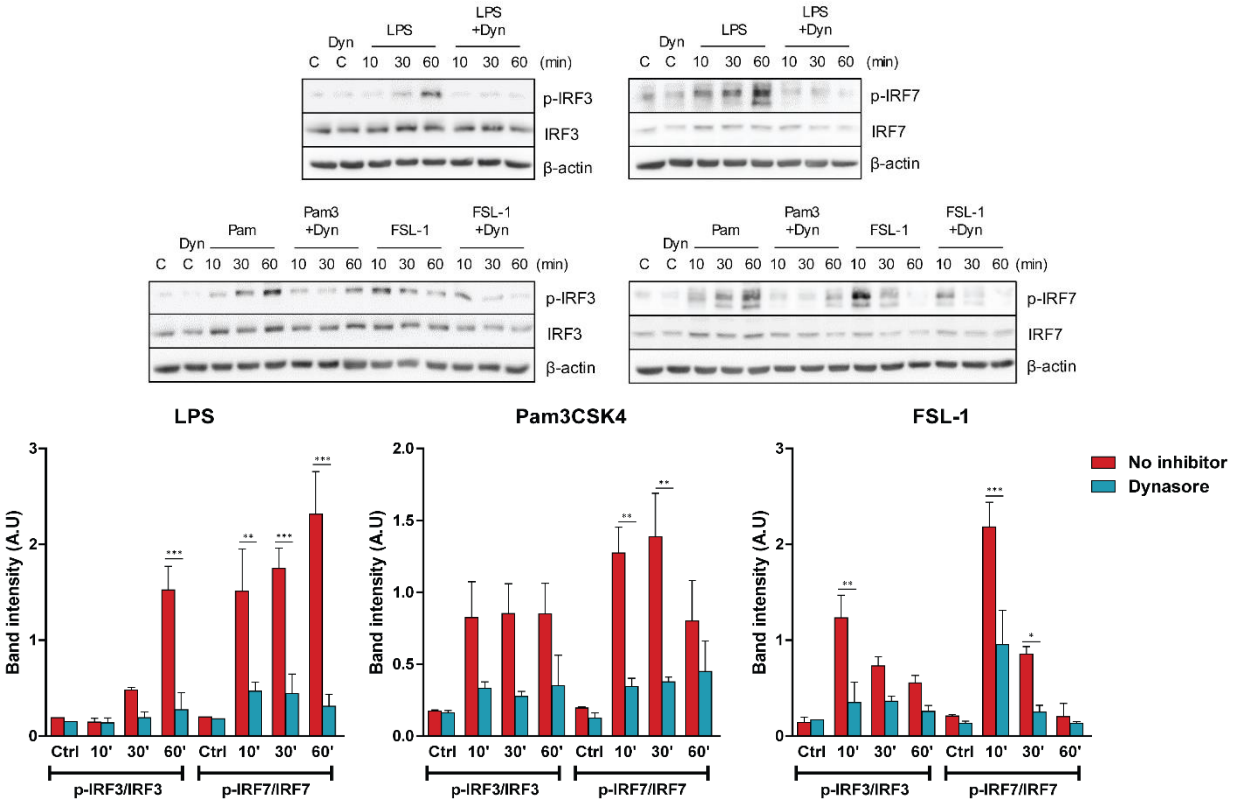

Fig. 25 TLR2- induced IRF3 and IRF7 phosphorylation is dependent of receptor endocytosis.

Peritoneal macrophages were pretreated with 80 μM dynasore ("Dyn") for 30 min and then stimulated with LPS and TLR2 ligands. Graphics show quantification of band intensities of the upper western blots. The values of p-IRF3 and p-IRF7 bands were normalized to the total IRF3 and IRF7 protein respectively. Data are representative of two independent experiments (mean ± SEM.) (*p < 0.05, **p < 0.01, and ***p < 0.001).

The activation of these transcription factors was also evaluated in bone marrow-derived macrophages. LPS induced IRF3 and IRF7 activation (Fig. 26), however, IRF3 phosphorylation was weakly induced by Pam3CSK4 and FSL-1. In addition, LPS induced IRF7 phosphorylation mainly at 60 min, whereas IRF7 phosphorylation is observed earlier at 10 min and maintains up to 60 min in response to TLR2 ligands. Furthermore, TRIF dependency for IRFs activation was evaluated. In TRIF-deficient macrophages, IRF3 and IRF7 phosphorylation was abrogated in response to stimuli. Thus, this data indicates that activation of these transcription factors is dependent of TRIF adaptor.

Previous studies reported that TLR4 activation induces IFN-β expression via TRIF signaling (Kagan et al., 2008). Therefore, the role of TRIF in IFN-production mediated by TLR2 ligands was accessed (Fig. 27). LPS-induced IFN-β transcription and expression was fully abolished in TRIF KO macrophages at 3 and 6 hours. In contrast, IFN-β was partially impaired in response to Pam3CSK4 at 3 and 6 hours, and a complete downregulation was observed for FSL-1-induced IFN-β at 6 hours (Fig. 27A and 27B). These results imply that IFN-β induction by TLR2 ligands is driven in part by TRIF activation and other pathways are likely contributing for the IFN expression at earlier stages (≤ 3 hours).

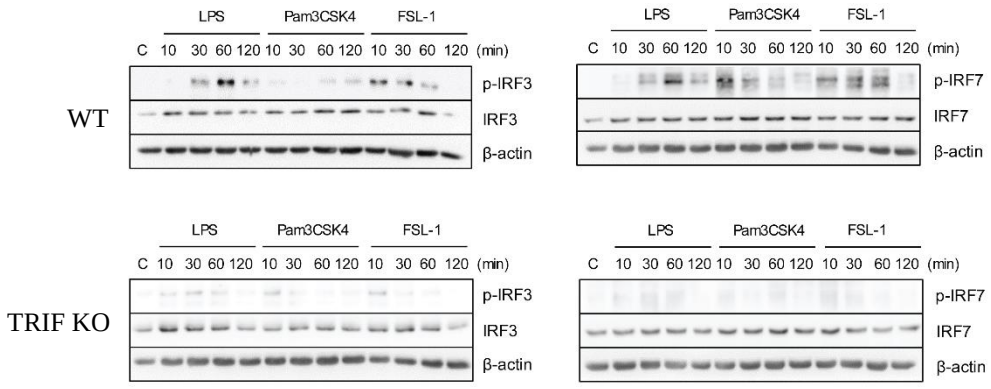

Fig. 26 TLR2 ligands activate IRF3 and IRF7 in bone marrow-derived macrophages, mediated by TRIF activation. WT and TRIF KO bone marrow-derived macrophages were left unstimulated (C) or stimulated with LPS, Pam3CSK4 and FSL-1 for 10, 30, 60 and 120 min. The images are representative of two independent experiments.

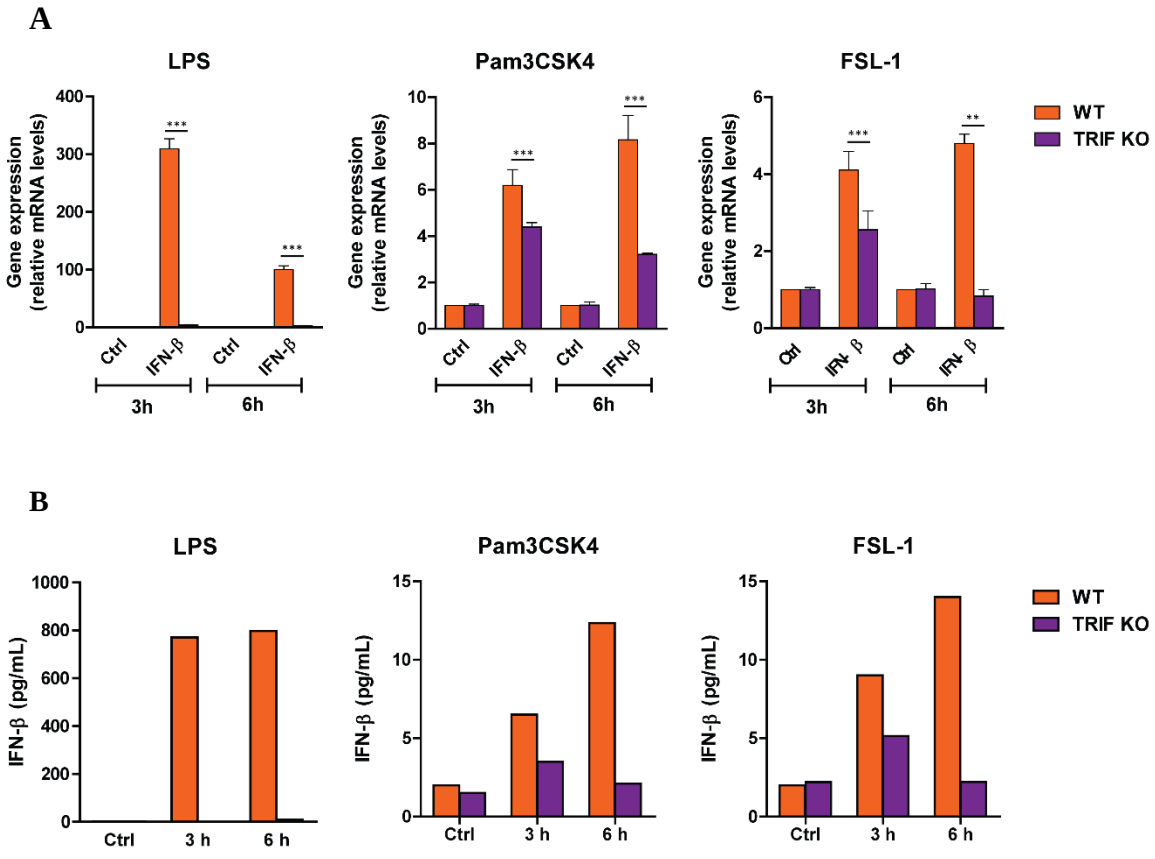

Fig. 27 TLR2 ligands induce IFN-β mediated in part by TRIF activation.

A) WT and TRIF KO bone marrow-derived macrophages were stimulated with LPS, Pam3CSK4 and FSL-1 for 3 and 6 hours and cytokine's mRNA transcription was assayed by quantitative RT-PCR. The results are shown as mean ± SEM of two independent experiments (* $p<0.05$, ** $p<0.01$, and *** $p<0.001$). **B)** IFN-β expression was also measured by ELISA. The graphic shows the results of one experiment

4.2.2.2 TRIF-IFN-β signaling pathway contributes to macrophage inflammatory response via TLR2 activation

TRIF-IFN-β signaling mediated by TLR4 is described to be important for the induction of pro and anti-inflammatory cytokines. Therefore, the involvement of the TRIF pathway in the regulation of TLR2-induced cytokines was determined (Fig. 28).

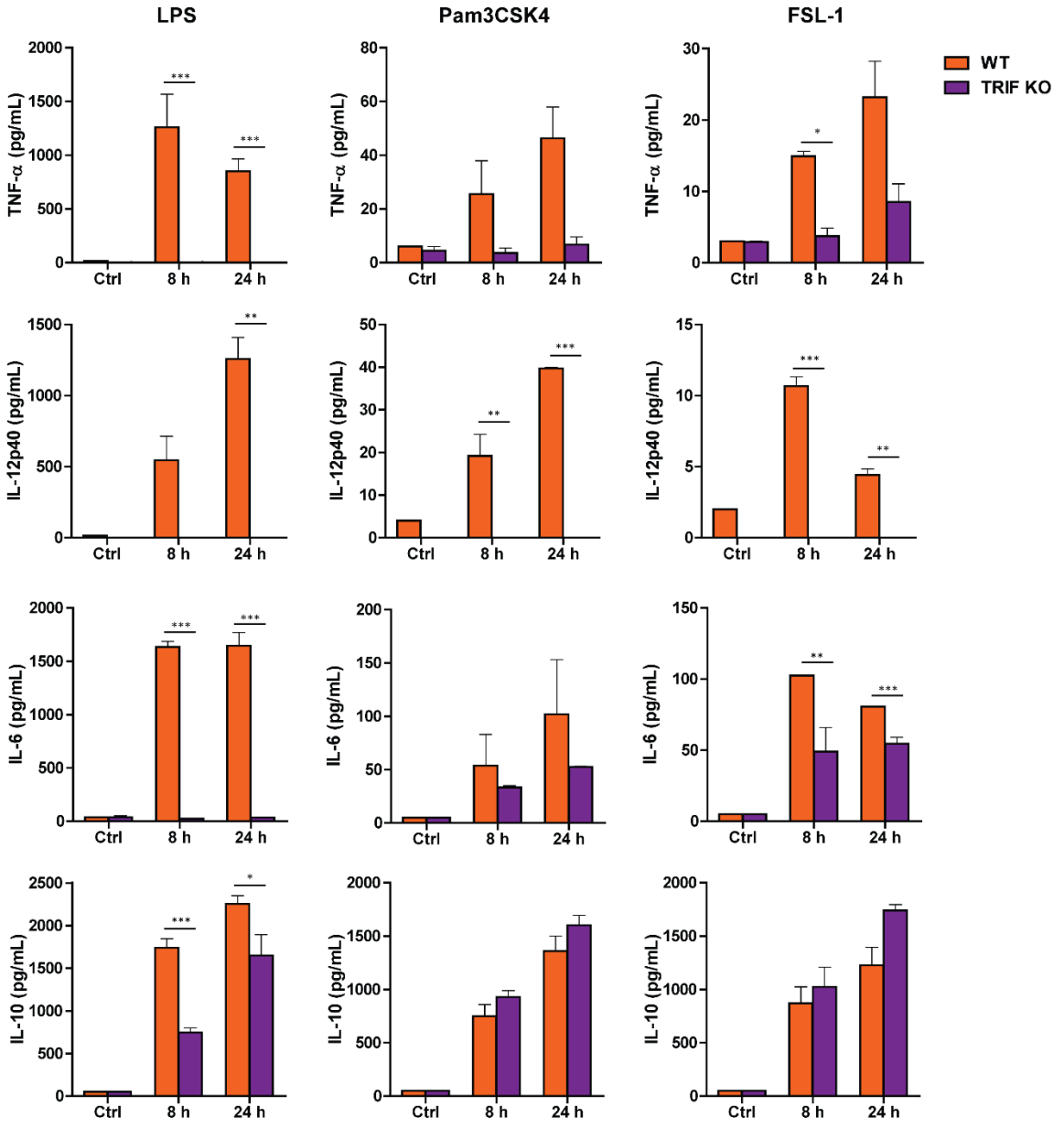

Fig. 28 TLR2 ligands induce pro-inflammatory cytokines, in part, mediated by TRIF activation.
WT and TRIF KO bone marrow-derived macrophages were stimulated with LPS, Pam3CSK4 and FSL-1 for 8 and 24 hours. Protein levels were measured by ELISA. The results are shown as mean ± SEM and are representative of three independent experiments (* $p<0.05$, ** $p<0.01$, and *** $p<0.001$).

LPS-stimulated TRIF KO macrophages displayed fully downregulation of the cytokines IL-12p40, IL-16 and TNF-α, while IL-10 was partially affected at 8 hours, and no differences were observed at 24 hours relatively to the WT cells. Moreover, Pam3CSK4 and FSL-1 responses in TRIF deficient macrophages were similar between both.

Specifically, TNF-α and mainly IL-12p40 induction was strongly impaired in TRIF KO macrophages, whereas IL-6 production was partially impaired and IL-10 was not affected. Therefore, at later stages of inflammation, unlike LPS, which strongly depends in the TRIF pathway for pro-inflammatory cytokine induction, TLR2 ligands depend mostly of TRIF for TNF-α and IL-12p40 induction.

To determine whether IFN-β per se contributes for TLR2-mediated cytokine induction, Raw264.7 cells were pretreated with a blocking antibody against IFN-β and consequently stimulated with TLR2 ligands (Fig. 9). IL-12 mRNA was strongly inhibited in the presence of the antibody, whereas IL-6 and IL-10 where only partially decreased. Therefore, TLR2-mediated TRIF-IFN-β signaling pathway plays an important role in late inflammatory response, mainly for IL-12p40 induction.

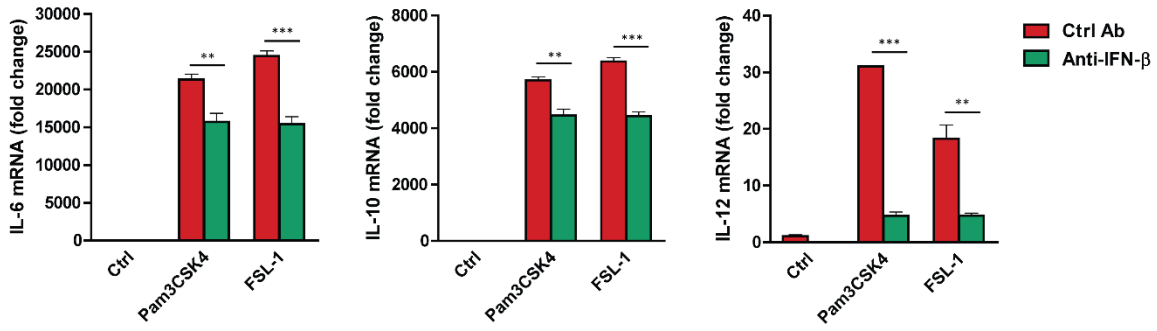

Fig. 29 IFN-β contributes to macrophage inflammatory response via TLR2 activation.

Raw264.7 cells were stimulated with Pam3CSK4 or FSL-1 for 24h in the presence of Ctrl Ab or 25 µg/mL anti-IFN-β. IL-12, IL-6 and IL-10 transcription was measured by qPCR. Results are shown as mean ± SEM of two independent experiments (* $p<0.05$, ** $p<0.01$, and *** $p<0.001$).

4.2.2 Effect of TLR2 ligand FSL-1 administration in neonatal listeriosis

Previous studies demonstrate that the PGN deacetylation of *Listeria monocytogenes* by the deacetylase pgdA avoids its degradation and the release of PAMPs (PGN, lipoproteins, LTA) recognized by TLR2 and NOD1/NOD2. Indeed, *Listeria* pgdA mutants induced a stronger IFN-β production compared to the WT strain, which was shown to be mediated by TLR2-TRIF signaling (Aubry et al., 2012; Boneca et al., 2007). Moreover, the timing of IFN-β production in response to *Listeria* is determinant to control the bacteria infection (Pontiroli et al., 2012). Our results show that TLR2 ligands can induce IFN-β expression and a previous study reported that diacylated lipoproteins are found in *Listeria monocytogenes* cell wall (Kurokawa et al., 2012). Therefore, since FSL-1 is a diacylated lipopeptide, a mouse model of neonatal listeriosis was developed to study the immunomodulatory and protective

effect of FSL-1 in Listeria infection (Fig 30). Pregnant mice were challenged intravenously with *L. monocytogenes* and with FSL-1 simultaneously. Four-day old neonates were chosen as they correspond to 1-month age in human neonates.

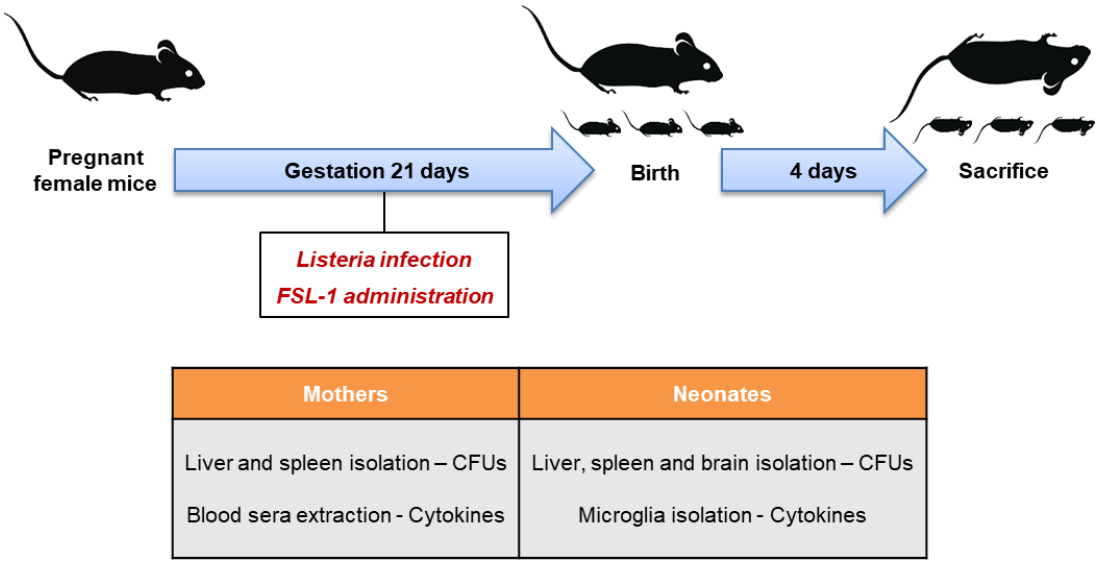

Fig. 30 Mouse model of neonatal listeriosis.

Pregnant mice were inoculated with *Listeria monocytogenes* during gestation phase and FSL-1 ligand was administered simultaneously. Organs from mothers and neonates were extracted after scarification to carry out the experiments.

Physical appearance and motility of neonates from infected mothers and infected and treated mothers was monitored during the birthday and four days after birth (Fig. 31). Previous data demonstrate that in the mouse model of neonatal listeriosis, infected mothers give birth to 2-4 pups whereas non-infected mothers present 6-9 pups per litter (Calderon-Gonzalez et al., 2017). In our hands, infected mothers gave birth to 4 pups whereas treated mothers gave birth to 5 pups. At day 4, the neonates survived from infected mothers as well as from treated mothers. FSL-1 treatment showed no improved effect in the birth number of neonates from infected mothers. However, at day 4, white spots due to lack of pigmentation and reduced movement were noticed in neonates from infected mothers, whereas these symptoms where not detected in neonates from treated mothers (Fig. 31A). Moreover, neonates from infected mothers showed lack of brain integrity compared to neonates from treated mothers (Fig. 31B). In addition, infected mothers showed fetal reabsorptions in the uterus, which were not visible in treated mothers (Fig. 31C). These data indicate that albeit FSL-1 treatment does not prevent the stillbirth in infected mothers, it confers some preventive effect on neonate brain disease.

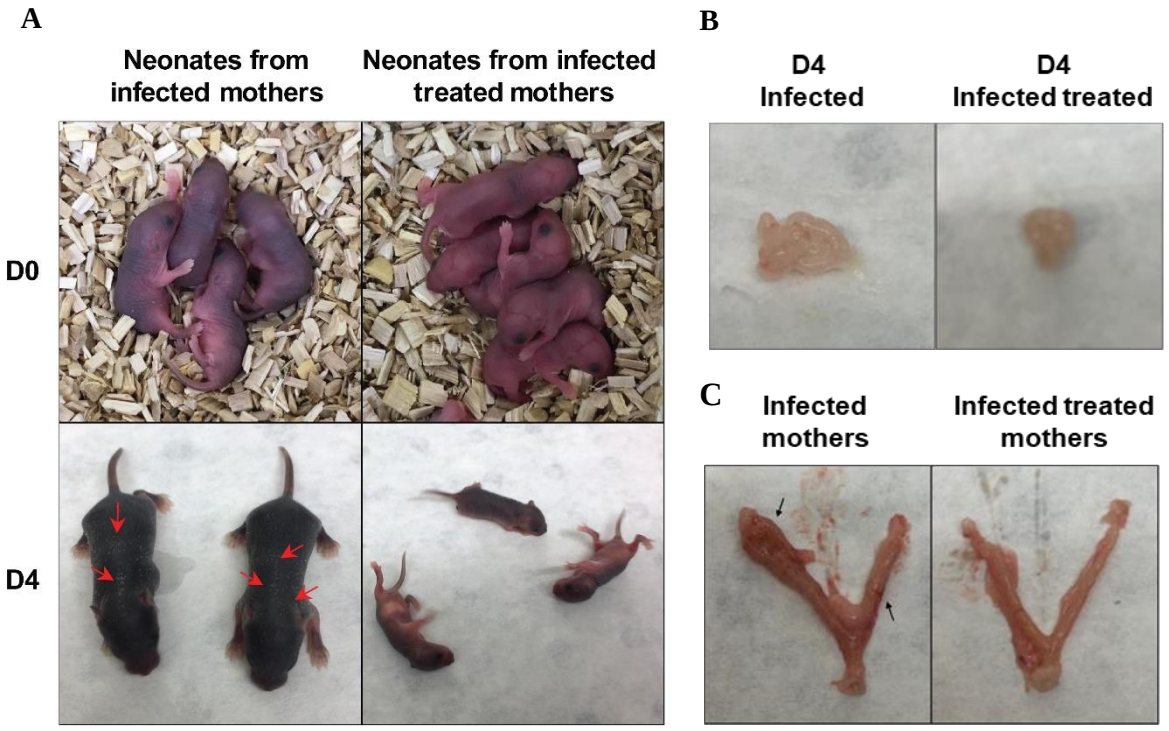

Fig. 31 Physical appearance of neonates from *Listeria* infected mothers and FSL-1 treated mothers at **birth (D0) and 4 days after birth (D4).**

A) Comparison of D0 neonates and D4 neonates from infected and infected treated mothers for physical and motility appearance. **B)** Brains isolated from D4 neonates of infected and infected treated mothers **C)** Uterus appearance from infected and infected treated mothers.

4.2.2.1 FSL-1 treatment decreases organ bacteria load in neonates and mothers

Reported studies demonstrate that TLR2-deficient mice show increased susceptibility to *Listeria* infection (Torres et al., 2004). In addition, our results demonstrated that FSL-1 administration in pregnant mice partially prevents the common clinical symptoms in neonatal listeriosis. Therefore, the effect of FSL-1 in organ bacterial clearance in the livers, spleen and brain of infected, treated mothers and neonates was analyzed (Fig. 32). Treated mothers displayed a 10 and 15-fold reduction of CFU counts in the liver and spleen respectively, compared to infected mothers. On the other hand, no difference in bacteria load was apparent in the liver of D4 neonates from infected and treated mothers. Neonates from treated mothers displayed a slight decrease in spleen bacteria load but the brain bacterial burden was reduced by 100-fold compared to neonates from infected mothers. These results demonstrate that the protective action of FSL-1 for both mothers and neonates Listeria infection is only partially due to the reduction of bacterial growth. This implies that additional mechanisms can contribute for the effects of FSL-1 treatment.

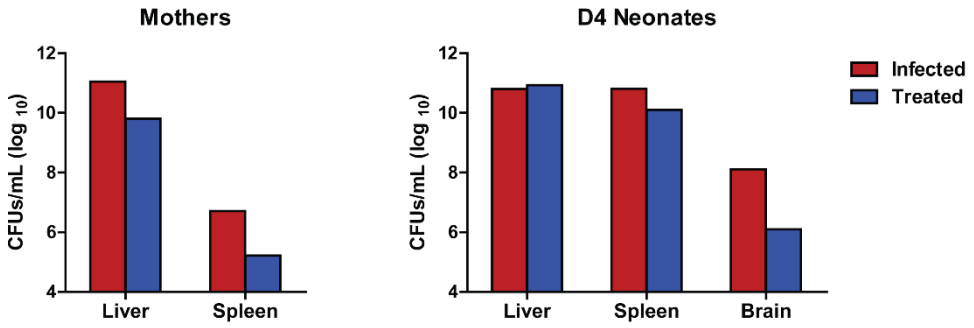

Fig. 32 Bacterial burden in distinct organs of mothers and D4 neonates.

Organs were extracted (2 mothers or 2 neonates per condition), homogenized and pooled for CFU counting. Results are expressed as CFUs/mL.

4.2.2.2 FSL-1 treatment increases IFN-β expression in *Listeria*-infected neonate's microglia

Inflammatory cytokines such as IFN-γ, TNF-α and IL-12p40 produced by NK cells, macrophages and DCs are critical for controlling a primary *L. monocytogenes* infection (Edelson and Unanue, 2000). Therefore, the effect of FSL-1 treatment in cytokine expression during the infection in mothers and neonates was evaluated (Fig. 33).

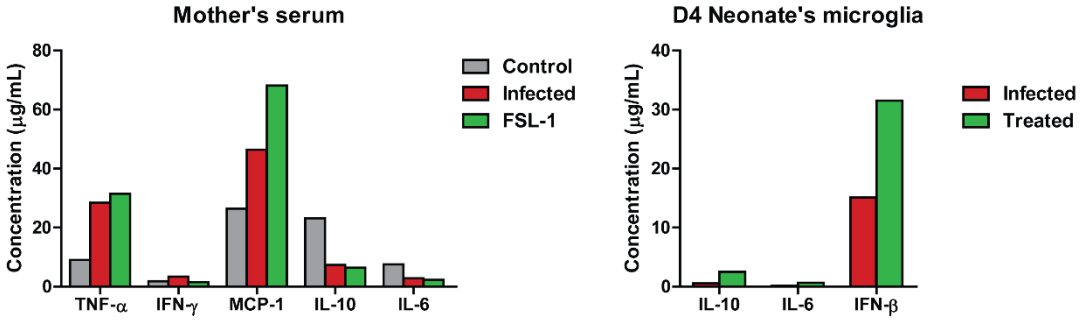

Fig. 33 FSL-1 treatment increases IFN-β expression in infected neonate's microglia.

Cytokine expression levels in serum from infected and treated mothers (1 mother per condition) and from D4 neonates' microglia supernatants (microglia from 3 neonates oer condition). Graphics are representative of one experiment.

Serum TNF-α and IFN-γ levels are similar from infected and treated mothers and TNF-α levels are higher compared to the control group, whereas IL-6 and IL-10 are reduced compared to the control group. On the other hand, MCP-1, a chemokine that recruits monocytes and dendritic cells to the sites of infection, showed high expression levels in infected mothers compared to non-infected cells and FSL-1 treatment increased its production. On the other hand, microglia of D4 neonates from infected mothers exhibited very low levels of IL-10, IL-6 but some expression of IFN-β, which was higher in neonates from treated mothers. These data correlate with the previous results where TLR2 ligands

induce IFN-β in macrophages. Overall, these results imply that *in vivo* FSL-1 treatment favors a Th1 response in *Listeria* infected mothers and particularly an increase in IFN-β expression in infected neonate's microglia.

4.2.2.3 TLR2 ligands induce the expression of IL-12 and IFN-β in *Listeria*-infected dendritic cells

In view of the FSL-1 beneficial role in the prevention of neonatal listeriosis symptoms and the IFN-β increment in the microglia of neonates from treated mothers, the modulatory effect of TLR2 ligands on cytokine's expression was further explored in *Listeria*-infected dendritic cells. One hour after bacterial infection, dendritic cells were stimulated with Pam3CSK4, FSL-1, IV1303 (Fig 34).

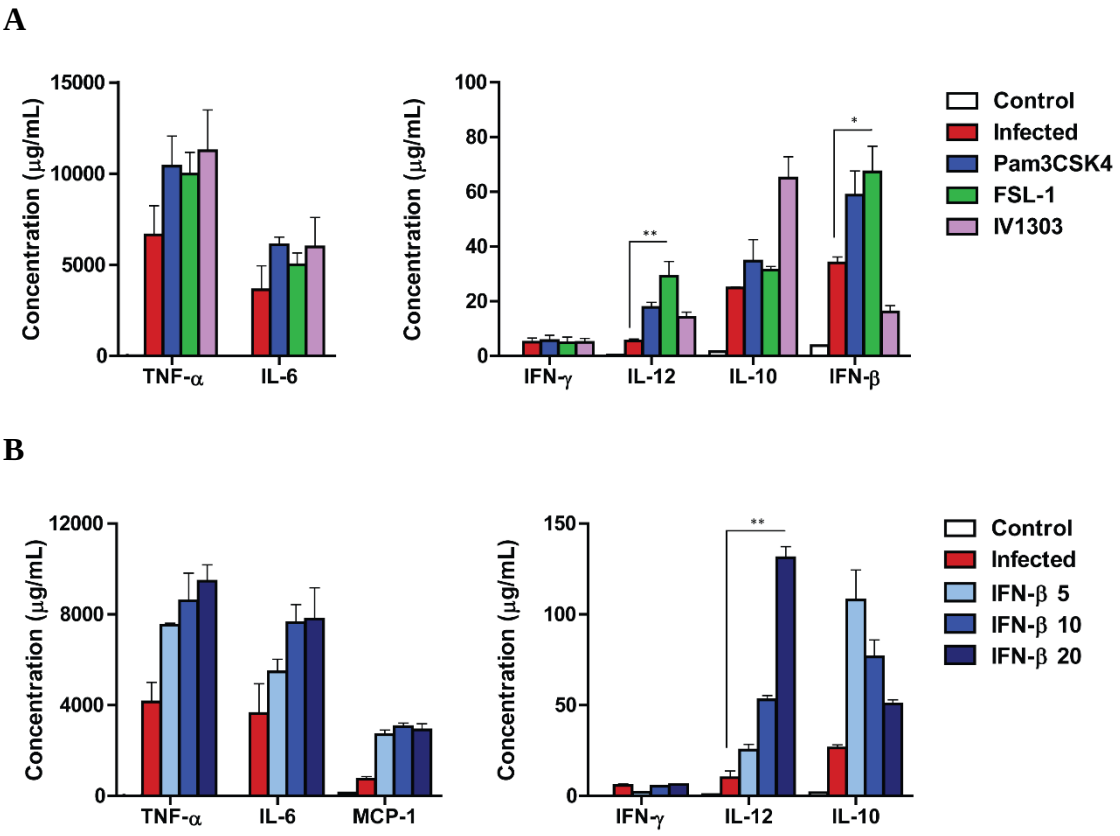

Fig. 34 TLR2 ligands increase Th1 cytokines IL-12 and IFN-β in *Listeria*-infected dendritic cells

Dendritic cells were infected with *Listeria* for 1 hour (infected) or infected and treated with: **A)** Pam3CSK4, FSL-1and IV1303; **B)** incremental doses of recombinant mouse IFN-β (5, 10 and 20 ng/mL). All treatments were performed for 24 hours and cell supernatants were used for cytokine quantification by CBA. Results are shown as mean ± SEM of three independent experiments (* $p<0.05$, ** $p<0.01$, and *** $p<0.001$).

.

IV1303 is a compound previously described as an adjuvant that elicits a protective Th1 response in neonatal listeriosis (Calderon-Gonzalez et al., 2017). Therefore, this compound was used as reference. Infected DCs showed strong expression levels of TNF-α and IL-6 compared to non-infected cells (Fig. 34A). These cytokines together with IL-12 are determinant for macrophage activation and increase of their bactericidal role. Moreover, IL-12, IL-10 and IFN-β expression was also observed in infected DCs. TLR2 ligands treatment showed increased levels of TNF-α and IL-6 and a similar pattern was observed in response to the compound IV1303, compared to infected non-treated DCs. In addition, infected DCs treated with IV1303 presented higher IL-10 expression levels compared to TLR2 ligands. On the other hand, TLR2 ligands administration incremented IL-12 and IFN-β expression in infected cells which was lower in response to IV1303. These results indicate that IV1303 and TLR2 ligands improve Th1 responses due to higher expression levels of pro-inflammatory cytokines (TNF-α, IL-6 and IL-12) However, TLR2 ligands differ due to their higher capacity of inducing IFN-β production

To determine the IFN-β role per se in cytokine regulation, infected DCs were treated with incremental doses of rIFN-β (Fig. 34B). Pro-inflammatory cytokines were found to be dose-dependently increased by an exogenous source of IFN-β, whereas IL-10 expression decreased. This result indicates that IFN-β contributes for pro-inflammatory cytokines induction and downregulates the expression of the anti-inflammatory cytokine IL-10. Given the positive effect of exogenous IFN-β in pro-inflammatory

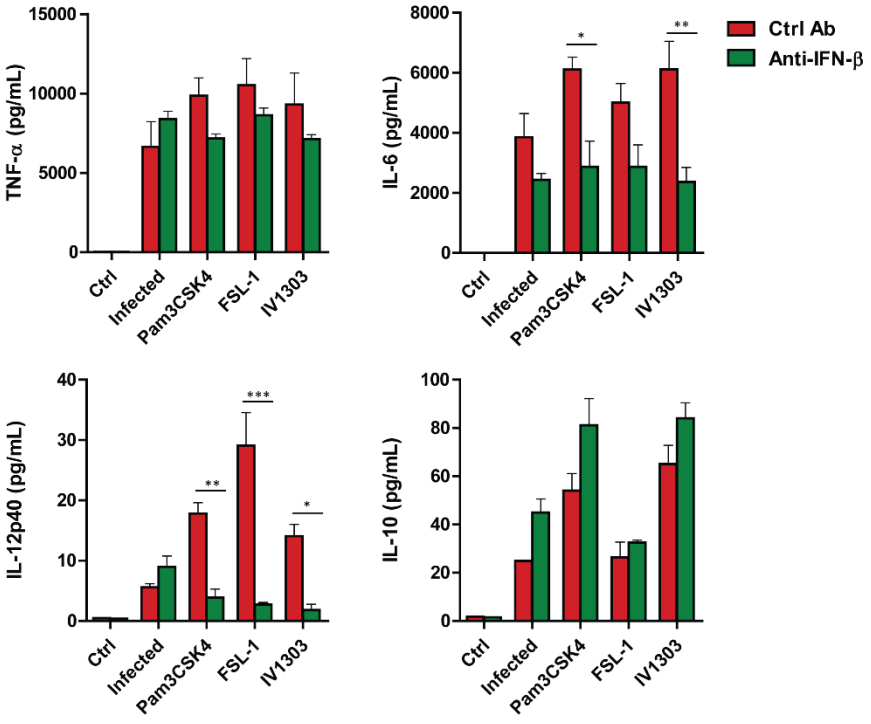

Fig. 35 IFN-β is involved in TLR2- mediated IL-12 induction and IL-10 regulation in *Listeria*-infected dendritic cells. Dendritic cells were left unstimulated (Ctrl) or were stimulated with Pam3CSK4, FSL1 and IV1303 for 24h in the presence of Ctrl Ab or 25 µg/mL anti-IFN-β. Cytokine's expression was measured by CBA. The data is representative of three independent experiments (mean ± SEM) (* $p<0.05$, ** $p<0.01$, and *** $p<0.001$).

cytokines and the regulation of IL-10 expression in infected dendritic cells, it was further studied whether TLR2-induced IFN-β is determinant for the modulatory effect of the cytokines induced in response to TLR2 ligands, during *Listeria* infection (Fig 35).

Infected DCs were pre-treated with a blocking antibody against IFN-β and subsequently stimulated with Pam3SCK4, FSL and IV1303 for 24 hours. Neutralization of IFN-β induced by TLR2 ligands partially downregulates IL-6 and TNF-α, whereas IL-10 expression is not affected. A similar result is observed in response to IV1303. On the other hand, IL-12 cytokine was found to be fully dependent on IFN-β induced by TLR2 ligands and IV1303 in infected dendritic cells. Altogether, the results indicate that TLR2 ligands provide a beneficial effect in neonatal listeriosis, in part by controlling the organ's bacterial growth and by eliciting a Th1 response with high induction of IFN-β in neonate's microglia, and a high induction of the pro-inflammatory cytokines mediated by IFN-β.

4.3 CHAPTER 3: *Ochrobactrum intermedium* LPS induces TLR4 and TLR2 heterodimerization

4.3.1 *O. intermedium* LPS induces an inflammatory response mediated by TLR4 and TLR2 receptors in primary mouse macrophages

Some type of LPS, termed atypical LPS are described to be dependent of TLR2 to induce inflammatory responses rather than TLR4 (Burns et al., 2010; Girard et al., 2003). In addition, previous studies performed in our laboratory indicate that *Ochrobactrum intermedium* LPS (*O. intermedium* LPS) requires the presence of both TLR4 and TLR2 receptors to induce a cytokine response in primary mouse macrophages. To confirm this, WT, TLR2 and TLR4 KO peritoneal macrophages were stimulated with two different doses of this LPS and compared with the controls: *E. Coli* LPS (TLR4 ligand) and FSL-1 (TLR2 ligand) (Fig. 36).

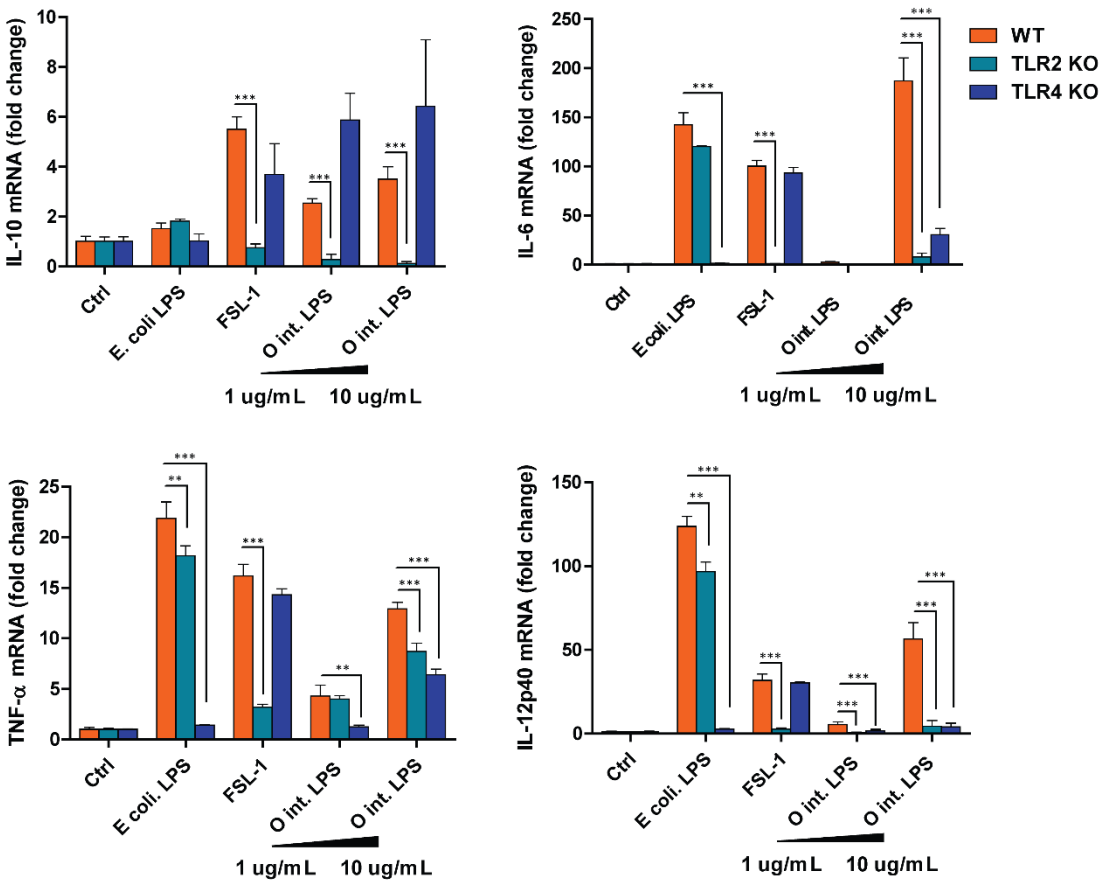

Fig. 36 *O. intermedium* LPS gives a weak inflammatory response, mediated by TLR2 and TLR4.

WT, TLR2 KO and TLR4 KO peritoneal macrophages were left unstimulated (Ctrl) or were stimulated with *E. coli* LPS (100 ng/mL), Pam3CSK4 (1 µg/mL), FSL-1 (100 ng/mL) and *O. intermedium* LPS (1 and 10 µg/mL) for 24 hours. Cytokines mRNA levels were measured by qPCR. The data shown is representative of two independent experiments (mean ± SEM) (*p < 0.05, **p < 0.01, and ***p < 0.001).

WT macrophages stimulated with *O. intermedium.* LPS showed a weaker induction of cytokines compared to *E. Coli* LPS. *O. intermedium* LPS only achieved similar cytokine levels to *E. coli* LPS at a 100-fold dosis of 10 ug/mL. Moreover, this LPS showed dependency on TLR4 and TLR2 in order to induce cytokines. IL-12, IL-6 and in part TNF-α were dependent on TLR2 and TLR4 signaling, whereas IL-10 induction was mostly TLR2-dependent. In addition, NF-κB and MAPKs activation induced by *O. intermedium* LPS increases in a dose dependent manner, however the response was always much weaker compared to *E. coli* LPS (Fig. 37). Thus, *O. intermedium* LPS is a TLR4/TLR2-dependent agonist.

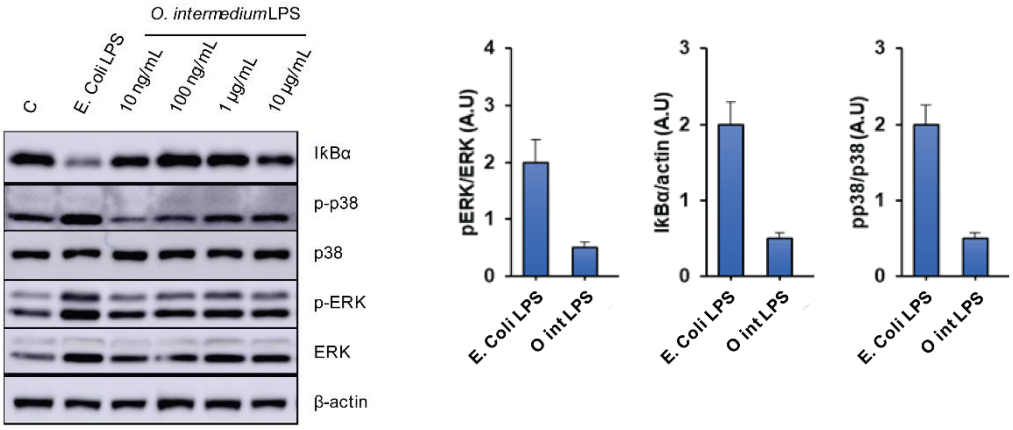

Fig. 37 *O. intermedium* LPS weakly induces NF-κB and MAPKs activation.

WT peritoneal macrophages were treated with *E. coli* LPS and four distinct doses of *O. intermedium* LPS for 30 min. NF-κB and MAPKs activation was determined by Western Blot. Graphics on the right panel show quantification of band intensities of the western blot. The values of p-ERK 1/2 and p-p38 bands were normalized to the total ERK 1/2 and p38 protein, respectively and IκBα levels were normalized to actin. The data are representative of three independent experiments (mean ± SEM.) (*p < 0.05, **p < 0.01, and ***p < 0.001).

4.3.2 Ligand-protein docking studies to access the ability of *O. intermedium* LPS to bind to hTLR2/TLR4-MD-2 heterodimer

4.3.2.1 Docking with the model hTLR2/TLR4-MD2 heterodimer and hTLR4/MD-2 homodimer

Since *O. intermedium* LPS is a TLR4 and TLR2-dependent agonist, the ability of this LPS to bind to a theoretical heterodimer formed by the human TLR2 and TLR4-MD2 receptors was explored by a molecular docking approach. The final structure of the hypothetical hTLR2/TLR4-MD2 heterodimer model constructed is displayed (Fig. 38).

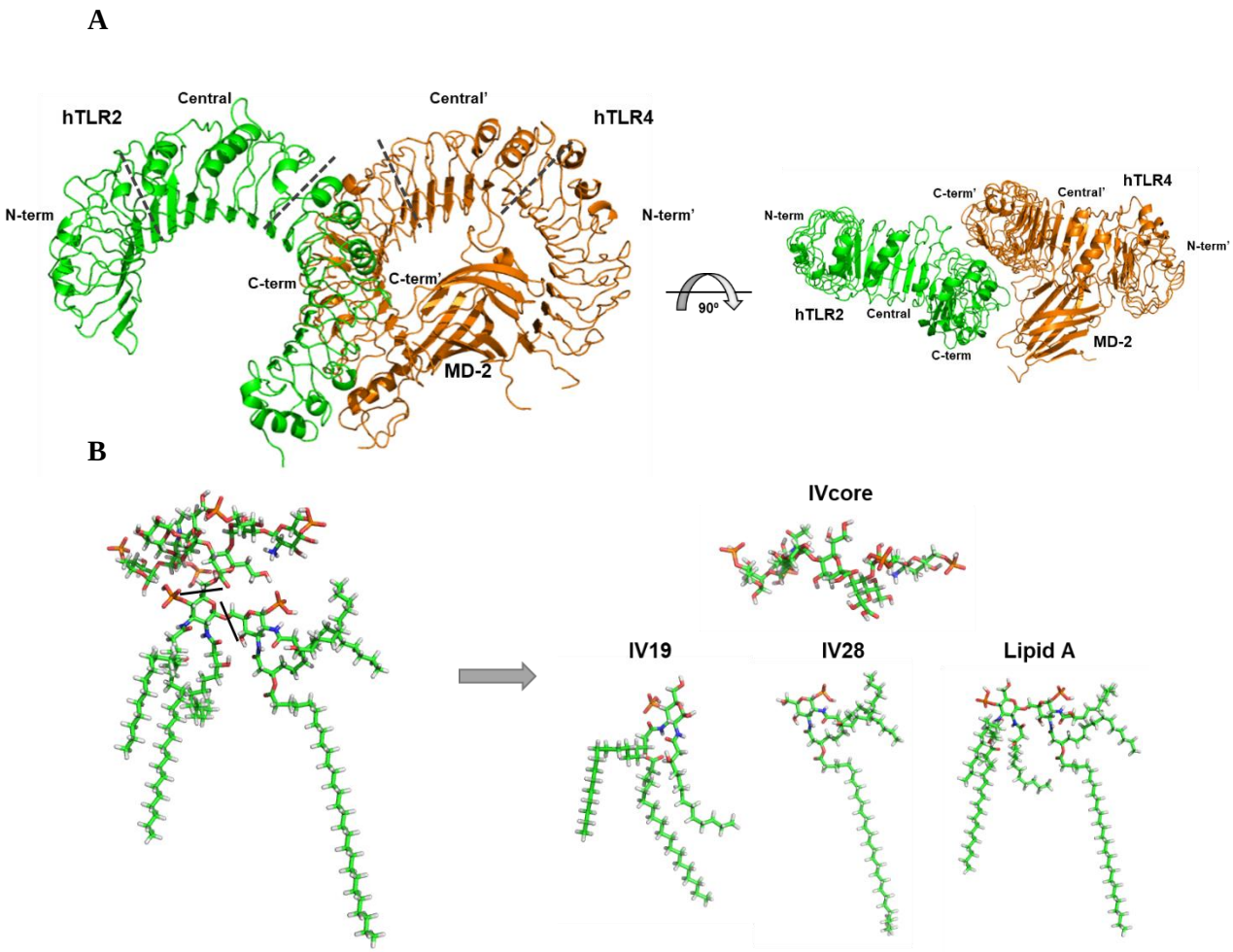

Fig. 38 A) 3D structure of hTLR2/TLR4/MD-2 heterodimer model in front view and upper view. TLR2 is represented in green and TLR4 and MD-2 in orange. **B)** Representation of the full *O. intermedium* LPS structure and the obtained fragments: the core saccharide (IV core), the fragment with the two fatty acid chains containing 12 and 16 carbons and the third 28 carbon acyl chain attached to C16 (IV28), the fragment containing the two lipid chains with 14 and 18 carbons and the third 19 carbon lipid chain attached to C18 (IV19), and the lipid A.

The *O. intermedium* LPS was divided in the different fragments, described in Material and Methods section. The importance of performing dockings with fragments is to minimize the atomic spatial energy. According to the literature and the crystal structure PDB ID 3FXI, *E coli* LPS accommodates five of its six lipid A chains inside the MD-2 pocket and the remaining chain is at the surface of MD-2 in a molecular channel where it interacts with the partner TLR4 (Park et al., 2009) . Given this, it was explored the ability of *O. intermedium* LPS fragments (IV19, IV28 and IVcore) to bind to the MD-2 pocket in the hTLR2/TLR4/MD-2 complex. From the docking calculations, favorable poses for the three fragments were found with predicted binding energies ranging from -6.8 to -6.6 and -7.3 to –6.9 kcal mol^{-1} respectively (Fig. 39A and 39B).

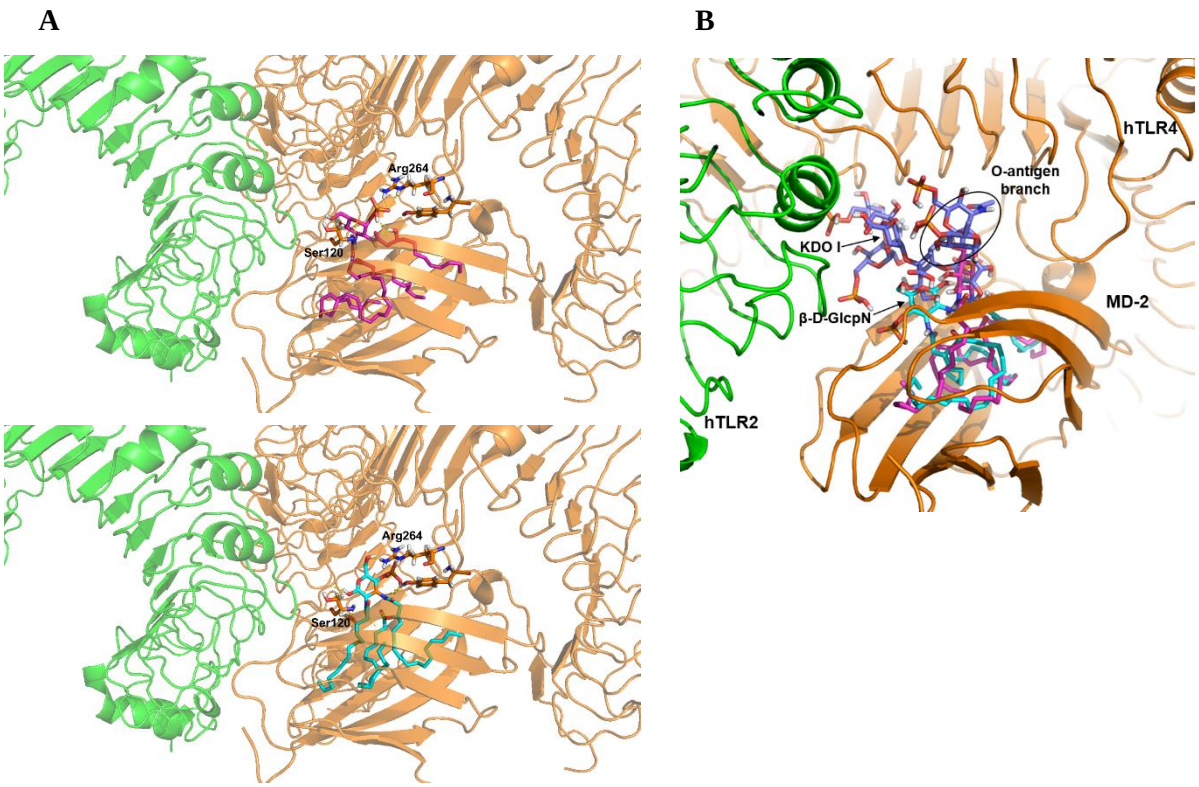

Fig. 39 View of the fragments IV28, IV19 and IVcore docked in the hTLR4/MD-2 pocket

A) IV28 (in magenta) and IV19 (in cyan) docked in the TLR4/MD-2 pocket. **B)** Superimposition of the three fragments (IV core in purple) docked in MD-2 pocket. (TLR4 and MD-2 are displayed in orange and TLR2 in green).

The two lipid A fragments showed their three FA chains buried in the MD-2 pocket. The glucosamine phosphate group was interacting with the NH2 groups of Arg264 (Fig. 39A), which is the same residue that interacts with the glucosamine of the *E. coli* LPS in the hTLR4/MD-2 crystal structure (PDB ID 3FXI). The core was near the entrance of MD-2 and the KDO I was spatially close to the glucosamine groups of the *O. intermedium* lipid A fragments (Fig. 39B).

E. coli LPS recognition by hTLR4/MD-2 complex was previously described (Park et al., 2009). The inner core of *E. coli* LPS is composed of KDO I, KDO II and heptoses, and these sugars stablish determinant interactions with MD-2 (e.g. Ser 118, Lys 122) and TLR4 residues (e.g. Lys 341, Tyr 296, Asp 294). Thus, besides the *E. coli* lipid A, the core is also important for inducing the dimerization of hTLR4/MD-2 monomers. Therefore, *O. intermedium* LPS was docked in hTLR4/MD-2 homodimer and superimposed with the *E. coli* LPS to compare binding orientation and interactions of these LPSs with the two TLR4 monomers. The docked poses were favorable with predictive binding energies ranging from -6.2 to -6.9 kcal mol^{-1}. The obtained binding poses showed that *O. intermedium* LPS FA chains were buried in the MD-2 pocket, however, the core saccharide dove towards TLR4*-TLR4 interface (Fig. 40A). This is more evident when the docked pose *O. intermedium* LPS is superimposed with *E. coli* LPS in the hTLR4/MD-2 homodimer (Fig. 40B). Despite *E. coli* LPS core established determinant interactions with TLR4 residues (e.g. Tyr296, Asp294 and Arg264) as well as with TLR4*

(Gln436), these interactions were not detected with *O. intermedium* LPS (Fig. 40C and D). This results theoretically indicates that in contrast to *E. coli* LPS, *O. intermedium* LPS does not favor the formation of stable TLR4 homodimers.

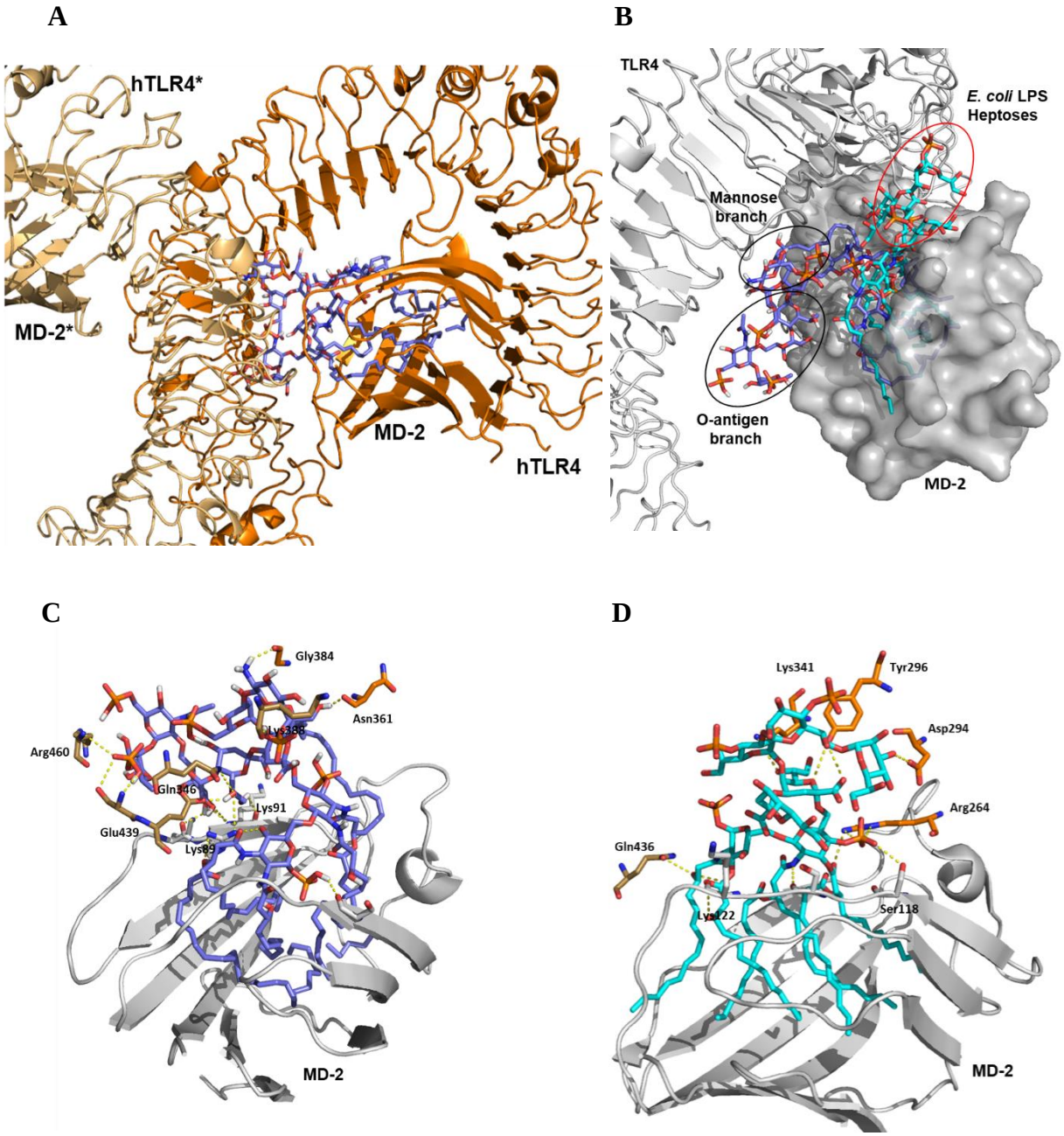

Fig. 40 General view of *O. intermedium* LPS and *E. coli* LPS docked in hTLR4/MD-2 dimer

A) Full *O. intermedium* LPS (in purple) conformation with the core diving towards TLR4*/TLR4 interface. **B)** *E. coli* LPS docked pose (in cyan) superimposed with *O. intermedium* LPS pose (in purple) in hTLR4/MD-2 dimer (hTLR4 and MD-2 are in grey and hTLR4/MD-2* was omitted for clarity). The polar interactions established between **C)** *O. intermedium* LPS and **D)** *E. coli* LPS with TLR4* (brown), TLR4 (in orange) and MD-2 (on grey) residues are presented. (An asterisk distinguishes the second TLR4/MD-2 monomer).

Full *O. intermedium* LPS was docked in the hTLR2/TLR4/MD-2 heterodimer to explore possible theoretical binding modes. The docked poses were favorable with predictive binding energies ranging from -7.4 to -6.9 kcal mol^{-1} (Fig. 41).

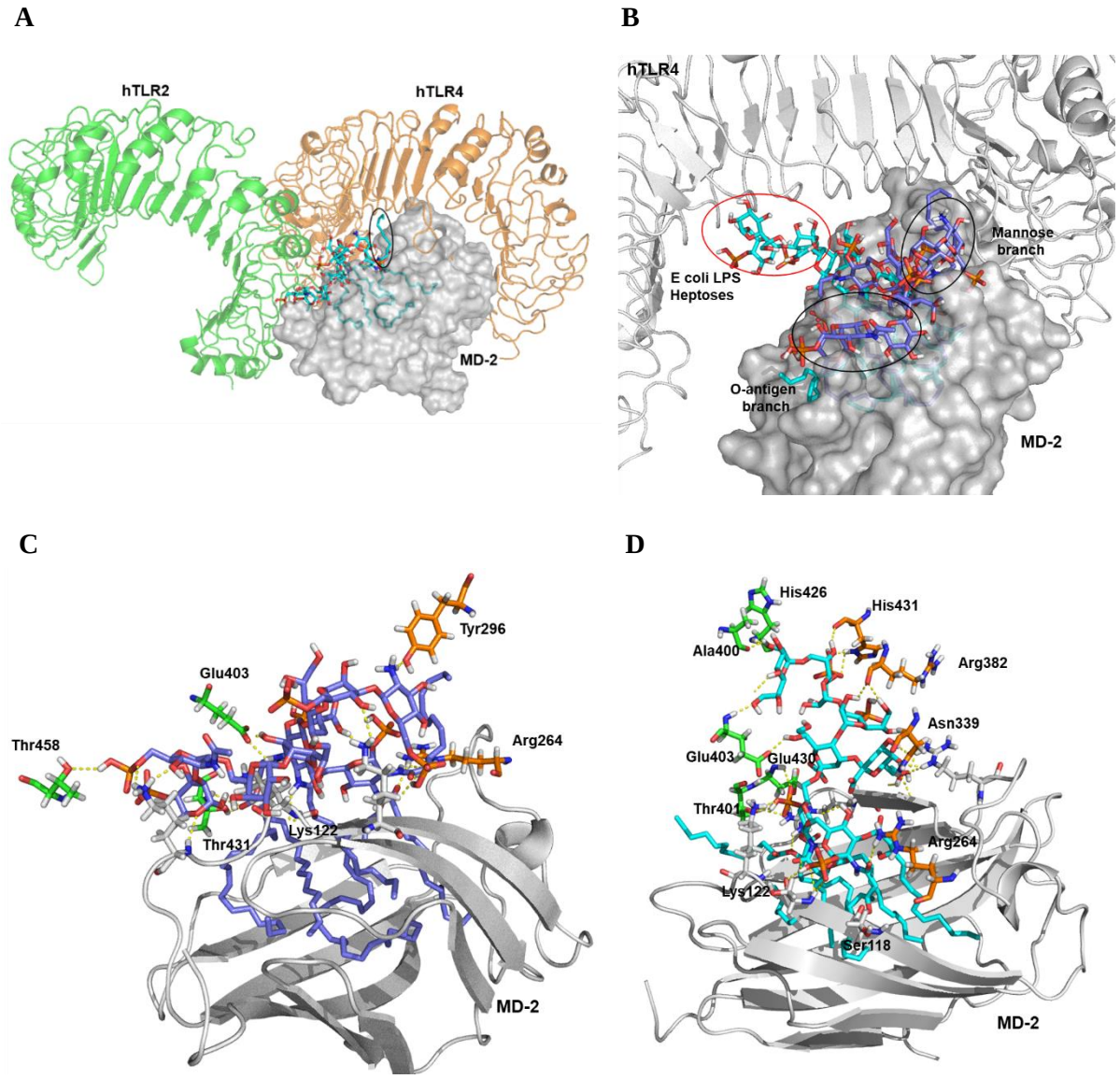

Fig. 41 General view of *O. intermedium* LPS and *E. coli* LPS docked in hTLR2/TLR4/MD-2 heterodimer

A) *O. intermedium* LPS (in cyan) conformation with one FA chain protruding out of the MD-2 pocket. **B)** *E. coli* LPS docked pose (in cyan) was superimposed with *O. intermedium* LPS pose (in purple) in hTLR2/TLR4/MD-2 complex (hTLR4 and MD-2 are in grey and hTLR2 was omitted for clarity). The polar interactions established between **C)** *O. intermedium* LPS and **D)** *E. coli* LPS with TLR2 (green), TLR4 (in orange) and MD-2 (on grey) residues are presented. (TLR4 and MD-2 are shown in orange and TLR2 in green).

The obtained binding poses showed that five FA chains of the LPS were buried in MD-2 pocket, remaining the sixth C12 chain on its surface (Fig. 41A). In this case, both LPSs showed their lipid A part accommodated in MD2-pocket. However, *E. coli* LPS core was diving towards TLR2/TLR4 interface (Fig. 41A and B). The interactions of the *E. coli* LPS core with the TLR4 residues described in the hTLR4/MD-2 dimer (Tyr 296, Lys 341 or Asp294) are not observed in the presence of the hTLR2 monomer (Fig. 41D). The TLR4 residues interacting with *E. coli* LPS core are nearer the TLR4 and TLR2 interface. This suggests that *E. coli* LPS does not favor the proximity of TLR4 and TLR2 receptors. On the other hand, *O. intermedium* LPS core maintains interactions with TLR4 residues such as Tyr 296 and Arg264, as well as with TLR2 residues far from the interface region (Fig. 41C). This imply that *O. intermedium* LPS accommodates in the hTLR2/TLR4/MD-2 complex in such a way that could favor the dimerization of both receptors. The *O. intermedium* LPS poses obtained from the dockings performed in hTLR2/TLR4/MD-2 heterodimer and hTLR4/MD-2 homodimer hint that the core composition and/or structure of this LPS might favor the formation of a hTLR2/TLR4 complexes rather than TLR4 homodimers.

The ability of *O. intermedium* LPS core to bind in the hTLR2 and TLR4 interface region was also investigated. The final docked poses gave favorable predicted binding energies, ranging from -7.2 to -6.3 kcal mol^{-1} (Fig. 42). In this docking, more diversity in the binding poses was observed, where despite most of the poses were near the entrance of MD-2 pocket, some poses features the ligand in the upper region of the TLR2/TLR4 interface and towards TLR2 central domain. This was not observed with *E. coli* core, were all the docked poses in the heterodimer are located only near the MD-2 pocket (data not shown).

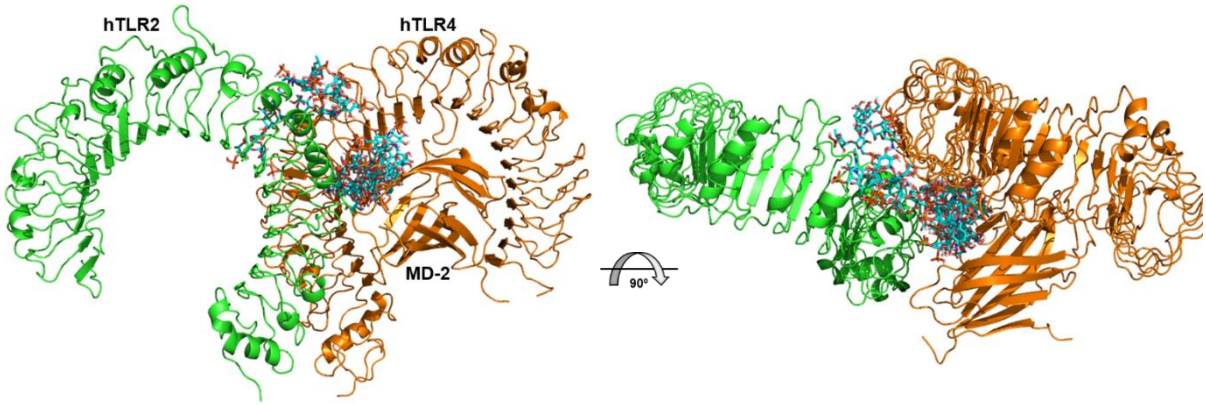

Fig. 42 Front and top view of IVcore fragment (in cyan) docked poses in hTLR2 (in green) and hTLR4/MD-2 (in orange) interface.

The ability of *O. intermedium* LPS core to interact with hTLR2 interface in the hTLR2/TLR4/MD-2 heterodimer was also explored. For this, a region spanning from the central domain (from Leu151 to

arg337) to the C-terminal domain (from Val338 to Iso506) was selected for docking. We found favorable docked poses with predictive binding energies ranging from -5.8 to -5.0 kcal mol^{-1} (Fig. 43).

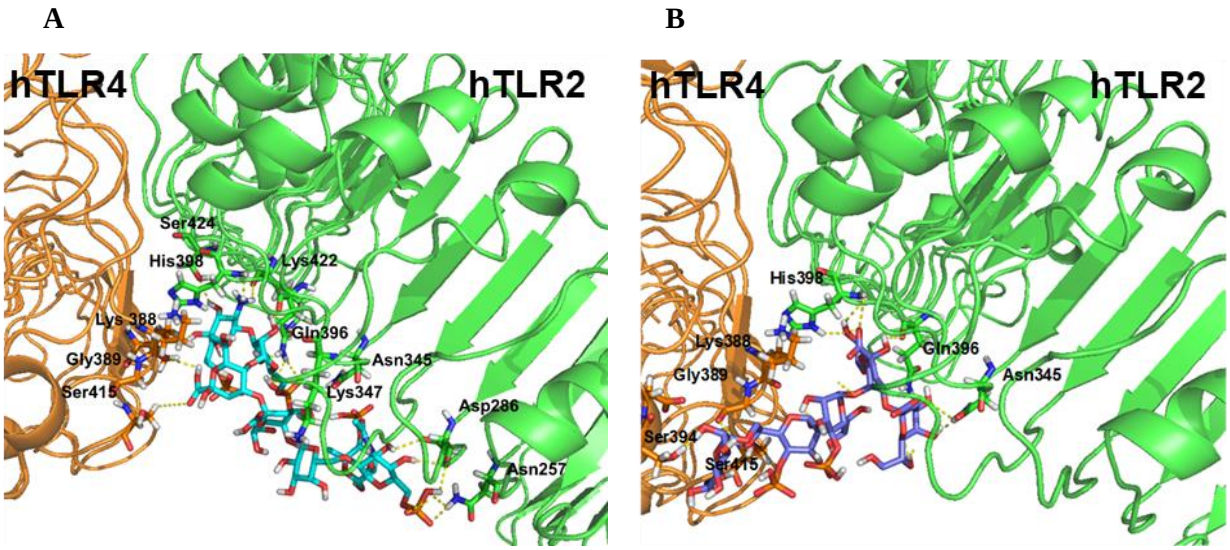

Fig. 43 Docking of IVcore fragment in hTLR2 central and C-terminal domain in the hTLR2/TLR4/MD-2 complex
A) Hydrogen interactions of IV core fragment with hTLR2 (green sticks) and hTLR4 residues (orange sticks). **B)** Hydrogen bonds of *E. coli* core fragment with hTLR2 (green sticks) and hTLR4 residues (orange sticks).

In many of the predicted binding poses of the IVcore fragment, the phosphate and hydroxyl groups were interacting with the backbone of TLR2, including residues His398, Ser425, Lys422, Gln396, Lys347, Asn345, Asp286 and Asn257 (Fig. 43A). Moreover, hydrogen bonds stablished with TLR4 residues Ser415, Gly389 and Lys388 were observed as well. The saccharide core from *E. coli* LPS was also docked in this region. The docked poses obtained, with predictive binding energies ranging from -5.5 to -5.2 kcal mol^{-1}, indicate that *E. coli* core can theoretically interact with the TLR2 C-terminal domain (Fig. 43B), in an energetically favorable manner. The core also established hydrogen bonds with TLR4 Ser415, Lys388 similarly to *O. intermedium* LPS core, however it showed fewer hydrogen interactions with TLR2 residues (His398, Gln396 and Asn345). These data indicate that the IVcore fragment has a higher probability of interacting with more TLR2 residues, located in the central and C-terminal domains. Therefore, *O. intermedium* LPS core is more favorable to establish interactions with TLR2 interface compared to *E. coli* LPS core.

4.3.2.2 Docking with the model hTLR2 monomer

TLR2 is described to associate with TLR1 or TLR6 receptors and this is required for recognition of the tri- and di-acylated lipopeptides, respectively (Alexopoulou et al., 2001; Buwitt-Beckmann et al., 2006; Takeuchi et al., 2001; Takeuchi et al., 2002). TLR2 contains an internal hydrophobic pocket located in the convex region formed at the border of the TLR2 central domain (from Leu151 to arg337) and C-terminal domain (from Val338 to Iso506), where it accommodates two lipid chains from TLR2-specific lipopeptides (Jin et al., 2007). Since TLR2 can hypothetically interact with TLR4 by *O. intermedium* LPS, docking studies were carried out using this LPS fragments in a region that covers the TLR2 pocket. Fragments IV19, IV28 and IVcore were docked in TLR2 pocket of the hTLR2 monomer model (Fig. 44). Docked poses with favorable predictive binding energies were found (ranging from -7.8 to -6.6 kcal mol^{-1}, from -6.9 to -6.5 kcal mol^{-1} and -5.7 to -4.9 kcal mol^{-1} for IV19, IV28 and IV core respectively).

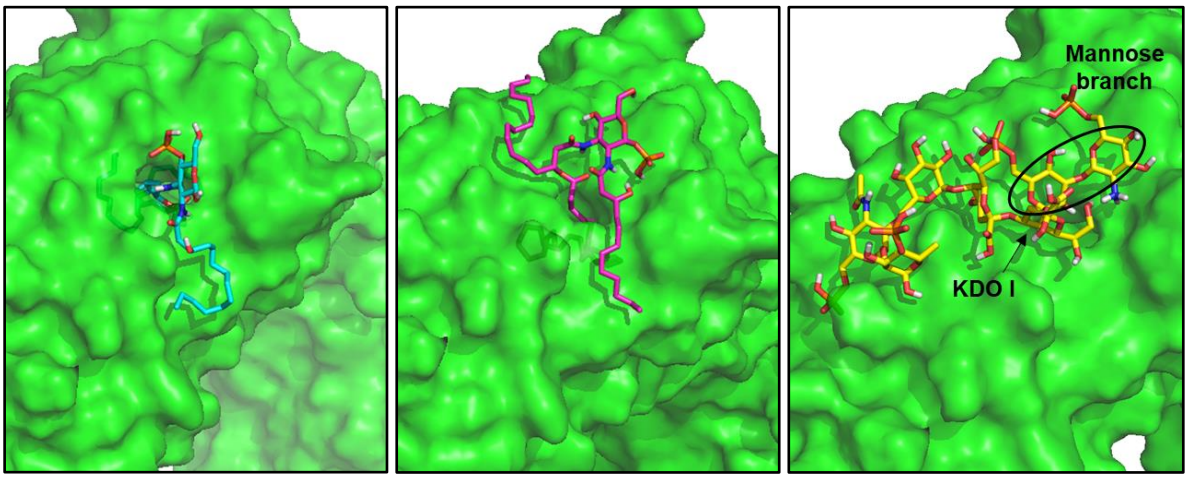

Fig. 44 Docking of the fragments IV19 (cyan), IV28 (magenta) and IVcore (yellow) in the hTLR2 pocket (TLR2 surface is represented in green for easier visualization of the pocket).

IV19 fragment docked in the TLR2 pocket showed the two fatty acid chains C19 and C18 buried in the pocket and the C14 chain was displayed in the solvent. On the other hand, IV28 fragment that comprises the large 28C chain was fully accommodated inside the pocket, whereas the C12 and C16 chain protruded out of the TLR2 pocket. Regarding the IV core, the obtained docked poses were interacting with TLR2, near to its pocket. Thus, the docking calculation showed that the lipid A component of *O. intermedium* LPS is theoretically able to interact with the hydrophobic TLR2 pocket, comprising a maximum of two acyl chains. This is consistent with the reported triacylated lipopeptide binding in the hTLR2/TLR1 receptor (Jin et al., 2007).

4.3.2.3 Redocking of *O. intermedium* LPS core in the hTLR2/TLR4/MD-2 complex, in the presence of LPS in the MD-2 pocket

O. intermedium LPS core is theoretically able to interact with hTLR2 monomer, near its pocket. Therefore, a redocking of the IV core fragment in the presence of an *O. intermedium* LPS in the MD-2 pocket was performed. The docked region covered the TLR4-TLR2 interface and TLR2 central and N-terminal domains (Fig. 45A). Favorable docked poses were obtained with binding energies ranging from -6.0 to -6.6 kcal mol^{-1}. In this redocking, most of the docked poses were observed in TLR2-TLR4 interface, in the presence of an LPS in the MD-2 pocket. The next step was to perform a redocking of the *O. intermedium* lipid A in the same region, in the presence of the core and the LPS molecule in the MD-2 pocket (Fig. 45B). Favorable docked poses for the lipid A fragment were found, with binding energies ranging from -5.9 to -5.2 kcal mol^{-1}. This redocking showed that only C28 or C19 chain can be accommodated in the TLR2 pocket. Moreover, the lipid A backbone is near to the sugar KDO I of the core. Thus, these redockings indicate that, in the presence of an *O. intermedium* LPS molecule in the MD-2 pocket, the core and the lipid A can theoretically bind to the hTLR2 interface, in the hTLR2/TLR4/MD-2 heterodimer. However, the lipid A is capable of accommodating only one FA chain in the TLR2 pocket (C28 or C19 chain).

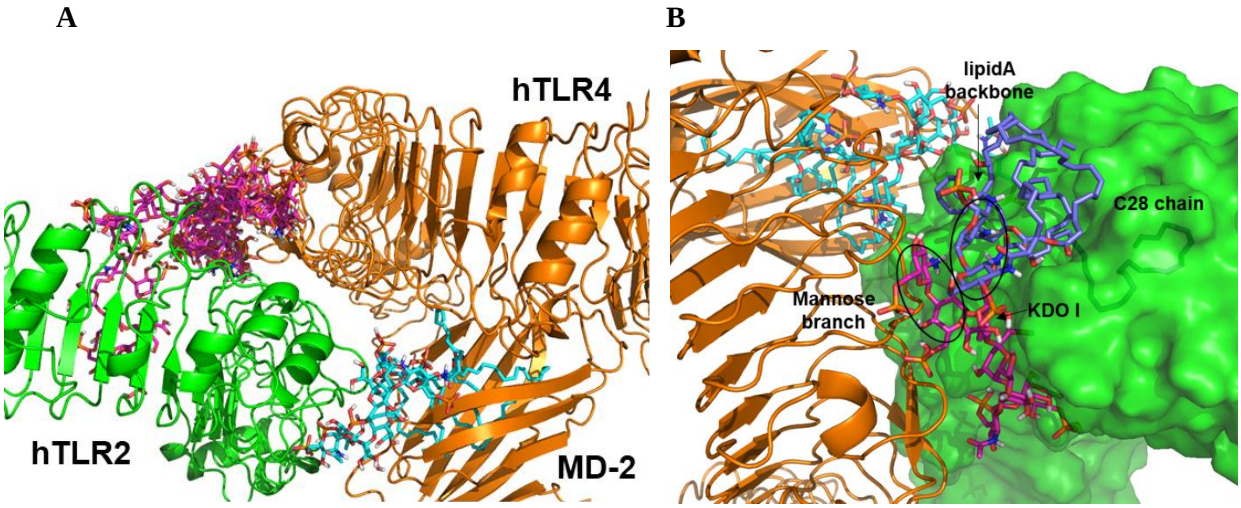

Fig. 45 A) Upper view IVcore (in magenta) redocked poses in the hTLR2 interface, in the presence of an *O. intermedium* LPS molecule (in cyan) in the MD-2 pocket. **B)** Redocking of the lipid A fragment (in purple) in the hTLR2 interface, in the presence of the IV core fragment and the *O. intermedium* LPS molecule in the MD-2 pocket (TLR2 represented in green and TLR4 in orange).

4.3.3 *O. intermedium* LPS induces hTLR4/MD-2 and hTLR2 heterodimerization

As receptor dimerization appears to be required for PAMPs recognition and TLRs activation, fluorescence resonance energy transfer (FRET) was performed to evaluate the intermolecular distance between TLR4 and TLR2 in the presence of *O. intermedium* LPS. HEK293 stably expressing MD-2 and CD14 were transiently transfected with TLR4-YFP (acceptor) and TLR2-CFP (donor) constructs and imaged *in vivo*. Unstimulated co-transfected cells showed a small FRET signal, with minute punctate-like structures present in the cell membrane and cytoplasm (Fig. 46).

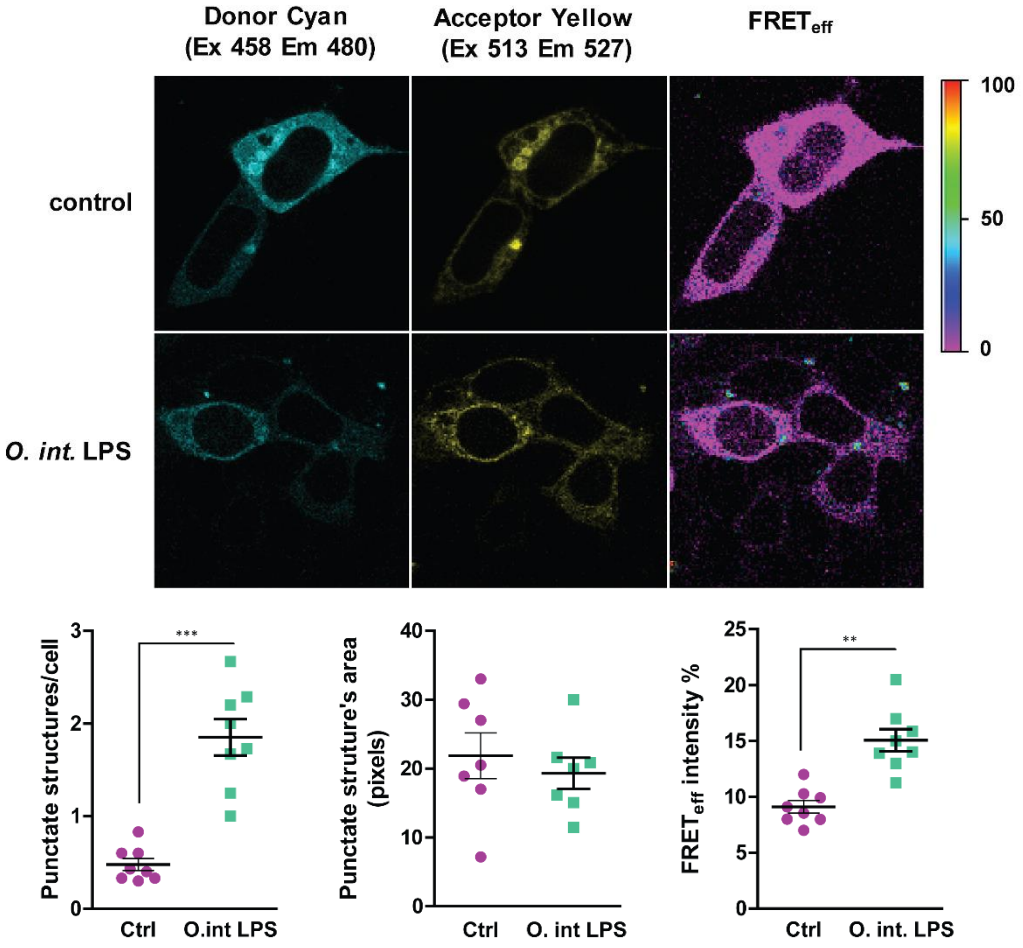

Fig. 46 *O. intermedium* LPS induces hTLR4-MD2 and hTLR2 heterodimerization.
HEK293T were transiently transfected with the plasmids TLR4-YFP (acceptor) and TLR2-CFP (donor). After transfection, cells were left unstimulated or were stimulated with *O. intermedium* LPS (1µg/mL). FRET between YFP and CFP was measured in *in vivo* cells, by sensitized emission fluorescence. Corrected FRET images (FRET $_{eff}$) are displayed using quantitative pseudocolor (right column). The graphics represent the quantification of FRET positive structures per total cell number, as well, as the area and mean fluorescence intensity of each punctate structure. The results are shown as mean ± SEM of two independent experiments (***, $p < 0.001$; **, $p < 0.01$; *, $p < 0.05$).

After stimulation with *O. intermedium* LPS, a significant FRET signal was observed by the presence of more punctate structures and with higher fluorescence intensity. A tandem vector construct of CFP and YFP was used as a positive control, with a FRET efficiency of around 40% (data not shown). The size of these punctate structures however did not change upon cell stimulation. These results demonstrate that in resting cells, TLR4 and TLR2 receptors are closer from each other but not sufficiently to induce downstream signaling activation. However, *O.intermedium* LPS stimulation promotes a closer interaction between TLR4 and TLR2 receptors that enables the activation of downstream intracellular signaling events. Thus, these data indicate that this particular LPS from *Ochrobactrum intermedium* can induce the rearrangement of both TLR2 and TLR4 receptors favoring their interaction.

DISCUSSION

5 DISCUSSION

5.1 TLR4 and TLR2 differential kinetics

Our results show that stimulation of macrophages with TLR4 or TLR2 ligands resulted in striking differences in cytokine production. Specifically, TLR2/6 and TLR2/1 ligands exhibit a higher induction of anti-inflammatory mediators, such as IL-10 and ARG1, whereas TLR4 favors the expression of pro-inflammatory cytokines such as TNF-α, IL-12, IL-6 and iNOS (see Fig. 1 and 2). The higher IL-10/IL-12 ratios observed in macrophages activated by TLR2 ligands suggest a change to a M2 and regulatory phenotype, whereas LPS induces a M1-type macrophage as previously described. This is concordant with previous published data in human DCs stimulated with LPS, PGN, zymosan and Pam3Cys, where TLR2 ligands favored a Th2 response in contrast to LPS (Agrawal et al., 2003; Dillon et al., 2006; Re and Strominger, 2001).

In this regard, several pathogens, such as *Brucella abortus*, *Candida albicans or Mycobacterium tuberculosis* may explore TLR2-mediated IL-10 induction as an virulence mechanism to induce M2 macrophages and suppress Th1 response against the pathogen (Netea et al., 2004; Richardson et al., 2015). Given this distinct cytokine profile, it was questionable if TLR4 and TLR2 ligands could activate exactly similar signaling pathways, including the activation of NF-κB and MAPKs p38 and ERK. Our results demonstrate different kinetics of activation between TLR4 and TLR2 ligands, however Pam3CSK4 and FSL-1 show similar kinetics of activation (see Fig. 3), which is in accordance with previous studies (Long et al., 2009). Our experiments were also performed in peritoneal macrophages, thus showing that this differential kinetics signaling occurs in both macrophage cell line and primary macrophages. Our work focused on the MAPKs ERK and p38 because they have a central role in activating and regulating a range of cellular responses. In macrophages, ERK and p38 are determinant in eliciting inflammatory responses through activation of nuclear transcription factors and through the stabilization and translation of cytokines mRNA that contain AU-rich elements. ERK is important for the induction of TNF-α, IL1-β, and IL-10, but negatively regulates IL-12 in response to LPS. On the other hand, p38 seems to be important in IL-12 induction and regulate TNF-α production at a posttranscriptional level. A possible explanation for the differential MAPKs activation by TLR4 and TLR2 could be due to activation of different upstream activators of p38 and ERK. TAK1 is a general upstream kinase described to be important for activation of NF-κB, p38, JNK and ERK (Shim et al., 2005). Our results show that TLR4 and TLR2 ligands are dependent of TAK1 to induce ERK and p38 and this is observed for the Raw264.7 cell line as well as for peritoneal macrophages (see Fig. 6). In most described cases, MEK1/2 is an upstream mediator of ERK1/2. Cell treatment with MEK1/2 inhibitor gave a different response. Raw264.7 cells treated with PD98059 or with U0126 still induced ERK phosphorylation, in response to TLR2 ligands, which was not observed in peritoneal or bone

marrow-derived macrophages (see Fig 7,9, 10 and 11). Thus, Raw264.7 cells can induce ERK by TLR2 ligands stimulation in a mechanism independent of MEK1/2. This uncoupling phenomenon was observed in previous studies, showing that TNF-α or LPS-stimulated human neutrophils or PBMCs induced ERK in a MEK independent mechanism (Foreback et al., 1998; Simard et al., 2015). Therefore, MEK-independent ERK activation appears to be cell-type specific and limited to certain kind of stimuli. Given this, the question of which kinases were activating ERK independently of MEK in Raw264.7 cells was explored. Several pathways have been reported to contribute for ERK activation in distinct cells systems and in response to different stimuli. These include Ras/Raf, a cascade usually activated by growth factors and cytokine receptors, PI3K-mTOR, TPL2 and classes of PKCs (Grammer and Blenis, 1997; Pathak et al., 2004; Shaul and Seger, 2007). Inhibitors of PI3K (wortmannin) and TPL2 (TPL2 inhibitor) were tested in Raw264.7 cells, however no effect was observed in ERK phosphorylation in response to TLR2 ligands (data not shown). Previous studies report that PKCζ inhibition was found to block MEK and ERK activation by LPS (Monick et al., 2000). This is in accordance with our results obtained in response to LPS, however a partial inhibition was observed for TLR2-mediated ERK phosphorylation. Nevertheless, treatment with Ras inhibitor (manumycin), not only impaired ERK activation by LPS, but also ERK phosphorylation mediated by Pam3CSK4 and FSL-1 (see Fig. 12). Thus, Ras, and in part PKCζ contribute to ERK activation in TLR2 ligands stimulated Raw264.7 cells, independently of MEK1/2.

Although macrophage cell lines such as Raw264.7, have been widely used as a surrogate of primary macrophages for signaling studies, previous studies demonstrate that unstimulated Raw264.7 cells contain about 1400 genes, which are differentially expressed relative to primary macrophages. In particular, this cell line has been described have higher expression of genes associated with mitosis and DNA metabolism whereas primary macrophages show higher expression of genes related to defense response and antigen processing and presentation (Maurya et al., 2007). Raw264.7 cells are transformed macrophage-like cell line derived from the lymphoma of a BALB/c mouse infected by the Abelson murine leukemia virus (Raschke et al., 1978). Particularly, an oncogenic form of the Abelson kinase, vAbl, is constitutively expressed in these cells, leading to a constitutive activation of proliferation-related signaling pathways, one of them being Ras (Shore et al., 2002). These changes in signaling mediator's activity should be taken into account when using macrophage-like cell lines as a validation model for signaling or infection studies performed in primary macrophages.

Our results also demonstrate that Raw264.7 cells, but not peritoneal macrophages, induce p38 phosphorylation by an alternative mechanism besides the classical MEKK3/6 axis, and is based on autophosphorylation (see Fig 13 and 14). However, this phenomenon occurred in response to LPS and Pam3CSK4, but not for FSL-1. As it was mentioned before, SB203580 inhibits p38 catalytic activity targeting p38α and p38β isoforms. By inhibiting p38 with SB203580, Ge et al. demonstrated that a TAB1-mediated p38α autophosphorylation mechanism occurs in response to bacterial components such as LPSs and CpG, but not in response to bacterial lipoproteins (Ge et al., 2002). Other study shows

that p38β has the capacity for autophosphorylation through spontaneous catalytic activity, triggered and regulated by MAPK insert and C-terminal motifs present in this isoform (Beenstock 2014). Moreover, autoactivation of p38α is also promoted in T cells (Salvador et al., 2005). Altogether, this data suggests that p38 autophosphorylation occurs in certain cell types and depends on the initial stimulus. This is in accordance with our results, where LPS-stimulated Raw264.7 cells activated p38 through this mechanism, and at a lesser extent in response to TLR2 ligands. Furthermore, this phenomenon was not observed in peritoneal macrophages. Indeed, a similar phenomenon was found by infecting bone marrow-derived macrophages with the parasite *Toxoplasma gondii*, which triggered TAB1-p38α autophosphorylation, but not LPS (Kim et al., 2005). Immune cells have developed distinct modes for p38 activation, one of them in the absence of MKK3/6 activation, probably to activate p38α and p38β isoforms rather than other isoforms. Therefore, our results elucidate that Raw 264.7 macrophage cell line use distinct and MEK-independent upstream activators for TLR2-mediated ERK activation as well as a p38 autophosphorylation mechanism for its activation, which is not observed in primary macrophages.

The TLR4 and TLR2 differential kinetics on ERK and p38 activation that we observed in macrophages cannot be ascribed to the differences on the signaling pathways activation that we tested. A plausible explanation for these kinetic activation differences could be the different recruitment of MyD88 and Mal/TIRAP adaptors to TLR2 and TLR4 receptor TIR domains, the termed TLR signalosome. TLR4 signalosome is formed by the recruitment of two Mal dimers that in turn recruit four MyD88-dimers. Then other six MyD88 molecules bind to this cluster, allowing IRAK4 and IRAK2 bind and initiate the signaling cascade (Guven-Maiorov et al., 2015). It turns out TLR2/6 and TLR2/1 heterodimers induce a different signalosome composition, where TLR2/1 binds a TIRAP and MyD88, and TLR2/6 recruits two TIRAP molecules. Additionally, three MyD88 molecules are recruited to the primary cluster, which are less that then the ones recruited by TLR4 (Piao et al., 2016). Therefore, the different composition and stoichiometry of MyD88 and TIRAP complexes in TLR4 and TLR2 heterodimers, can likely contribute for the different kinetics of NF-κB and MAPKs activation by TLR4 and TLR2 ligands.

Dephosphorylation of MAPKs is likely to be one of the most efficient mechanisms to control their activation. Dual specificity phosphatases (DUSP), also termed MKP can negatively regulate MAPKs activation through dephosphorylation of phosphotyrosine and phosphothreonine residues. DUSPs can be induced by TLR-mediated activation of MAPKs, creating a negative feedback loop to limit MAPKs activation. Among DUSPs, MKP-1 is highly expressed in macrophages. Our results show that TLR4 and TLR2 ligands induce MKP-1, however with different kinetics of activation (see Fig. 15A and B), similarly to ERK and p38 MAPKs. It is likely that this spatiotemporal difference in MKP-1 induction via TLR4 and TLR2 ligands is due to the same differences observed in ERK and p38 induction. Interestingly, MKP-1 mRNA levels induced by TLR2 ligands decay completely after 2 hours, whereas in response to LPS the levels drop much later, at 6 hours after stimulation. A similar pattern occurs at

protein expression, however, since MKP-1 is likely stabilized, the decay levels are observed at 4 hours after TLR2 stimulation (see Fig 15C and D). Therefore, the duration of MKP1 activation and stabilization is longer by TLR4 activation but shorter by TLR2. Distinct upstream mediators are likely contributing and regulating MKP1 expression. Indeed, MKP-1 can be induced and stabilized by ERK in LPS-stimulated Raw264.7 cells, and bone marrow-derived macrophages (Crowell et al., 2014). Our data shows that inhibition of ERK in Raw264.7 cells impairs MKP-1 induction by TLR4 and for TLR2 ligands, being more evident for FSL-1, whereas p38 inhibition only affected MKP-1 levels upon stimulation by LPS (see Fig 16A). These results are in accordance with previous published work, where LPS stimulated-Raw264.7 cells induce MKP-1 primarily by ERK and at a lesser extent by p38 (Chen et al., 2002). In addition, when using peritoneal macrophages, our results gave an ERK and p38-dependency for full MKP-1 induction for the distinct ligands (see Fig. 16B). Hu et al reported a similar conclusion using the same cell type, but stimulating with LPS and PGN, and found a p38-MK2 regulation feedback, through MKP-1 induction (Hu et al., 2007). However, there are conflicting reported results regarding MKP-1 induction in primary macrophages. Published data shows that JNK is required for MKP-1 induction in bone marrow-derived macrophages, in response to LPS or M-CSF (Sanchez-Tillo et al., 2007). However, in this study, BALB/c mice macrophages were used. Other study points that MKP-1 is induced by the kinases MSK1/2, which are downstream targets of ERK and p38 (Ananieva et al., 2008). Therefore, ERK, p38 and JNK drive MKP-1 induction, however the contribution of each MAPK seems to depend on the mice genetic background, cell type and stimuli.

MKP-1 induction is determinant for controlling the length of MAPK responses in macrophages. Previous studies demonstrated that MKP-1 KO peritoneal, alveolar macrophages and bone marrow-derived macrophages showed prolonged activation of p38 and JNK, suggesting that MKP-1 regulates primarily p38 and JNK, but has little effect on ERK, in response to LPS (Chi et al., 2006; Hammer et al., 2006; Zhao et al., 2005). Our results show a similar result in response to the TLR2 ligand FSL-1, where MKP-1 KO PM exhibit a prolonged p38 phosphorylation whereas ERK phosphorylation was not affected (see Fig. 17). In the absence of MKP-1, p38 is likely to eventually become inactivated by other MKPs, though at a much slower rate. This is consistent with the observation that deactivation of p38 in MKP-1 KO macrophages was delayed. Overall, MKP-1 has a central role in the regulation of p38.

MKP-1 was previously described to regulate pro and anti-inflammatory cytokines in response to LPS stimulation (Chi et al., 2006). We addressed the role of MKP-1 in the inflammatory response mediated by TLR2 ligands. Using MKP-1 KO PM, our data shows that this phosphatase contributes to the induction of pro-inflammatory cytokines such as IL-6, IL-12 and TNF-α, but regulates IL-10 expression at later time points (8 and 24h), whereas at 4 hours of stimulation, cytokine levels are similar to WT cells (see Fig. 18). MKP-1 regulation, however, is stronger for TLR2 ligands in comparison to TLR4. In contrast, Salojin et al reported that MKP-1 KO BMDM not only exhibit an increase in TNF-α, IL-6, IL-12, and IFN-γ levels but also of IL-10 after 24-hour stimulation with LPS (Salojin et al.,

2006). However, Chi et al demonstrates that MKP-1 BMDM deficient macrophages induce more IL-10, observed for different stimuli such as PGN and Pam3CSK4, which are more in accordance with our results. This induction was blocked by a p38 inhibitor, showing that p38 mediates IL-10 synthesis (Chi et al., 2006). In our hands, TNF-α levels were enhanced in MKP-1 KO cells at earlier time points, but at later stages, no differences were observed comparing with WT cells. On the other hand, Zhao et al also observed that MKP-1 KO PM prolonged p38 activation and leads to augmented production of TNF-α, IL-6, and IL-10, however, IL-12 is downregulated. This was observed at 6 and 24 hours after LPS stimulation (Zhao et al., 2006). Together with our results, MKP1 regulates pro and anti-inflammatory cytokines, likely by downregulation of p38 activity. In addition, we demonstrate MKP-1 is important for pro-inflammatory cytokine's production in response to TLR2 ligands. Nevertheless, the outcome of MKP1 regulation in cytokine's expression seems to depend on the cell type, the stimuli and the stage where inflammation is being analyzed.

Our results also demonstrate that p38 is critical for later anti-inflammatory IL-10 induction but not for pro-inflammatory cytokines, regardless of the stimuli (see Fig. 20). This is in accordance with Chi et al, which demonstrates that IL-10 induction mediated by LPS was blocked by a p38 inhibitor, implying that p38 mediates IL-10 synthesis (Chi et al., 2006). Our results demonstrate that TLR2 ligands also induce IL-10 expression fully dependent of p38 at later stages. The higher levels of IL-10 expression could be due to the early activation of p38 by these ligands, in contrast with LPS. Furthermore, it is described that IL-10 inhibits the transcription of pro-inflammatory cytokines via IL10R-Janus kinase-

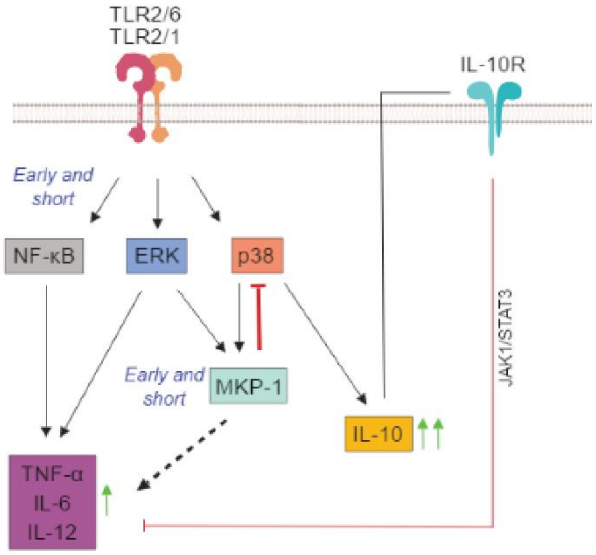

Fig 1D. Model Hypothetical model of the molecular events leading to high IL-10 levels in response to TLR2 ligands. TLR2 ligands such as Pam3CSK4 or FSL-1 activate NF-κB, ERK and p38 earlier and faster (≈ 3 min) compared to LPS (≈ 30 min), allowing a faster induction of cytokines such as TNF-α, mediated by NF-κB and IL-12, IL-6 and IL-10 by ERK. The earlier induction of MKP-1 by TLR2 activation contributes for upregulation of pro-inflammatory cytokines and MKP-1 can dephosphorylate 38. On the other hand, the early TLR2-mediated p38 induction contributes for later and high IL-10 levels of expression. Consequently, IL-10 activates the STAT3 pathway which amplifies IL-10 production and regulates pro-inflammatory cytokines induction.

STAT3 pathway (Murray, 2006). Therefore, the earlier activation of this pathway could contribute for the higher IL-10 levels and lower pro-inflammatory cytokines observed via TLR2 activation at later stages (Fig. D1).

The transcription factors also influence cytokine expression. SP1, c/EBPβ. CREB/AP1 and MAF have been shown to bind to IL-10 promoter. MSK1/MSK2-mediated activation of CREB and ATF1 induced IL-10 in response to LPS. However, the different stimuli may induce different transcription factors activated in a same cell type. For example, p38 induce IL-10 promoter via SP1 in response to LPS, whereas c/EBP5 was found to be recruited in response to cAMP (Brenner et al., 2003; Ma et al., 2001). Further studies are required to identify the downstream targets of p38 that mediate IL-10 regulation in response to TLR2 ligands.

5.2 TRIF-IFN-β signaling dependence in TLR2 inflammatory responses and *Listeria* infection

Similar to TLR4 and endosomal TLRs, it was recently found that TLR2 activation induces not only inflammatory cytokines but also type I IFNs. Thus, Dietrich et al. observed that TLR2 ligands induced IFN-β mediated by MyD88- IRF1 and IRF7 mechanism in macrophages (Dietrich et al., 2010). Furthermore, this TLR2 signaling occurs in endosomes, similar to other TLRs. So far, these results were observed only in BMDMs. We evaluated TLR2-mediated IFN-β production in peritoneal macrophages and the Raw264.7 cell line, observing that TLR2 ligands induce IFN-β although at lower levels than TLR4 ligands (see Fig. 21). This is consistent with the reported studies performed in BMDMs. Moreover, IFN-β induction in response to TLR2 ligands was dependent of the receptor endocytosis in peritoneal macrophages, demonstrating that distinct macrophage types require TLR2 internalization to induce IFN-β (see Fig. 22). Indeed, Pam3CSK4 and FSL-1 rapidly triggered TLR2 internalization, however to a lesser extent compared to LPS-stimulated TLR4 internalization.

Our results further show that TLR2 ligands induce IRF3 and IRF7 activation in peritoneal macrophages earlier compared to LPS and mediated by endocytosis (see Fig. 24 and 25). On the other hand, LPS-stimulated BMDMs displayed IRF3 and IRF7 phosphorylation. In this cell type, Pam3CSK4 failed in activating IRF3, whereas IRF7 was phosphorylated in response to both TLR2 ligands, Pam3CSK4 and FSL-1 (see Fig. 26). Published data demonstrated BMDMs deficient in IRF1 and IRF7, but not IRF3, failed in producing IFN-β mediated by TLR2 ligands, demonstrating that IRF3 is dispensable for IFN-β production in these macrophages (Dietrich et al., 2010). Our results support that the ligand Pam3CSK4 weakly activates IRF3 in BMDMs. Previous studies reported that IRF3 and IRF7 are activated in response to vaccinia virus (Barbalat et al., 2009; Dietrich et al., 2010). Moreover, both IRF1 and IRF2 had a role on TLR2-dependent-IFN production in Raw264.7 cells (Liljeroos et al., 2008). Therefore, it is feasible that IFN-β activation is controlled by different IRFs, which depend on the initial stimulus or type of microbe and cell type.

It is well characterized the TLR4 dependence in TRIF signaling for type I IFN induction. We demonstrated that TLR2 activation requires TRIF signaling in part, to induce IFN-β. Indeed, IFN-β production is only slightly affected in TRIF deficient cells after TLR2 stimulation for 3 hours. However, at 6 hours, a stronger TRIF dependency for IFN-β production is observed, mainly in response to FSL-1 (see Fig. 27). Our results are in accordance with Stack et al, which demonstrated a strong dependency of MyD88 for Pam3CSK4-mediated IFN-β production (Stack et al., 2014). Indeed, Stack et al demonstrated an endosomal localization of TLR2, TRAM, Mal and MyD88 within 20 min after TLR2 ligands stimulation, whereas Nilsen et al implied that TLR2 is recruited and co-localized with TRAM and TRIF upon stimulation with FSL-1 for 1 hour (Nilsen et al., 2015). Thus, in addition to the previous findings, our results support that in contrast to TLR4, TLR2 is rapidly internalized, likely complexed with MyD88 and induce a first wave of IFN-β, whereas in later endosomes, TRIF is

required to induce the second wave of IFN-β. Given the TRIF-signaling dependency for TLR2-mediated IFN-β induction, we also observed that TLR2 can utilize this pathway to induce a specific set of cytokines. Our results show that TNF-α and IL-12p40 induction are strongly dependent of TRIF and IFN-β at later stages, whereas the anti-inflammatory cytokine IL-10 is not affected (see Fig. 28 and 29).

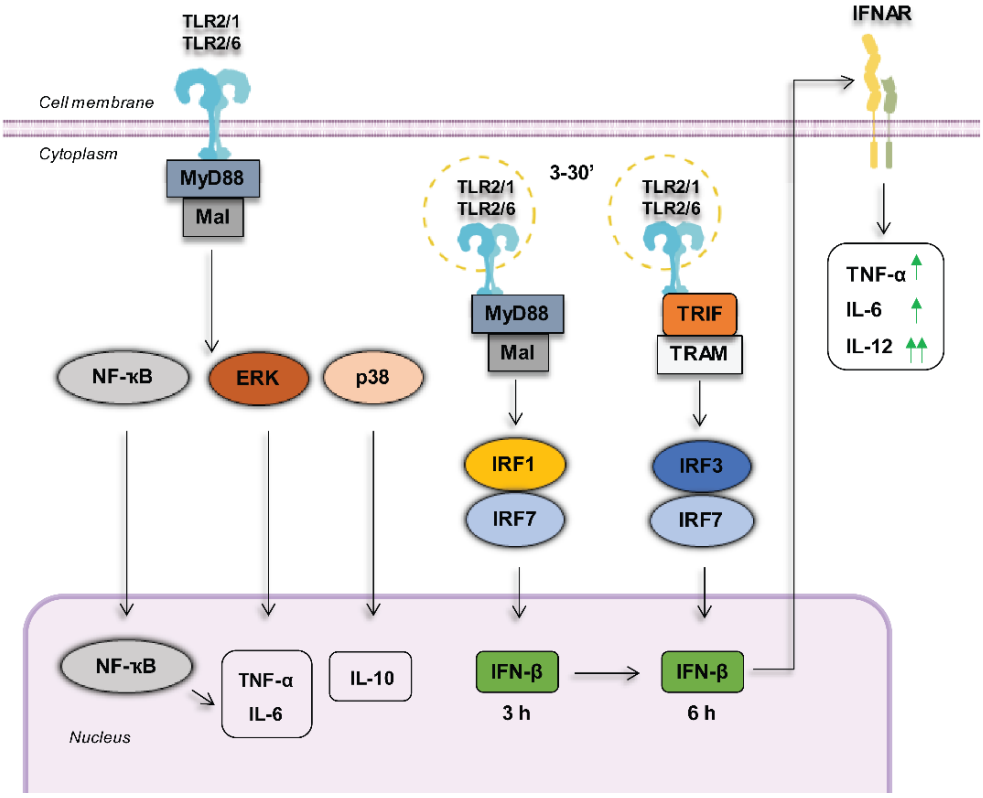

Fig. D2 Proposed model for TRIF signaling contribution to TLR2-mediate inflammatory responses in macrophages. In an initial phase, TLR2 ligands recruit MyD88 and Mal adaptors to activate the transcription factors NF-κB and the MAPKs ERK and p38. NF-κ and ERK contribute for the first wave of pro-inflammatory cytokines and p38 is determinant for IL-10 induction. Upon TLR2 stimulation, a fast internalization of this receptor occurs, either complexed with MyD88 or by recruiting MyD88 in endosomes. This signaling promotes the activation of the transcription factors IRF1 and IRF7, which contribute for IFN-β transcription at earlier time points (3h). Once in the endosomes, TLR2 recruits TRIF adaptor. The activation of these pathways induces IRF3 and IRF7, which in turns promote IFN-β at later time points (6 h). The expressed IFN-β activates IFN receptor and downstream signaling pathways are activated in order to induce pro-inflammatory cytokines, especially IL-12.

Indeed, this is in accordance with our results, showing that IL-10 induction is dependent of the MAPK p38 (see Fig. 19 and 20). Moreover, MyD88 and TRIF dependency for TLR2-mediated Ccl5 and Ccl4 chemokines was previously reported in peritoneal macrophages (Nilsen et al., 2015). Thus, it feasible that both TRIF and MyD88 pathways mediate TLR2-induced TNF-α and IL-12 expression in macrophages, which may be necessary to mount optimal host inflammatory responses towards certain infections (Fig. D2).

Bacteria such as *Lactobacillus acidophilus, Staphylococcus aureus, Borrelia burgdorferi* and *Legionella pneumophila* have been found to trigger type I IFN production in a TLR2-dependent manner in the host (Liljeroos et al., 2008; Opitz et al., 2006; Petnicki-Ocwieja et al., 2013; Weiss et al., 2010). Therefore, type I IFNs appear to play a key role as immunomodulatory cytokines capable of enhancing protective immune responses during bacterial infections. However, different roles of type I IFN during *Listeria monocytogenes* infection were suggested. Initial studies showed that type I IFN production is harmful to the host in *Listeria monocytogenes* infection. IFNAR1 KO mice were found to be resistant to *L. monocytogenes* infection (O'Connell et al., 2004) and the mechanism attributed to this resistance was a reduced lymphocyte and macrophage apoptosis mediated by type I IFNs, sensitizing these cells to bacteria invasion (Carrero et al., 2004). However, recent investigations suggest that these results depend greatly on the route of infection (Kernbauer et al., 2013; Pitts et al., 2016). Moreover, the timing of type I IFN production by the host is likely to be determinant for the beneficial and protective role of this mediators during *Listeria* infection (Pontiroli et al., 2012).

Neonatal listeriosis represents between 16 and 27% of invasive listeriosis cases and is associated to high mortality rates (20-60%). In addition, neonates commonly develop symptoms of septicemia and meningitis. Pregnancy increases the susceptibility to *L. monocytogenes* infection since placental-derived Th1 antagonistic cytokines confer a Th2 type response in the fetus. Thus, suppression of Th1 responses is advantageous for survival of the fetus but increases the newborn susceptibility to infections. Neonates have an immature immune system, associated with a downregulation of Th1-dependent anti-microbial immunity. Indeed, neonatal macrophages are defective in the secretion of Th1-type cytokines such as IL-12, IFN-γ, TNF-α, IL-6, and show a low degree in TLRs expression compared to adult macrophages. Consequently, induction of cytotoxic T cells is compromised, rendering neonates more susceptible to *Listeria* infections (Marodi, 2006). In view of previous published data, TLR2 appears to be important for recognition of *L. monocytogenes* during *in vivo* infection (Boneca et al., 2007). Moreover, our results together with published data supports that TLR2 signaling induces IFN-β, mediated by endocytosis (Dietrich et al., 2010; Torres et al., 2004). In addition, IFN-β shows protective effects against *Listeria* infection when administered in the initial phase of bacteria challenge (Pontiroli et al., 2012). Therefore, we prompted to explore the *in vivo* effect of TLR2 ligands in the prevention of neonatal listeriosis.

The experimental murine model of neonatal listeriosis can mimic several human clinical symptoms of listeriosis. The number of neonates from infected mothers is reduced compared to non-infected mothers, which resembles spontaneous abortion or stillbirth (Calderon-Gonzalez et al., 2017). Our results show a reduced number of neonates from infected mothers compared to FSL-1-treated mothers, but not significant. However, neonates from infected mothers presented impaired coordinated movements and lesser brain integrity compared to neonates from treated mothers (see Fig. 31). These symptoms are related with brain dysfunction and resemble severe brain disease. Moreover, lack of skin pigmentation is observed in listeriosis patients because the bacteria impairs melanoblast’s migration to

the epidermis (Bronchalo-Vicente et al., 2015). Our results show that skin spots lacking pigmentation were observed in infected neonates but not in treated neonates. In addition, FSL-1-treated mothers presented a uterus with less fetal resorptions compared to infected non-treated mothers. These results indicate that FSL-1 attenuates neonate brain disease symptoms and reduces the chance of fetal loss during pregnancy. Moreover, FSL-1 treatment reduced in some extent the bacterial growth in the liver and spleen of infected mothers, however the effect was more evident in infected neonates' brain, with 100-fold reduction in bacteria load (see Fig. 32). It is likely that a stronger regulation of bacterial growth is observed in the brain due to the lower bacterial load compared to the liver and spleen. On the other hand, in intravenously bacteria injection, all the inoculum enters as a bolus into the bloodstream and almost all bacteria deposited in the liver and spleen within 15 min (Gregory et al., 1996). Moreover, FSL-1 administration was performed at the same time of *Listeria* challenge, which could explain the weak effect of FSL-1 in bacterial burden reduction in primary targeting organs. Nevertheless, the FSL-1 role in the reduction of bacterial load in neonates' brain is likely related with the higher levels of IFN-β observed in infected and treated neonates' microglia. Ponteroli et al observed an increment of IFN-γ production by NK cells and reduced bacterial burden when treated with exogenous IFN-β during early infection (Pontiroli et al., 2012). It is feasible that IFN-β induction mediated by FSL-1 treatment in early infection stage determines the protective effect in reducing the bacterial growth in the brain. In addition, infected and FSL1- treated mothers presented higher levels of MCP-1 and slightly higher levels of TNF-α in the serum, whereas IL-10 and IL-6 levels were not altered (see Fig. 33). Secreted TNF-α is determinant for neutrophils and NK cells activation and MCP-1 chemokine is secreted by neutrophils to recruit macrophages to the sites of infection (Zenewicz and Shen, 2007). Therefore, FSL-1 treatment likely modulated the immune system of infected mothers to induce TNF-α over Th2 cytokines (IL-6 and IL-10) and the recruitment of phagocytic cells. Our results further indicate that *Listeria*-infected dendritic cells exhibited higher levels of TNF-α, IL-6 and IL-12 as well as increased IFN-β levels upon treatment with Pam3CSK4 and FSL-1 compared to infected non-treated cells (see Fig. 34A). DCs are determinant to bridge innate and adaptive immunity. In response to *Listeria*, this antigen-presenting cells stimulate specific types of T cells and, DCs prime $CD4^+$ T and $CD8^+$ T cells for bacteria killing and to mount a proper memory T cell population. Treatment with TLR2 ligands increments Th1 cytokines in infected DCs but maintains IL-10 levels, thus exerting a Th1/Th2 balance. Moreover, treatment with exogenous IFN-β increased pro-inflammatory cytokines but decreased IL-10 in a dose dependent manner (see Fig. 34B). These results show the modulatory role of IFN-β in cytokines during the bacterial infection. Furthermore, TLR2-induced TNF-α and IL-6 were partially impaired by neutralizing IFN-β activity and IL-12 was fully inhibited in infected DCs (see Fig. 35). This data demonstrates that TLR2 ligands can modulate cytokine levels, in *Listeria*-infected cells, eliciting IL-6, TNF-α and IL-12 expression, mediated by IFN-β. Therefore, TLR2 ligands induce a tuned immunomodulatory effect, with proper IFN-β and pro-inflammatory cytokine levels, that could prevent *Listeria* dissemination in neonate's brain. Further

studies with TLR2 ligands in this model of Listeriosis are necessary to better elucidate the beneficial effects of these ligands in controlling the pathogen dissemination in the brain, and the mechanisms associated to it.

5.3 *Ochrobactrum intermedium* LPS induces TLR4 and TLR2 heterodimerization

TLR4 is considered the major receptor involved in the recognition of all LPS. However, this paradigm is being questioned and debated. Despite the general structure, lipidA, Core and O-saccharide repeats, LPS from Gram-bacteria have many different compositions in those 3 parts. Previous data reported that LPSs from *Legionella pneumofila, Rhizobium species or Porphyromonas gingivalis* require TLR2 rather than TLR4 to elicit innate immune responses (Darveau et al., 2004; Girard et al., 2003; Hirschfeld et al., 2001; Werts et al., 2001). Nonetheless, this is a debated issue since a recent publication, demonstrates that pure *Porphyromonas gingivalis* LPS activity is mediated exclusively through TLR4. A possible explanation for all those discrepancies is contamination from other cell wall components. Thus, the standard purified *Porphyromonas gingivalis* LPS can be contaminated by lipoproteins that bind TLR2 that can explain these controversial results. Nevertheless, purity may not be the full explanation since those above mentioned LPSs present a structure and composition very different from the enterobacterial LPSs, the archetypical TLR4 ligand. One of the common features is the presence of very long fatty acid chains in the lipid A that reduce the affinity of the LPS. Members of α-Proteobacteria such as *Brucella* and *Ochrobactrum* also express these atypical LPSs, comprising at least two very long FA chains, a disaccharide backbone and core saccharide and O-antigen with distinct sugars and, importantly, different net charge compared with the classical *E. coli* LPS. It is evident that the peculiar structure of those LPSs confers to this class of bacteria a stealthy strategy for immune system recognition. Indeed, our results show that the response by *Ochrobactrum intermedium* LPS requires higher concentrations to induce similar cytokine levels or signaling activation compared to *E. coli* LPS (see Fig. 36). Moreover, *O. intermedium* LPS induces inflammatory responses mediated not only by TLR4 but also by TLR2, as shown by the experiments with TLR deficient macrophages (Ovejero Guisasola, 2012). This TLR2-dependence is contradicting the current dogma that LPS molecules are strictly recognized by TLR4/MD-2 homodimers. Our FRET analysis indicates that *O. intermedium* LPS potentiates the association of TLR4/MD-2 and TLR2 *in vivo* (see Fig. 46). Indeed, our molecular dockings analysis contribute to elucidate the predictive interaction of *O. intermedium* LPS with TLR4/MD-2 homodimers, where the *O. intermedium* LPS is displaced from MD2- pocket and the core saccharide is diving towards the interface of the complex (see Fig. 40). Moreover, determinant interactions with TLR4 (e.g. Tyr296, Asp294 and Arg264) and TLR4* residues (Gln436) are lost. This implies that *O. intermedium* LPS impairs the formation of stable TLR4/MD-2 homodimers. On the other hand, the docking of this LPS in a putative TLR2/TLR4 MD-2 heterodimer demonstrated that the lipid A accommodates in MD-2 pocket, however the core side branch stablishes

determinant interaction with TLR4 (Tyr 296 and Arg 264) and the O-antigen portion seems to be determinant for the interaction with TLR2 (see Fig. 41). Therefore, *O. intermedium* LPS is likely to favor the formation of TLR2/TLR4/MD-2 heterodimers rather than TLR4/MD-2 homodimers. Nonetheless, our FRET results demonstrate that interaction of TLR2 and TLR4 is somehow weak (5-10 nm). The weak contact between TIR domains of the dimers may impair the recruitment of downstream adaptors and consequently leading to a poor activation of signaling cascades. This could explain the very weak agonist activity by *O. intermedium* LPS.

On the other hand, published studies demonstrate that a mutation in *Brucella* LPS core, leading to the specific removal of the side branch increased the inflammatory response compared to the *Brucella* WT LPS (Conde-Alvarez et al., 2012). The core side branch is composed of positive charge Glc*p*N residues linked to a mannosyl residue. It is suggested that these positive charges neutralize the KDO groups and the phosphate groups of the diaminoglucose backbone, thus displacing the *Brucella* LPS from the MD-2 pocket (Fontana et al., 2016). It was proposed that the core saccharide and the peculiar long acyl chain of the lipid A of the *Brucella* LPS hampers its MD-2 recognition. So far, it is only considered that this leads to the impairment of TLR4/MD-2 dimerization. However, it is feasible that TLR4 can also stablish interaction with other receptors in response to this type of atypical LPSs, rendering a lower inflammatory response. We further compared the composition of the cores between *Brucella abortus*, *O. Anthropi* and *O. intermedium* to evaluate the differences in sugar composition and net charge (Fig. 3). *Brucella* core is composed of glucosamines, which confer a strong positive charge and displacement of the LPS from MD-2 pocket, thus hampering TLR4 activation. O. *anthropi* contains a similar composition, but only harbors one glucosamine on the core side branch and a negative Gal*p*A residue linked to KDO II, which confers less positive net charge. Interestingly *O. intermedium* core contains the same side branch than *O. anthropi*, but the two residues are phosphorylated. This confers a more negative charge in the core compared to the *O. anthropi* core (Fig.3). Eventually, the less positive charge can lead to a lower displacement of the lipid A from MD-2, however this shift is likely to be less pronounced compared to *E. coli* lipid A. This could explain the findings from Barquero-Calvo et al., where *O. anthropi* triggers inflammatory responses lower than *Salmonella enterica*, but higher than *Brucella abortus* (Barquero-Calvo et al., 2009).

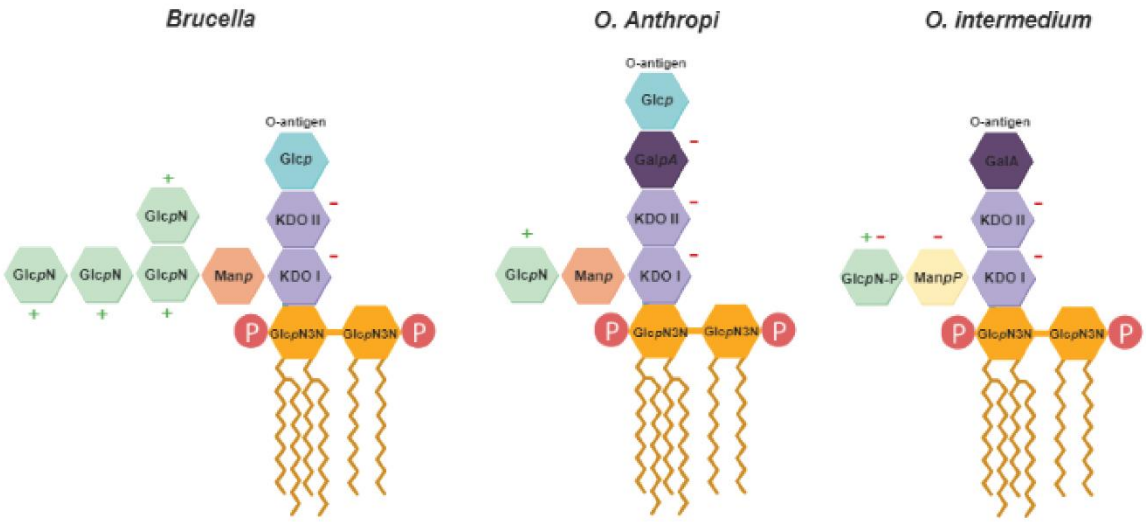

Bacterium	*B. abortus*	*O. anthropi*	*O. intermedium*	*E. coli*
Net core charge (KDO I and KDO II included)	+2	-2	-3	-5

Fig. 3 Structure model of *Brucella, O. Anthropi* and *O. intermedium* LPS core.

The three LPSs carry a similar lipid A with two very long FA chains but different cores. *Brucella* LPS contains four glucosamines in the side branch of the core, whereas *O. Anthropi* LPS only have one residue. Moreover, *O. Anthropi* LPS contains a negatively charged GalpA in the core branch that links to the O-antigen portion. *O. intermedium* LPS contains one glucosamine and mannose on the side branch of the core but both are negatively charged. The table represents the net charge of each LPS core including the KDO I and KDO II charges. *E. coli* LPS core contains an overall charge of -5.

An important aspect to consider is the LPS moieties existent in aqueous solvents since different species besides the full LPS may exist. Portions of the lipid A or the core saccharide can be present as well. Moreover, the O-antigen, which is known to serve as a "camouflage" for bacteria phagocytosis, may also be present in fragments. Considering this, lipid A fragments as well as the core were docked in the interface of TLR2 heterodimerized with TLR4/MD-2 plus an LPS accommodated in MD-2. The core distributes in the interface of TLR2, whereas docked poses in a TLR2 monomer show that one fatty acid chain of the lipid A can be accommodated in the TLR2 pocket and the core can stablish interactions near the TLR2 pocket. A proposed model consists first in the dimerization step of TLR2 and TLR4/MD-2 monomers induced by full *O. intermedium* LPS binding in MD-2 pocket and consequently, LPS moieties can bind to TLR2 and likely contribute for the final dimerization process of both TLR2 and TLR4/MD-2. Therefore, our results have clearly pointed out to the possibility of previously undescribed TLR2/TLR4 heterodimers in response to a particular set of atypical LPSs, and the important role of the core structures in the binding besides the well-known lipid A.

Bacteria have developed distinct mechanisms to escape and low the recognition by the immune system. The LPS number of acyl chains and the length greatly influence the endotoxicity of the LPS. On example is *Yersinia pesti*s and *Porphyromonas gengivalis*, which express mainly hexaacylated LPS at 28ºC, however at 37 ºC (host temperature) the LPS is mostly in tetraacylated form, avoiding innate immune cell activation (Kawahara et al., 2002; Knirel et al., 2005). In addition, the core saccharide and O-antigen composition and surface charge confer an efficient mechanism in masking the pathogen from host recognition. *Brucella* is an opportunistic pathogen usually found in immunocompromised patients. On the hand, although, *Ochrobactrum* is a living soil organism, it has been reported to display some degree of pathogenicity (Berg et al., 2005; Mahmood et al., 2000). Both bacteria, phylogenetically closed, are likely to share similar mechanistic strategies of host evasion. Brucella LPS weakly activates TLRs activation, impairing the induction of Th1 responses determinant for the bacteria clearance. Furthermore, most of the infectious diseases lack for efficient vaccines. This limitation comes from the incorrect use of adjuvants to induce an appropriate immune response. Moreover, the toxicity of the adjuvant in human vaccines formulation is another concern due to the exacerbated Th1 responses. Since the core saccharide, besides the VLFCAs, shows an impact in the induction of inflammatory mediators, the use of *Brucella* core mutants are being developed as adjuvants for vaccines (Conde-Alvarez et al., 2013). Our group previously characterized the potential use of *O. intermedium* LPS as an adjuvant for vaccines in immunocompromised and septic animals with no side toxicity (Ovejero Guisasola, 2012). Besides, the inflammation response induced by the *O. intermedium* LPS depend on TLR4 and TLR2 receptors. Given this, further studies are necessary to elucidate in a molecular and biological perspective the impact of the cores and O-antigen of these type of LPS for the development of vaccine adjuvants or better immunomodulators.

CONCLUSIONS

6. CONCLUSIONS

1. TLR2 ligands induce higher levels of anti-inflammatory IL-10 and lower levels of pro-inflammatory cytokines IL-12, TNF-α compared to TLR4 ligands. TLR2 ligands activate NF-κB and MAPKs earlier compared to TLR4 ligands.

2. TLR2 ligands induce ERK by a MEK1/2-independent but Ras-dependent in the Raw264.7 cell line. Moreover, Raw264.7 cells induce p38 by an autophosphorylation mechanism only in response to TLR4. These phenomena were not observed in primary macrophages.

3. MKP-1 controls p38 phosphorylation and differentially controls pro and anti-inflammatory cytokines in response to TLR2 activation. The early p38 is critical for the higher levels of IL-10 induction in response to TLR2 ligands.

4. TLR2 ligands induce IRF3, IRF7 and IFN-β in peritoneal macrophages in an endocytosis dependent manner. TRIF-IFNβ signaling contributes for later IL-12 cytokine expression in response to TLR2 ligands. TLR2/6 ligand FSL-1 treatment in neonatal listeriosis confer a preventive effect on neonate's brain disease, by decreasing bacteria load and increasing protective Th1 cytokines. TLR2 ligands treatment in *Listeria*-infected DC cells exert a Th1/Th2 balance, through an increase in IL-12 levels mediated by IFN-β.

5. *Ochrobactrum intermedium* LPS induces a weaker inflammatory response mediated by TLR4 and TLR2 compared to the TLR4-dependent *E. coli* LPS, in primary macrophages. *Ochrobactrum intermedium* LPS favors the heterodimerization of TLR4 and TLR2 receptors.

CONCLUSIONES

1. Los ligandos de TLR2, Pam3CSK4 (TLR2/TLR1) y FSL-1 (TLR2/TLR6) inducen niveles más elevados de la citoquina antiinflamatoria IL-10 and niveles más bajos de citoquinas proinflamatorias en comparación a los ligandos TLR4. Además, los ligandos TLR2 activan NF-κB y MAPKs más temprano que el LPS.

2. Los ligandos TLR2 inducen la MAPK ERK por un mecanismo independiente de MEK1/2, pero dependiente de Ras en la línea celular Raw264.7. Este fenómeno no se observa en macrófagos primarios.

3. MKP-1 controla la fosforilación de p38 y regula diferencialmente la expresión de citoquinas pro y antiinflamatorias por la activación de TLR2. La activación temprana de p38 es importante para los altos niveles de inducción de IL-10 en respuesta a los ligandos TLR2.

4. Los ligandos TLR2 inducen IRF3, IRF7 y IFN-β en macrófagos peritoneales por un mecanismo dependiente de endocitosis. La ruta de señalización TRIF-IFN-β contribuye a la expresión de IL-12 por la activación de TLR2. El tratamiento con el ligando FSL-1 en listeriosis neonatal tiene un efecto preventivo en la enfermedad cerebral de los neonatos, por disminución de la carga bacteriana y incremento de la expresión de citoquinas Th1 protectoras. Además, el tratamiento de células dendríticas infectadas con *Listeria* con los ligandos TLR2 incrementa los niveles de IL-12 mediado por IFN-β, creando un balance Th1/Th2.

5. El LPS de *Ochrobactrum intermedium* induce un respuesta inflamatoria mas debil en comparacion al LPS de E coli, y dependiente de TLR4 y TLR2. O interermedium LPS favorece la dimerizacion de TKR4 y TLR2.

REFERENCES

7. REFERENCES

Agrawal, S., Agrawal, A., Doughty, B., Gerwitz, A., Blenis, J., Van Dyke, T., and Pulendran, B. (2003). Cutting edge: different Toll-like receptor agonists instruct dendritic cells to induce distinct Th responses via differential modulation of extracellular signal-regulated kinase-mitogen-activated protein kinase and c-Fos. J Immunol *171*, 4984-4989.

Akira, S., and Takeda, K. (2004a). Functions of toll-like receptors: lessons from KO mice. C R Biol *327*, 581-589.

Akira, S., and Takeda, K. (2004b). Toll-like receptor signalling. Nat Rev Immunol *4*, 499-511.

Akira, T.K.a.S. (2010). The role of pattern-recognition receptors in innate immunity: update on Toll-like receptors. Nat Immunol 11(5), 373-384.

Alessi, D.R., Cuenda, A., Cohen, P., Dudley, D.T., and Saltiel, A.R. (1995). PD 098059 is a specific inhibitor of the activation of mitogen-activated protein kinase kinase in vitro and in vivo. J Biol Chem *270*, 27489-27494.

Alexopoulou, L., Holt, A.C., Medzhitov, R., and Flavell, R.A. (2001). Recognition of double-stranded RNA and activation of NF-kappaB by Toll-like receptor 3. Nature *413*, 732-738.

Ananieva, O., Darragh, J., Johansen, C., Carr, J.M., McIlrath, J., Park, J.M., Wingate, A., Monk, C.E., Toth, R., Santos, S.G., *et al.* (2008). The kinases MSK1 and MSK2 act as negative regulators of Toll-like receptor signaling. Nat Immunol *9*, 1028-1036.

Andrade, W.A., Souza Mdo, C., Ramos-Martinez, E., Nagpal, K., Dutra, M.S., Melo, M.B., Bartholomeu, D.C., Ghosh, S., Golenbock, D.T., and Gazzinelli, R.T. (2013). Combined action of nucleic acid-sensing Toll-like receptors and TLR11/TLR12 heterodimers imparts resistance to Toxoplasma gondii in mice. Cell Host Microbe *13*, 42-53.

Archer, K.A., Durack, J., and Portnoy, D.A. (2014). STING-dependent type I IFN production inhibits cell-mediated immunity to Listeria monocytogenes. PLoS Pathog *10*, e1003861.

Arthur, J.S., and Ley, S.C. (2013). Mitogen-activated protein kinases in innate immunity. Nat Rev Immunol *13*, 679-692.

Aubry, C., Corr, S.C., Wienerroither, S., Goulard, C., Jones, R., Jamieson, A.M., Decker, T., O'Neill, L.A., Dussurget, O., and Cossart, P. (2012). Both TLR2 and TRIF contribute to interferon-beta production during Listeria infection. PLoS One *7*, e33299.

Auerbuch, V., Brockstedt, D.G., Meyer-Morse, N., O'Riordan, M., and Portnoy, D.A. (2004). Mice lacking the type I interferon receptor are resistant to Listeria monocytogenes. J Exp Med *200*, 527-533.

Bakardjiev, A.I., Stacy, B.A., and Portnoy, D.A. (2005). Growth of Listeria monocytogenes in the guinea pig placenta and role of cell-to-cell spread in fetal infection. J Infect Dis *191*, 1889-1897.

Barbalat, R., Lau, L., Locksley, R.M., and Barton, G.M. (2009). Toll-like receptor 2 on inflammatory monocytes induces type I interferon in response to viral but not bacterial ligands. Nat Immunol *10*, 1200-1207.

Barquero-Calvo, E., Conde-Alvarez, R., Chacon-Diaz, C., Quesada-Lobo, L., Martirosyan, A., Guzman-Verri, C., Iriarte, M., Mancek-Keber, M., Jerala, R., Gorvel, J.P., *et al.* (2009). The differential interaction of Brucella and ochrobactrum with innate immunity reveals traits related to the evolution of stealthy pathogens. PLoS One *4*, e5893.

Bell, J.K., Botos, I., Hall, P.R., Askins, J., Shiloach, J., Segal, D.M., and Davies, D.R. (2005). The molecular structure of the Toll-like receptor 3 ligand-binding domain. Proc Natl Acad Sci U S A *102*, 10976-10980.

Bell, J.K., Mullen, G.E., Leifer, C.A., Mazzoni, A., Davies, D.R., and Segal, D.M. (2003). Leucine-rich repeats and pathogen recognition in Toll-like receptors. Trends Immunol *24*, 528-533.

Berg, G., Eberl, L., and Hartmann, A. (2005). The rhizosphere as a reservoir for opportunistic human pathogenic bacteria. Environ Microbiol *7*, 1673-1685.

Boneca, I.G., Dussurget, O., Cabanes, D., Nahori, M.A., Sousa, S., Lecuit, M., Psylinakis, E., Bouriotis, V., Hugot, J.P., Giovannini, M., *et al.* (2007). A critical role for peptidoglycan N-deacetylation in Listeria evasion from the host innate immune system. Proc Natl Acad Sci U S A *104*, 997-1002.

Brenner, S., Prosch, S., Schenke-Layland, K., Riese, U., Gausmann, U., and Platzer, C. (2003). cAMP-induced Interleukin-10 promoter activation depends on CCAAT/enhancer-binding protein expression and monocytic differentiation. J Biol Chem *278*, 5597-5604.

Bronchalo-Vicente, L., Rodriguez-Del Rio, E., Freire, J., Calderon-Gonzalez, R., Frande-Cabanes, E., Gomez-Roman, J.J., Fernandez-Llaca, H., Yanez-Diaz, S., and Alvarez-Dominguez, C. (2015). A novel therapy for melanoma developed in mice: transformation of melanoma into dendritic cells with Listeria monocytogenes. PLoS One *10*, e0117923.

Brondello, J.M., Pouyssegur, J., and McKenzie, F.R. (1999). Reduced MAP kinase phosphatase-1 degradation after p42/p44MAPK-dependent phosphorylation. Science *286*, 2514-2517.

Brooke, J.S., and Valvano, M.A. (1996). Biosynthesis of inner core lipopolysaccharide in enteric bacteria identification and characterization of a conserved phosphoheptose isomerase. J Biol Chem *271*, 3608-3614.

Burdette, D.L., Monroe, K.M., Sotelo-Troha, K., Iwig, J.S., Eckert, B., Hyodo, M., Hayakawa, Y., and Vance, R.E. (2011). STING is a direct innate immune sensor of cyclic di-GMP. Nature *478*, 515-518.

Burns, E., Eliyahu, T., Uematsu, S., Akira, S., and Nussbaum, G. (2010). TLR2-dependent inflammatory response to Porphyromonas gingivalis is MyD88 independent, whereas MyD88 is required to clear infection. J Immunol *184*, 1455-1462.

Buwitt-Beckmann, U., Heine, H., Wiesmuller, K.H., Jung, G., Brock, R., Akira, S., and Ulmer, A.J. (2006). TLR1- and TLR6-independent recognition of bacterial lipopeptides. J Biol Chem *281*, 9049-9057.

Cabanes, D., Sousa, S., Cebria, A., Lecuit, M., Garcia-del Portillo, F., and Cossart, P. (2005). Gp96 is a receptor for a novel Listeria monocytogenes virulence factor, Vip, a surface protein. EMBO J *24*, 2827-2838.

Calderon-Gonzalez, R., Frande-Cabanes, E., Teran-Navarro, H., Marimon, J.M., Freire, J., Salcines-Cuevas, D., Carmen Farinas, M., Onzalez-Rico, C., Marradi, M., Garcia, I., *et al.* (2017). GNP-GAPDH1-22 nanovaccines prevent neonatal listeriosis by blocking microglial apoptosis and bacterial dissemination. Oncotarget *8*, 53916-53934.

Carrero, J.A., Calderon, B., and Unanue, E.R. (2004). Type I interferon sensitizes lymphocytes to apoptosis and reduces resistance to Listeria infection. J Exp Med *200*, 535-540.

Case, D.B., V.; Berryman, J.; Betz, R.; Cai, Q.; Cerutti, D.; Cheatham III, T.; Darden, T.; Duke, R.; Gohlke, H.; Goetz, A.; Gusarov, S.; Homeyer, N.; Janowski, P.; Kaus, J.; Kolossváry, I.; Kovalenko, A.; Lee, T.; LeGrand, S.; Luchko, T.; Luo, R.; Madej, B.; Merz, K. M.; Paesani, F.; Roe, D.; Roitberg, A.; Sagui, C.; Salomon-Ferrer, R.; Seabra, G.; Simmerling, C.; Smith, W.; Swails, J.; Walker, R. C.; Wang, J.; Wolf, R. M.; Wu, X.; Kollman, P. A (2014). AMBER 14, University of California, San Francisco.

Chandler, C.E., and Ernst, R.K. (2017). Bacterial lipids: powerful modifiers of the innate immune response. F1000Res *6*.

Charles A. Janeway, J.a.R.M. (2002). Innate Immune Recognition. Annu Rev Immunol 20, 197-216.

Chen, P., Li, J., Barnes, J., Kokkonen, G.C., Lee, J.C., and Liu, Y. (2002). Restraint of proinflammatory cytokine biosynthesis by mitogen-activated protein kinase phosphatase-1 in lipopolysaccharide-stimulated macrophages. J Immunol *169*, 6408-6416.

Chi, H., Barry, S.P., Roth, R.J., Wu, J.J., Jones, E.A., Bennett, A.M., and Flavell, R.A. (2006). Dynamic regulation of pro- and anti-inflammatory cytokines by MAPK phosphatase 1 (MKP-1) in innate immune responses. Proc Natl Acad Sci U S A *103*, 2274-2279.

Chiba, S., Nagai, T., Hayashi, T., Baba, Y., Nagai, S., and Koyasu, S. (2011). Listerial invasion protein internalin B promotes entry into ileal Peyer's patches in vivo. Microbiol Immunol *55*, 123-129.

Choe, J., Kelker, M.S., and Wilson, I.A. (2005). Crystal structure of human toll-like receptor 3 (TLR3) ectodomain. Science *309*, 581-585.

Conde-Alvarez, R., Arce-Gorvel, V., Gil-Ramirez, Y., Iriarte, M., Grillo, M.J., Gorvel, J.P., and Moriyon, I. (2013). Lipopolysaccharide as a target for brucellosis vaccine design. Microb Pathog *58*, 29-34.

Conde-Alvarez, R., Arce-Gorvel, V., Iriarte, M., Mancek-Keber, M., Barquero-Calvo, E., Palacios-Chaves, L., Chacon-Diaz, C., Chaves-Olarte, E., Martirosyan, A., von Bargen, K., *et al.*

(2012). The lipopolysaccharide core of Brucella abortus acts as a shield against innate immunity recognition. PLoS Pathog *8*, e1002675.

Cossart, P. (2011). Illuminating the landscape of host-pathogen interactions with the bacterium Listeria monocytogenes. Proc Natl Acad Sci U S A *108*, 19484-19491.

Crowell, S., Wancket, L.M., Shakibi, Y., Xu, P., Xue, J., Samavati, L., Nelin, L.D., and Liu, Y. (2014). Post-translational regulation of mitogen-activated protein kinase phosphatase (MKP)-1 and MKP-2 in macrophages following lipopolysaccharide stimulation: the role of the C termini of the phosphatases in determining their stability. J Biol Chem *289*, 28753-28764.

Darveau, R.P., Pham, T.T., Lemley, K., Reife, R.A., Bainbridge, B.W., Coats, S.R., Howald, W.N., Way, S.S., and Hajjar, A.M. (2004). Porphyromonas gingivalis lipopolysaccharide contains multiple lipid A species that functionally interact with both toll-like receptors 2 and 4. Infect Immun *72*, 5041-5051.

DeLano, W.L. (2002). PyMOL Molecular Graphics System, Version 1.6.0.0. Schrödinger (LLC).

Diebold, S.S., Kaisho, T., Hemmi, H., Akira, S., and Reis e Sousa, C. (2004). Innate antiviral responses by means of TLR7-mediated recognition of single-stranded RNA. Science *303*, 1529-1531.

Dietrich, N., Lienenklaus, S., Weiss, S., and Gekara, N.O. (2010). Murine toll-like receptor 2 activation induces type I interferon responses from endolysosomal compartments. PLoS One *5*, e10250.

Dillon, S., Agrawal, S., Banerjee, K., Letterio, J., Denning, T.L., Oswald-Richter, K., Kasprowicz, D.J., Kellar, K., Pare, J., van Dyke, T., *et al.* (2006). Yeast zymosan, a stimulus for TLR2 and dectin-1, induces regulatory antigen-presenting cells and immunological tolerance. J Clin Invest *116*, 916-928.

Dinarello, C.A. (1991). Interleukin-1 and interleukin-1 antagonism. Blood *77*, 1627-1652.

Drevets, D.A. (1999). Dissemination of Listeria monocytogenes by infected phagocytes. Infect Immun *67*, 3512-3517.

Duenas, A.I., Orduna, A., Crespo, M.S., and Garcia-Rodriguez, C. (2004). Interaction of endotoxins with Toll-like receptor 4 correlates with their endotoxic potential and may explain the proinflammatory effect of Brucella spp. LPS. Int Immunol *16*, 1467-1475.

Dussurget, O., Bierne, H., and Cossart, P. (2014). The bacterial pathogen Listeria monocytogenes and the interferon family: type I, type II and type III interferons. Front Cell Infect Microbiol *4*, 50.

Echchannaoui, H., Frei, K., Schnell, C., Leib, S.L., Zimmerli, W., and Landmann, R. (2002). Toll-like receptor 2-deficient mice are highly susceptible to Streptococcus pneumoniae meningitis because of reduced bacterial clearing and enhanced inflammation. J Infect Dis *186*, 798-806.

Edelson, B.T., and Unanue, E.R. (2000). Immunity to Listeria infection. Curr Opin Immunol *12*, 425-431.

Faith, N., Kathariou, S., Cheng, Y., Promadej, N., Neudeck, B.L., Zhang, Q., Luchansky, J., and Czuprynski, C. (2009). The role of L. monocytogenes serotype 4b gtcA in gastrointestinal listeriosis in A/J mice. Foodborne Pathog Dis *6*, 39-48.

Favata, M.F., Horiuchi, K.Y., Manos, E.J., Daulerio, A.J., Stradley, D.A., Feeser, W.S., Van Dyk, D.E., Pitts, W.J., Earl, R.A., Hobbs, F., *et al.* (1998). Identification of a novel inhibitor of mitogen-activated protein kinase kinase. J Biol Chem *273*, 18623-18632.

Fontana, C., Conde-Alvarez, R., Stahle, J., Holst, O., Iriarte, M., Zhao, Y., Arce-Gorvel, V., Hanniffy, S., Gorvel, J.P., Moriyon, I., *et al.* (2016). Structural Studies of Lipopolysaccharide-defective Mutants from Brucella melitensis Identify a Core Oligosaccharide Critical in Virulence. J Biol Chem *291*, 7727-7741.

Foreback, J.L., Sarma, V., Yeager, N.R., Younkin, E.M., Remick, D.G., and Ward, P.A. (1998). Blood mononuclear cell production of TNF-alpha and IL-8: engagement of different signal transduction pathways including the p42 MAP kinase pathway. J Leukoc Biol *64*, 124-133.

Gantner, B.N., Simmons, R.M., Canavera, S.J., Akira, S., and Underhill, D.M. (2003). Collaborative induction of inflammatory responses by dectin-1 and Toll-like receptor 2. J Exp Med *197*, 1107-1117.

Ge, B., Gram, H., Di Padova, F., Huang, B., New, L., Ulevitch, R.J., Luo, Y., and Han, J. (2002). MAPKK-independent activation of p38alpha mediated by TAB1-dependent autophosphorylation of p38alpha. Science *295*, 1291-1294.

Girard, R., Pedron, T., Uematsu, S., Balloy, V., Chignard, M., Akira, S., and Chaby, R. (2003). Lipopolysaccharides from Legionella and Rhizobium stimulate mouse bone marrow granulocytes via Toll-like receptor 2. J Cell Sci *116*, 293-302.

Good, D.W., George, T., and Watts, B.A., 3rd (2012). Toll-like receptor 2 is required for LPS-induced Toll-like receptor 4 signaling and inhibition of ion transport in renal thick ascending limb. J Biol Chem *287*, 20208-20220.

Grammer, T.C., and Blenis, J. (1997). Evidence for MEK-independent pathways regulating the prolonged activation of the ERK-MAP kinases. Oncogene *14*, 1635-1642.

Gregory, S.H., Sagnimeni, A.J., and Wing, E.J. (1996). Bacteria in the bloodstream are trapped in the liver and killed by immigrating neutrophils. J Immunol *157*, 2514-2520.

Guan, Y., Ranoa, D.R., Jiang, S., Mutha, S.K., Li, X., Baudry, J., and Tapping, R.I. (2010). Human TLRs 10 and 1 share common mechanisms of innate immune sensing but not signaling. J Immunol *184*, 5094-5103.

Guven-Maiorov, E., Keskin, O., Gursoy, A., VanWaes, C., Chen, Z., Tsai, C.J., and Nussinov, R. (2015). The Architecture of the TIR Domain Signalosome in the Toll-like Receptor-4 Signaling Pathway. Sci Rep *5*, 13128.

Hammer, M., Mages, J., Dietrich, H., Servatius, A., Howells, N., Cato, A.C., and Lang, R. (2006). Dual specificity phosphatase 1 (DUSP1) regulates a subset of LPS-induced genes and protects mice from lethal endotoxin shock. J Exp Med *203*, 15-20.

Harder, E., Damm, W., Maple, J., Wu, C., Reboul, M., Xiang, J.Y., Wang, L., Lupyan, D., Dahlgren, M.K., Knight, J.L., *et al.* (2016). OPLS3: A Force Field Providing Broad Coverage of Drug-like Small Molecules and Proteins. J Chem Theory Comput *12*, 281-296.

Hawn, T.R., Verbon, A., Lettinga, K.D., Zhao, L.P., Li, S.S., Laws, R.J., Skerrett, S.J., Beutler, B., Schroeder, L., Nachman, A., *et al.* (2003). A common dominant TLR5 stop codon polymorphism abolishes flagellin signaling and is associated with susceptibility to legionnaires' disease. J Exp Med *198*, 1563-1572.

Haziot, A., Ferrero, E., Kontgen, F., Hijiya, N., Yamamoto, S., Silver, J., Stewart, C.L., and Goyert, S.M. (1996). Resistance to endotoxin shock and reduced dissemination of gram-negative bacteria in CD14-deficient mice. Immunity *4*, 407-414.

Heil, F., Hemmi, H., Hochrein, H., Ampenberger, F., Kirschning, C., Akira, S., Lipford, G., Wagner, H., and Bauer, S. (2004). Species-specific recognition of single-stranded RNA via toll-like receptor 7 and 8. Science *303*, 1526-1529.

Hemmi, H., Takeuchi, O., Kawai, T., Kaisho, T., Sato, S., Sanjo, H., Matsumoto, M., Hoshino, K., Wagner, H., Takeda, K., *et al.* (2000). A Toll-like receptor recognizes bacterial DNA. Nature *408*, 740-745.

Hidmark, A., von Saint Paul, A., and Dalpke, A.H. (2012). Cutting edge: TLR13 is a receptor for bacterial RNA. J Immunol *189*, 2717-2721.

Hirschfeld, M., Weis, J.J., Toshchakov, V., Salkowski, C.A., Cody, M.J., Ward, D.C., Qureshi, N., Michalek, S.M., and Vogel, S.N. (2001). Signaling by toll-like receptor 2 and 4 agonists results in differential gene expression in murine macrophages. Infect Immun *69*, 1477-1482.

Hoebe, K., Georgel, P., Rutschmann, S., Du, X., Mudd, S., Crozat, K., Sovath, S., Shamel, L., Hartung, T., Zahringer, U., *et al.* (2005). CD36 is a sensor of diacylglycerides. Nature *433*, 523-527.

Honda, K., Takaoka, A., and Taniguchi, T. (2006). Type I interferon [corrected] gene induction by the interferon regulatory factor family of transcription factors. Immunity *25*, 349-360.

Hoshino, K., Takeuchi, O., Kawai, T., Sanjo, H., Ogawa, T., Takeda, Y., Takeda, K., and Akira, S. (1999). Cutting edge: Toll-like receptor 4 (TLR4)-deficient mice are hyporesponsive to lipopolysaccharide: evidence for TLR4 as the Lps gene product. J Immunol *162*, 3749-3752.

Hu, J.H., Chen, T., Zhuang, Z.H., Kong, L., Yu, M.C., Liu, Y., Zang, J.W., and Ge, B.X. (2007). Feedback control of MKP-1 expression by p38. Cell Signal *19*, 393-400.

Janakiraman, V. (2008). Listeriosis in pregnancy: diagnosis, treatment, and prevention. Rev Obstet Gynecol *1*, 179-185.

Jin, M.S., Kim, S.E., Heo, J.Y., Lee, M.E., Kim, H.M., Paik, S.G., Lee, H., and Lee, J.O. (2007). Crystal structure of the TLR1-TLR2 heterodimer induced by binding of a tri-acylated lipopeptide. Cell *130*, 1071-1082.

Kagan, J.C., Su, T., Horng, T., Chow, A., Akira, S., and Medzhitov, R. (2008). TRAM couples endocytosis of Toll-like receptor 4 to the induction of interferon-beta. Nat Immunol *9*, 361-368.

Kang, J.Y., Nan, X., Jin, M.S., Youn, S.J., Ryu, Y.H., Mah, S., Han, S.H., Lee, H., Paik, S.G., and Lee, J.O. (2009). Recognition of lipopeptide patterns by Toll-like receptor 2-Toll-like receptor 6 heterodimer. Immunity *31*, 873-884.

Kawahara, K., Tsukano, H., Watanabe, H., Lindner, B., and Matsuura, M. (2002). Modification of the structure and activity of lipid A in Yersinia pestis lipopolysaccharide by growth temperature. Infect Immun *70*, 4092-4098.

Kernbauer, E., Maier, V., Rauch, I., Muller, M., and Decker, T. (2013). Route of Infection Determines the Impact of Type I Interferons on Innate Immunity to Listeria monocytogenes. PLoS One *8*, e65007.

Kim, C., Sano, Y., Todorova, K., Carlson, B.A., Arpa, L., Celada, A., Lawrence, T., Otsu, K., Brissette, J.L., Arthur, J.S., *et al.* (2008). The kinase p38 alpha serves cell type-specific inflammatory functions in skin injury and coordinates pro- and anti-inflammatory gene expression. Nat Immunol *9*, 1019-1027.

Kim, L., Del Rio, L., Butcher, B.A., Mogensen, T.H., Paludan, S.R., Flavell, R.A., and Denkers, E.Y. (2005). p38 MAPK autophosphorylation drives macrophage IL-12 production during intracellular infection. J Immunol *174*, 4178-4184.

Knirel, Y.A., Lindner, B., Vinogradov, E.V., Kocharova, N.A., Senchenkova, S.N., Shaikhutdinova, R.Z., Dentovskaya, S.V., Fursova, N.K., Bakhteeva, I.V., Titareva, G.M., *et al.* (2005). Temperature-dependent variations and intraspecies diversity of the structure of the lipopolysaccharide of Yersinia pestis. Biochemistry *44*, 1731-1743.

Kumar, H., Kawai, T., and Akira, S. (2011). Pathogen recognition by the innate immune system. Int Rev Immunol *30*, 16-34.

Kurokawa, K., Ryu, K.H., Ichikawa, R., Masuda, A., Kim, M.S., Lee, H., Chae, J.H., Shimizu, T., Saitoh, T., Kuwano, K., *et al.* (2012). Novel bacterial lipoprotein structures conserved in low-GC content gram-positive bacteria are recognized by Toll-like receptor 2. J Biol Chem *287*, 13170-13181.

Lapaque, N., Takeuchi, O., Corrales, F., Akira, S., Moriyon, I., Howard, J.C., and Gorvel, J.P. (2006). Differential inductions of TNF-alpha and IGTP, IIGP by structurally diverse classic and non-classic lipopolysaccharides. Cell Microbiol *8*, 401-413.

Latz, E., Visintin, A., Lien, E., Fitzgerald, K.A., Monks, B.G., Kurt-Jones, E.A., Golenbock, D.T., and Espevik, T. (2002). Lipopolysaccharide rapidly traffics to and from the Golgi apparatus

with the toll-like receptor 4-MD-2-CD14 complex in a process that is distinct from the initiation of signal transduction. J Biol Chem *277*, 47834-47843.

Leber, J.H., Crimmins, G.T., Raghavan, S., Meyer-Morse, N.P., Cox, J.S., and Portnoy, D.A. (2008). Distinct TLR- and NLR-mediated transcriptional responses to an intracellular pathogen. PLoS Pathog *4*, e6.

Lecuit, M., Vandormael-Pournin, S., Lefort, J., Huerre, M., Gounon, P., Dupuy, C., Babinet, C., and Cossart, P. (2001). A transgenic model for listeriosis: role of internalin in crossing the intestinal barrier. Science *292*, 1722-1725.

Lee, H.K., Dunzendorfer, S., and Tobias, P.S. (2004). Cytoplasmic domain-mediated dimerizations of toll-like receptor 4 observed by beta-lactamase enzyme fragment complementation. J Biol Chem *279*, 10564-10574.

Lemaitre, B., Nicolas, E., Michaut, L., Reichhart, J.M., and Hoffmann, J.A. (1996). The dorsoventral regulatory gene cassette spatzle/Toll/cactus controls the potent antifungal response in Drosophila adults. Cell *86*, 973-983.

Liljeroos, M., Vuolteenaho, R., Rounioja, S., Henriques-Normark, B., Hallman, M., and Ojaniemi, M. (2008). Bacterial ligand of TLR2 signals Stat activation via induction of IRF1/2 and interferon-alpha production. Cell Signal *20*, 1873-1881.

Liu, L., Botos, I., Wang, Y., Leonard, J.N., Shiloach, J., Segal, D.M., and Davies, D.R. (2008). Structural basis of toll-like receptor 3 signaling with double-stranded RNA. Science *320*, 379-381.

Liu, Y., Shepherd, E.G., and Nelin, L.D. (2007). MAPK phosphatases--regulating the immune response. Nat Rev Immunol *7*, 202-212.

Long, E.M., Millen, B., Kubes, P., and Robbins, S.M. (2009). Lipoteichoic acid induces unique inflammatory responses when compared to other toll-like receptor 2 ligands. PLoS One *4*, e5601.

Ma, W., Lim, W., Gee, K., Aucoin, S., Nandan, D., Kozlowski, M., Diaz-Mitoma, F., and Kumar, A. (2001). The p38 mitogen-activated kinase pathway regulates the human interleukin-10 promoter via the activation of Sp1 transcription factor in lipopolysaccharide-stimulated human macrophages. J Biol Chem *276*, 13664-13674.

Mahmood, M.S., Sarwari, A.R., Khan, M.A., Sophie, Z., Khan, E., and Sami, S. (2000). Infective endocarditis and septic embolization with Ochrobactrum anthropi: case report and review of literature. J Infect *40*, 287-290.

Maier, J.A., Martinez, C., Kasavajhala, K., Wickstrom, L., Hauser, K.E., and Simmerling, C. (2015). ff14SB: Improving the Accuracy of Protein Side Chain and Backbone Parameters from ff99SB. J Chem Theory Comput *11*, 3696-3713.

Mancuso, G., Gambuzza, M., Midiri, A., Biondo, C., Papasergi, S., Akira, S., Teti, G., and Beninati, C. (2009). Bacterial recognition by TLR7 in the lysosomes of conventional dendritic cells. Nat Immunol *10*, 587-594.

Marodi, L. (2006). Innate cellular immune responses in newborns. Clin Immunol *118*, 137-144.

Matzinger, P. (1994). Tolerance, danger, and the extended family. Annu Rev Immunol *12*, 991-1045.

Maurya, M.R., Benner, C., Pradervand, S., Glass, C., and Subramaniam, S. (2007). Systems biology of macrophages. Adv Exp Med Biol *598*, 62-79.

Medzhitov, R., Preston-Hurlburt, P., and Janeway, C.A., Jr. (1997). A human homologue of the Drosophila Toll protein signals activation of adaptive immunity. Nature *388*, 394-397.

Molinaro, A., Holst, O., Di Lorenzo, F., Callaghan, M., Nurisso, A., D'Errico, G., Zamyatina, A., Peri, F., Berisio, R., Jerala, R., *et al.* (2015). Chemistry of lipid A: at the heart of innate immunity. Chemistry *21*, 500-519.

Monick, M.M., Carter, A.B., Flaherty, D.M., Peterson, M.W., and Hunninghake, G.W. (2000). Protein kinase C zeta plays a central role in activation of the p42/44 mitogen-activated protein kinase by endotoxin in alveolar macrophages. J Immunol *165*, 4632-4639.

Mosser, D.M., and Edwards, J.P. (2008). Exploring the full spectrum of macrophage activation. Nat Rev Immunol *8*, 958-969.

Murray, P.J. (2006). Understanding and exploiting the endogenous interleukin-10/STAT3-mediated anti-inflammatory response. Curr Opin Pharmacol *6*, 379-386.

Nagai, Y., Akashi, S., Nagafuku, M., Ogata, M., Iwakura, Y., Akira, S., Kitamura, T., Kosugi, A., Kimoto, M., and Miyake, K. (2002). Essential role of MD-2 in LPS responsiveness and TLR4 distribution. Nat Immunol *3*, 667-672.

Netea, M.G., Sutmuller, R., Hermann, C., Van der Graaf, C.A., Van der Meer, J.W., van Krieken, J.H., Hartung, T., Adema, G., and Kullberg, B.J. (2004). Toll-like receptor 2 suppresses immunity against Candida albicans through induction of IL-10 and regulatory T cells. J Immunol *172*, 3712-3718.

Nilsen, N.J., Vladimer, G.I., Stenvik, J., Orning, M.P., Zeid-Kilani, M.V., Bugge, M., Bergstroem, B., Conlon, J., Husebye, H., Hise, A.G., *et al.* (2015). A role for the adaptor proteins TRAM and TRIF in toll-like receptor 2 signaling. J Biol Chem *290*, 3209-3222.

O'Connell, R.M., Saha, S.K., Vaidya, S.A., Bruhn, K.W., Miranda, G.A., Zarnegar, B., Perry, A.K., Nguyen, B.O., Lane, T.F., Taniguchi, T., *et al.* (2004). Type I interferon production enhances susceptibility to Listeria monocytogenes infection. J Exp Med *200*, 437-445.

O'Connell, R.M., Vaidya, S.A., Perry, A.K., Saha, S.K., Dempsey, P.W., and Cheng, G. (2005). Immune activation of type I IFNs by Listeria monocytogenes occurs independently of TLR4, TLR2, and receptor interacting protein 2 but involves TNFR-associated NF kappa B kinase-binding kinase 1. J Immunol *174*, 1602-1607.

O'Neill, L.A., Bryant, C.E., and Doyle, S.L. (2009). Therapeutic targeting of Toll-like receptors for infectious and inflammatory diseases and cancer. Pharmacol Rev *61*, 177-197.

Ohto, U., Fukase, K., Miyake, K., and Satow, Y. (2007). Crystal structures of human MD-2 and its complex with antiendotoxic lipid IVa. Science *316*, 1632-1634.

Ohto, U., Fukase, K., Miyake, K., and Shimizu, T. (2012). Structural basis of species-specific endotoxin sensing by innate immune receptor TLR4/MD-2. Proc Natl Acad Sci U S A *109*, 7421-7426.

Okan, N.A., and Kasper, D.L. (2013). The atypical lipopolysaccharide of Francisella. Carbohydr Res *378*, 79-83.

Oldenburg, M., Kruger, A., Ferstl, R., Kaufmann, A., Nees, G., Sigmund, A., Bathke, B., Lauterbach, H., Suter, M., Dreher, S., *et al.* (2012). TLR13 recognizes bacterial 23S rRNA devoid of erythromycin resistance-forming modification. Science *337*, 1111-1115.

Oleg Trott, A.J.O. (2010). AutoDock Vina: improving the speed and accuracy of docking with a new scoring function, efficient optimization and multithreading. In J Comput Chem 31(2), pp. 455–461.

Oosting, M., Cheng, S.C., Bolscher, J.M., Vestering-Stenger, R., Plantinga, T.S., Verschueren, I.C., Arts, P., Garritsen, A., van Eenennaam, H., Sturm, P., *et al.* (2014). Human TLR10 is an anti-inflammatory pattern-recognition receptor. Proc Natl Acad Sci U S A *111*, E4478-4484.

Opitz, B., Vinzing, M., van Laak, V., Schmeck, B., Heine, G., Gunther, S., Preissner, R., Slevogt, H., N'Guessan, P.D., Eitel, J., *et al.* (2006). Legionella pneumophila induces IFNbeta in lung epithelial cells via IPS-1 and IRF3, which also control bacterial replication. J Biol Chem *281*, 36173-36179.

Oshiumi, H., Matsumoto, M., Funami, K., Akazawa, T., and Seya, T. (2003). TICAM-1, an adaptor molecule that participates in Toll-like receptor 3-mediated interferon-beta induction. Nat Immunol *4*, 161-167.

Ovejero Guisasola, J.I., Fresno Escudero, Manuel (2012). Lipopolysaccharide of ochrobactrum intermedium and their use as immunostimulant of mammalians (Spain: LABORATORIOS OVEJERO, S.A. Patent number: 20120107352).

Pamer, E.G. (2004). Immune responses to Listeria monocytogenes. Nat Rev Immunol *4*, 812-823.

Park, B.S., Song, D.H., Kim, H.M., Choi, B.S., Lee, H., and Lee, J.O. (2009). The structural basis of lipopolysaccharide recognition by the TLR4-MD-2 complex. Nature *458*, 1191-1195.

Pathak, S.K., Bhattacharyya, A., Pathak, S., Basak, C., Mandal, D., Kundu, M., and Basu, J. (2004). Toll-like receptor 2 and mitogen- and stress-activated kinase 1 are effectors of Mycobacterium avium-induced cyclooxygenase-2 expression in macrophages. J Biol Chem *279*, 55127-55136.

Petnicki-Ocwieja, T., Chung, E., Acosta, D.I., Ramos, L.T., Shin, O.S., Ghosh, S., Kobzik, L., Li, X., and Hu, L.T. (2013). TRIF mediates Toll-like receptor 2-dependent inflammatory responses to Borrelia burgdorferi. Infect Immun *81*, 402-410.

Piao, W., Ru, L.W., and Toshchakov, V.Y. (2016). Differential adapter recruitment by TLR2 co-receptors. Pathog Dis *74*.

Pitts, M.G., Myers-Morales, T., and D'Orazio, S.E. (2016). Type I IFN Does Not Promote Susceptibility to Foodborne Listeria monocytogenes. J Immunol *196*, 3109-3116.

Pontiroli, F., Dussurget, O., Zanoni, I., Urbano, M., Beretta, O., Granucci, F., Ricciardi-Castagnoli, P., Cossart, P., and Foti, M. (2012). The timing of IFNbeta production affects early innate responses to Listeria monocytogenes and determines the overall outcome of lethal infection. PLoS One *7*, e43455.

Psylinakis, E., Boneca, I.G., Mavromatis, K., Deli, A., Hayhurst, E., Foster, S.J., Varum, K.M., and Bouriotis, V. (2005). Peptidoglycan N-acetylglucosamine deacetylases from Bacillus cereus, highly conserved proteins in Bacillus anthracis. J Biol Chem *280*, 30856-30863.

Raschke, W.C., Baird, S., Ralph, P., and Nakoinz, I. (1978). Functional macrophage cell lines transformed by Abelson leukemia virus. Cell *15*, 261-267.

Re, F., and Strominger, J.L. (2001). Toll-like receptor 2 (TLR2) and TLR4 differentially activate human dendritic cells. J Biol Chem *276*, 37692-37699.

Richardson, E.T., Shukla, S., Sweet, D.R., Wearsch, P.A., Tsichlis, P.N., Boom, W.H., and Harding, C.V. (2015). Toll-like receptor 2-dependent extracellular signal-regulated kinase signaling in Mycobacterium tuberculosis-infected macrophages drives anti-inflammatory responses and inhibits Th1 polarization of responding T cells. Infect Immun *83*, 2242-2254.

Salojin, K.V., Owusu, I.B., Millerchip, K.A., Potter, M., Platt, K.A., and Oravecz, T. (2006). Essential role of MAPK phosphatase-1 in the negative control of innate immune responses. J Immunol *176*, 1899-1907.

Salvador, J.M., Mittelstadt, P.R., Guszczynski, T., Copeland, T.D., Yamaguchi, H., Appella, E., Fornace, A.J., Jr., and Ashwell, J.D. (2005). Alternative p38 activation pathway mediated by T cell receptor-proximal tyrosine kinases. Nat Immunol *6*, 390-395.

Sanchez-Tillo, E., Comalada, M., Xaus, J., Farrera, C., Valledor, A.F., Caelles, C., Lloberas, J., and Celada, A. (2007). JNK1 Is required for the induction of Mkp1 expression in macrophages during proliferation and lipopolysaccharide-dependent activation. J Biol Chem *282*, 12566-12573.

Sanner, M.F. (1999). Python: a programming language for software integration and development. J Mol Graph Model *17*, 57-61.

Schrödinger (2018), Schrödinger, ed. (LLC, New York).

Shaul, Y.D., and Seger, R. (2007). The MEK/ERK cascade: from signaling specificity to diverse functions. Biochim Biophys Acta *1773*, 1213-1226.

Shi, Z., Cai, Z., Sanchez, A., Zhang, T., Wen, S., Wang, J., Yang, J., Fu, S., and Zhang, D. (2011). A novel Toll-like receptor that recognizes vesicular stomatitis virus. J Biol Chem *286*, 4517-4524.

Shim, J.H., Xiao, C., Paschal, A.E., Bailey, S.T., Rao, P., Hayden, M.S., Lee, K.Y., Bussey, C., Steckel, M., Tanaka, N., *et al.* (2005). TAK1, but not TAB1 or TAB2, plays an essential role in multiple signaling pathways in vivo. Genes Dev *19*, 2668-2681.

Shizuo Akira, S.U.a.O.T. (2006). Pathogen Recognition and Innate Immunity. Cell 124, 783-801.

Shore, S.K., Tantravahi, R.V., and Reddy, E.P. (2002). Transforming pathways activated by the v-Abl tyrosine kinase. Oncogene *21*, 8568-8576.

Sica, A., and Mantovani, A. (2012). Macrophage plasticity and polarization: in vivo veritas. J Clin Invest *122*, 787-795.

Silipo, A., and Molinaro, A. (2010). The diversity of the core oligosaccharide in lipopolysaccharides. Subcell Biochem *53*, 69-99.

Simard, F.A., Cloutier, A., Ear, T., Vardhan, H., and McDonald, P.P. (2015). MEK-independent ERK activation in human neutrophils and its impact on functional responses. J Leukoc Biol *98*, 565-573.

Stack, J., Doyle, S.L., Connolly, D.J., Reinert, L.S., O'Keeffe, K.M., McLoughlin, R.M., Paludan, S.R., and Bowie, A.G. (2014). TRAM is required for TLR2 endosomal signaling to type I IFN induction. J Immunol *193*, 6090-6102.

Stockinger, S., Reutterer, B., Schaljo, B., Schellack, C., Brunner, S., Materna, T., Yamamoto, M., Akira, S., Taniguchi, T., Murray, P.J., *et al.* (2004). IFN regulatory factor 3-dependent induction of type I IFNs by intracellular bacteria is mediated by a TLR- and Nod2-independent mechanism. J Immunol *173*, 7416-7425.

Tabeta, K., Georgel, P., Janssen, E., Du, X., Hoebe, K., Crozat, K., Mudd, S., Shamel, L., Sovath, S., Goode, J., *et al.* (2004). Toll-like receptors 9 and 3 as essential components of innate immune defense against mouse cytomegalovirus infection. Proc Natl Acad Sci U S A *101*, 3516-3521.

Takeuchi, O., Kawai, T., Muhlradt, P.F., Morr, M., Radolf, J.D., Zychlinsky, A., Takeda, K., and Akira, S. (2001). Discrimination of bacterial lipoproteins by Toll-like receptor 6. Int Immunol *13*, 933-940.

Takeuchi, O., Sato, S., Horiuchi, T., Hoshino, K., Takeda, K., Dong, Z., Modlin, R.L., and Akira, S. (2002). Cutting edge: role of Toll-like receptor 1 in mediating immune response to microbial lipoproteins. J Immunol *169*, 10-14.

Thedieck, K., Hain, T., Mohamed, W., Tindall, B.J., Nimtz, M., Chakraborty, T., Wehland, J., and Jansch, L. (2006). The MprF protein is required for lysinylation of phospholipids in listerial membranes and confers resistance to cationic antimicrobial peptides (CAMPs) on Listeria monocytogenes. Mol Microbiol *62*, 1325-1339.

Torres, D., Barrier, M., Bihl, F., Quesniaux, V.J., Maillet, I., Akira, S., Ryffel, B., and Erard, F. (2004). Toll-like receptor 2 is required for optimal control of Listeria monocytogenes infection. Infect Immun *72*, 2131-2139.

Trent, M.S., Stead, C.M., Tran, A.X., and Hankins, J.V. (2006). Diversity of endotoxin and its impact on pathogenesis. J Endotoxin Res *12*, 205-223.

Uematsu, S., Fujimoto, K., Jang, M.H., Yang, B.G., Jung, Y.J., Nishiyama, M., Sato, S., Tsujimura, T., Yamamoto, M., Yokota, Y., *et al.* (2008). Regulation of humoral and cellular gut immunity by lamina propria dendritic cells expressing Toll-like receptor 5. Nat Immunol *9*, 769-776.

Underhill, D.M., and Ozinsky, A. (2002). Toll-like receptors: key mediators of microbe detection. Curr Opin Immunol *14*, 103-110.

Vazquez-Boland, J.A., Kuhn, M., Berche, P., Chakraborty, T., Dominguez-Bernal, G., Goebel, W., Gonzalez-Zorn, B., Wehland, J., and Kreft, J. (2001). Listeria pathogenesis and molecular virulence determinants. Clin Microbiol Rev *14*, 584-640.

Velasco, J., Bengoechea, J.A., Brandenburg, K., Lindner, B., Seydel, U., Gonzalez, D., Zahringer, U., Moreno, E., and Moriyon, I. (2000). Brucella abortus and its closest phylogenetic relative, Ochrobactrum spp., differ in outer membrane permeability and cationic peptide resistance. Infect Immun *68*, 3210-3218.

Vollmer, W., and Tomasz, A. (2000). The pgdA gene encodes for a peptidoglycan N-acetylglucosamine deacetylase in Streptococcus pneumoniae. J Biol Chem *275*, 20496-20501.

Wang, G., Olczak, A., Forsberg, L.S., and Maier, R.J. (2009). Oxidative stress-induced peptidoglycan deacetylase in Helicobacter pylori. J Biol Chem *284*, 6790-6800.

Wang, T., Town, T., Alexopoulou, L., Anderson, J.F., Fikrig, E., and Flavell, R.A. (2004). Toll-like receptor 3 mediates West Nile virus entry into the brain causing lethal encephalitis. Nat Med *10*, 1366-1373.

Warren, S.E., Mao, D.P., Rodriguez, A.E., Miao, E.A., and Aderem, A. (2008). Multiple Nod-like receptors activate caspase 1 during Listeria monocytogenes infection. J Immunol *180*, 7558-7564.

Weinberg, E.D. (1987). Pregnancy-associated immune suppression: risks and mechanisms. Microb Pathog *3*, 393-397.

Weiss, G., Rasmussen, S., Zeuthen, L.H., Nielsen, B.N., Jarmer, H., Jespersen, L., and Frokiaer, H. (2010). Lactobacillus acidophilus induces virus immune defence genes in murine dendritic cells by a Toll-like receptor-2-dependent mechanism. Immunology *131*, 268-281.

Werts, C., Tapping, R.I., Mathison, J.C., Chuang, T.H., Kravchenko, V., Saint Girons, I., Haake, D.A., Godowski, P.J., Hayashi, F., Ozinsky, A., *et al.* (2001). Leptospiral lipopolysaccharide activates cells through a TLR2-dependent mechanism. Nat Immunol *2*, 346-352.

Woodward, J.J., Iavarone, A.T., and Portnoy, D.A. (2010). c-di-AMP secreted by intracellular Listeria monocytogenes activates a host type I interferon response. Science *328*, 1703-1705.

Yamamoto, M., Sato, S., Mori, K., Hoshino, K., Takeuchi, O., Takeda, K., and Akira, S. (2002). Cutting edge: a novel Toll/IL-1 receptor domain-containing adapter that preferentially activates the IFN-beta promoter in the Toll-like receptor signaling. J Immunol *169*, 6668-6672.

Yarovinsky, F., Zhang, D., Andersen, J.F., Bannenberg, G.L., Serhan, C.N., Hayden, M.S., Hieny, S., Sutterwala, F.S., Flavell, R.A., Ghosh, S., *et al.* (2005). TLR11 activation of dendritic cells by a protozoan profilin-like protein. Science *308*, 1626-1629.

Zenewicz, L.A., and Shen, H. (2007). Innate and adaptive immune responses to Listeria monocytogenes: a short overview. Microbes Infect *9*, 1208-1215.

Zhang, D., Zhang, G., Hayden, M.S., Greenblatt, M.B., Bussey, C., Flavell, R.A., and Ghosh, S. (2004). A toll-like receptor that prevents infection by uropathogenic bacteria. Science *303*, 1522-1526.

Zhang, S.Y., Jouanguy, E., Ugolini, S., Smahi, A., Elain, G., Romero, P., Segal, D., Sancho-Shimizu, V., Lorenzo, L., Puel, A., *et al.* (2007). TLR3 deficiency in patients with herpes simplex encephalitis. Science *317*, 1522-1527.

Zhao, G.N., Jiang, D.S., and Li, H. (2015). Interferon regulatory factors: at the crossroads of immunity, metabolism, and disease. Biochim Biophys Acta *1852*, 365-378.

Zhao, Q., Shepherd, E.G., Manson, M.E., Nelin, L.D., Sorokin, A., and Liu, Y. (2005). The role of mitogen-activated protein kinase phosphatase-1 in the response of alveolar macrophages to lipopolysaccharide: attenuation of proinflammatory cytokine biosynthesis via feedback control of p38. J Biol Chem *280*, 8101-8108.

Zhao, Q., Wang, X., Nelin, L.D., Yao, Y., Matta, R., Manson, M.E., Baliga, R.S., Meng, X., Smith, C.V., Bauer, J.A., *et al.* (2006). MAP kinase phosphatase 1 controls innate immune responses and suppresses endotoxic shock. J Exp Med *203*, 131-140.